Understanding mangrove regrowth

A problem analysis of the mangrove system of Las Brujas, situated in the Biotopo Monterrico-Hawaii, Guatemala

CEGM3000: Multidisciplinary Project (2025/2026)

Eva van der Weegen, Ilja de Goede, Jorrit van Heijst, Lena ten Wolde, Robin Bruins and Saana Taal

Delft University of Technology

TU Delft

Understanding mangrove regrowth

A problem analysis of the mangrove system of Las Brujas, situated in the Biotopo Monterrico-Hawaii, Guatemala

by

Eva van der Weegen, Ilja de Goede, Jorrit van Heijst, Lena ten Wolde, Robin Bruins and Saana Taal

Name Student	Education
E.A. (Eva) van der Weegen	Environmental Engineering
G.I. (Ilja) de Goede	Hydraulic Engineering
J.J.W. (Jorrit) van Heijst	Environmental Engineering
H.E. (Lena) ten Wolde	Hydraulic Structures Engineering
R. (Robin) Bruins	Structural Engineering
S.A. (Saana) Taal	Hydraulic Structures Engineering

Supervisor TU Delft:	Astrid Blom and Marcus Hrachowitz
Partner Organisations:	CECON, Alas y Raíces Resilientes and FUNDAECO
Project timespan:	1/09/2025 - 06/11/2025
Faculty:	Faculty of Civil Engineering (CiTG), Delft
MDP Group number:	387

Preface

This report was written for the course ”CEGM3000 Multidisciplinary Project (MDP)” in Q1 of the academic year 2025/2026. Research was conducted at both the Faculty of Civil and Geosciences, Delft University of Technology (TU Delft), in the Netherlands, and at the project location in Monterrico, Guatemala. The required fieldwork for this project has been conducted in and around the research site *Las Brujas*, situated in the Biotopo Monterrico-Hawaii in Monterrico, Guatemala.

This report would not have been possible without the guidance and help we received throughout the project. We would like to express our gratitude to the following: Dr.Ir. Astrid Blom (TU Delft), Dr. Markus Hrachowitz (TU Delft) and Myrnamaría Galindo (FUNDAECO) for their supervision. We would like to thank Dr. Bregje van Wesenbeeck (TU Delft), Ir. Marcel Taal (Deltares), Dr.Ir. Stuart Pearson (TU Delft), Prof.Dr. Thom Bogaard (TU Delft) and Prof.Dr.Ir. Han Winterwerp for their helpful insights and advice.

Dr.Ir. Astrid Blom and Dr. Markus Hrachowitz were our supervisors from the TU Delft, who helped by giving useful advice and feedback, both during the project preparations and throughout our time in Guatemala. Myrnamaría Galindo, our local supervisor from the company of FUNDAECO, supported us by sharing information about the study area, coordinating the fieldwork, and assisting with any questions we had. We are also grateful to Dr. Bregje van Wesenbeeck, Ir. Marcel Taal, Dr.Ir. Stuart Pearson and Prof.Dr.Ir. Han Winterwerp for their valuable input on specific aspects of our research, and to Prof.Dr. Thom Bogaard, who provided important advice on fieldwork-related matters.

With great appreciation,
Eva van der Weegen, Ilja de Goede, Jorrit van Heijst, Lena ten Wolde, Robin Bruins and Saana Taal
Delft, November 2025

Abstract

Situated at the southern coast of Guatemala is the protected nature reserve of Biotopo Monterrico-Hawaii. This biotope contains a mangrove forest consisting of three tree species: the *Rhizophora Mangle*, *Lagunculeria Racemosa* and *Avicenna Germinans*. At the beginning of the 21st century, human-induced fires destroyed parts of the mangrove forest. After this disturbance, the mangrove forest has shown signs of natural regeneration, although the extent of recovery remains low and spatially restricted. The area of Las Brujas currently shows one of the lowest natural regeneration rates of mangroves within the reserve. This study aimed to identify the main factors limiting mangrove regrowth in Las Brujas.

An extensive literature review was conducted, key stakeholders were interviewed, and field measurements were taken to investigate precipitation data, tidal influence, flow dynamics, ground level, and physical-chemical parameters. Results indicate that visually, the precipitation patterns have been undergoing small changes in the past years. These changes elongate the time during which young mangrove saplings are submerged by water, increasing their risk of drowning. Tidal influence in Las Brujas is minimal. The flow is driven mainly by wind and river discharge. Moreover, flow velocities are low, not exceeding 0.12 m/s, and are stagnated by invasive species. This reduces nutrient, sediment, and propagule transport, and therefore stresses mangrove regrowth. Satellite data reveal no significant changes in ground level, yet sediment flow was observed, indicating that natural heightening of the ground level is possible. A higher ground level could reduce the mortality rate of young saplings by decreasing the risk of drowning. The physical-chemical parameters were within optimal ranges for mangrove growth, suggesting that water quality is not limiting mangrove regeneration during the wet season.

The most critical parameters influencing natural regeneration during the wet season appear to be water depth and flow dynamics. Submergence of saplings for more than 15 days results in high mortality due to oxygen deprivation. In addition, reduced flow conditions limit the dispersal of propagules and restrict nutrient exchange within the water column. To better understand these processes, further hydrological and hydrodynamic investigations during the dry season are recommended.

Contents

1

Introduction

The ecological importance of mangrove forests has become increasingly recognised over the last decades. Mangrove forests are unique coastal ecosystems in tropical and subtropical regions characterised by salt-tolerant trees (Friess, 2016). The knotted roots of the trees, periodically submerged in saltwater, make ideal underwater perches for shrimps, crabs, and other marine organisms. These animals, in their turn, serve as an important source of food for a wide range of juvenile fish, as well as birds, reptiles, and an abundance of other wildlife both above and below the water surface (Waters, 2016). However, a better understanding of the importance of mangroves has not stopped their destruction so far. Proximate drivers such as aquaculture, agriculture, and urban development have caused large-scale mangrove deforestation worldwide, and mangroves are further degraded by overexploitation of resources and by pollution (Friess et al., 2019).

Problem analysis

Mangrove forests are present along the southern coast of Guatemala. The second largest of these forests is the Biotopo Monterrico-Hawaii near the town of Monterrico. This ecosystem is undergoing significant degradation. In the early 21st century, parts of the mangrove forest were destroyed by fires (CONRED, 2013). Furthermore, the construction of an artificial channel has altered the natural hydrological dynamics of the area, leading to disturbances in the water system (Coromac et al., 2024). During the dry season, severe water shortages and low water levels occur, while in the wet season, water levels can become excessively high. These fluctuations create unfavourable conditions for tree growth (Enschedé et al., 2017). Such challenges highlight the need for research on current hydrological conditions to develop strategies to regulate water levels, thereby stimulating the natural regeneration of mangrove forests.

Figure 1.1: Location of the Biotopo Monterrico-Hawaii (Google Earth, 2025)

Objective

During this multidisciplinary research project, the following research question will be put at the centre:

¨What are the possible causes for the limited regrowth of mangrove forests in Las Brujas, Monterrico, Guatemala?¨

To address the main question, the problem is divided into sub-questions:

- ¨How do precipitation patterns over the last 40 years influence the water regime of Las Brujas?¨
- ¨To what extent do the present tidal dynamics influence Las Brujas?¨
- ¨How does water flow affect transport processes in Las Brujas?¨
- ¨What are the changes in ground level in the Biotopo Monterrico-Hawaii?¨
- ¨How do current physical–chemical conditions in Las Brujas compare to those characteristic of a healthy mangrove environment?¨

The research will be conducted in Monterrico, Guatemala, through on-site fieldwork and measurements combined with a literature study and information gathered by conducting interviews.

Reading guide

The second chapter presents a literature study on mangrove ecosystems, focusing on their growth characteristics and the environmental conditions that support healthy development. The third chapter introduces the Biotopo Monterrico-Hawaii, discussing its current state, historical background, and prior restoration efforts. Chapter four outlines the methodology used during the fieldwork, while the research results are presented in chapter five. Chapter six summarises the main conclusions, which are further discussed in chapter seven. Finally, chapter eight provides recommendations for future research.

2

Literature study on Mangrove Ecosystems

This chapter provides an overview of mangrove forests in general. The first section introduces key characteristics, global occurrence, and dominant species, while the second outlines the main parameters regulating healthy mangrove performance.

2.1. What are mangroves?

Mangroves are salt-tolerant, evergreen forests that are located in intertidal zones. These are coastal areas that lie between the high and low tide marks, regularly exposed to air at low tide and submerged under seawater at high tide (National Geographic Society, n.d.). They only grow along tropical and subtropical coastlines, as they cannot withstand average temperatures below 20 $°C$ (Komiyama et al., 2008). They mainly appear in deltas, shallow-water lagoons, rivers, and estuaries. In these places, they receive a daily input of salt water from the ocean and fresh water, sediments and nutrients from upstream sources (Food and Agriculture organization of the United Nations, 2025). Many mangrove forests are known for their dense, tangled roots that resemble stilts and grow above the water. These structures allow mangrove trees to obtain nutrients even during high water levels so that they can withstand tidal changes, as most forests are flooded multiple times a day (National Oceanic and Atmospheric Administration, 2024). In addition to coping with tides, mangrove forests can also provide coastal protection during heavy storms. Their roots help to reduce erosion, buffer storm surges, and dissipate the energy of tsunamis (Massel et al., 1999). The roots also slow the movement of tidal waters down, which causes sediments to settle and form nutrient-rich muddy floors. In this way, mangrove forests not only build, but also restore their environment.

Distribution of mangroves

In total, around 80 mangrove species exist worldwide, of which around 60 species live exclusively on coasts in the intertidal zones (American Museum of Natural History, n.d.). In figure 2.1, the amount of mangrove species present at a variety of locations on the globe is shown.

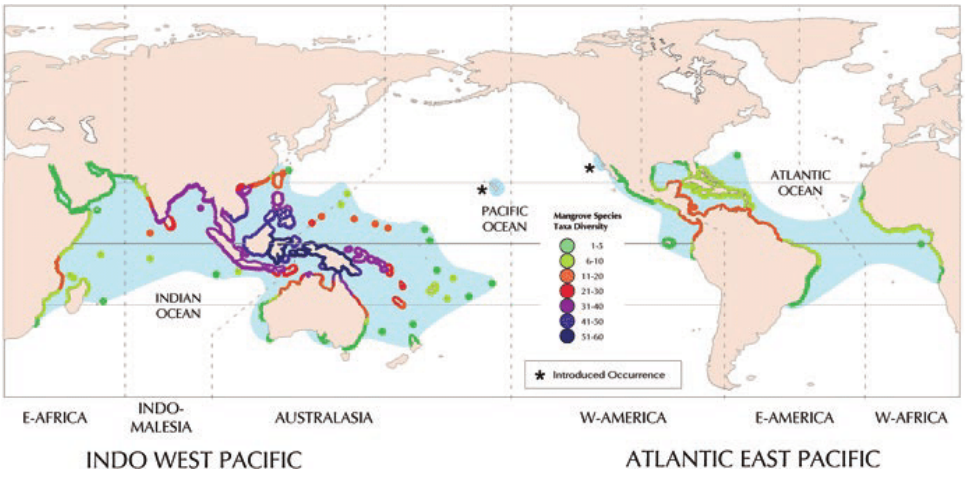

Figure 2.1: The distribution of mangrove species (blue shading) showing the diversity as numbers of specific taxa (species and nominal hybrids) (Duke, 2017)

Mangrove forests once covered three-quarters of the intertidal zones worldwide, with Southeast Asia hosting the greatest diversity. Besides a great variety in species, the size of mangrove trees can also vary greatly. They range in size from small shrubs to trees over 60 meters tall, as illustrated in figure 2.2. Across the globe, numerous species occupy distinct districts within mangrove forests. Those that tolerate full tidal flooding grow along the open sea, on outlying islands or in sheltered bays. The other three species are adapted to drier and less saline conditions, which commonly occur further inland away from the shoreline. A smaller group of species even thrives along riverbanks far inland, where freshwater currents meet the influence of the oceans' saltwater (American Museum of Natural History, n.d.).

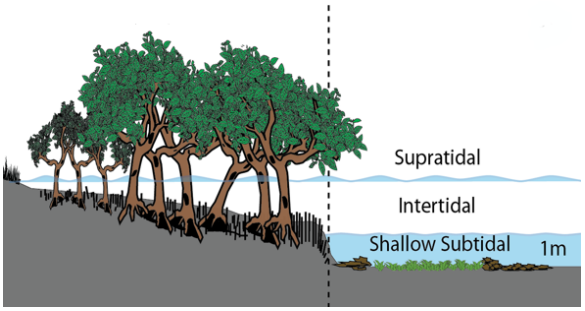

Figure 2.2: Intertidal zone ("File:Mangrove ecosystem in the coastal intertidal zone.png - Wikimedia Commons," 2020)

Mangrove species

As explained in section 2.1, there are many different species of mangroves. The three most common species of mangroves are:

1. Red Mangroves - *Rhizophora mangle*
2. White Mangroves - *Laguncularia racemosa*
3. Black Mangroves - *Avicenna germinans*

(González et al., 2023)

Red Mangroves - Rhizophora mangle

The red mangrove typically grows along the shoreline, where conditions are harsh as a result of tidal influences. Red mangroves are recognised by their long stilt-like roots. These roots originate from the trunk and grow downward mainly to provide stability to relatively slim trees. They also serve to transport oxygen to roots that are below ground level (Florida Museum of Natural History, 2025). The red mangrove species produces propagules as seedlings to reproduce itself (see figure 2.3 on the left). Propagules are seeds with a tail that are buoyant and will float in the water once they fall from the tree. The propagule can float up to 15 days until it either dies or finds a suitable location to nest.

Figure 2.3: Red mangrove species and a propagule (left) (Florida Museum of Natural History, 2025)

The propagule thrives best in muddy soil with desired salinity levels (section 2.2) and a stable tidal environment. Once this location is found, the root end of the propagule will anchor itself in the soil, and a new mangrove tree can emerge.

White Mangroves - Laguncularia racemosa

The white mangrove species are mainly found in coastal areas such as bays, lagoons, and tidal creeks. They typically grow inland of other mangrove species, well above the high tide line (Ellison et al., 2000). Depending on the environmental conditions, pneumatophore roots may be present. Pneumatophore roots are roots that enable plants to breathe air in habitats with waterlogged soil (Hiller, 1998). These roots grow upwards towards the air, which is the inverse of typical soil-bound roots. Besides, the white mangrove species is cryptoviviparous in its way of reproduction. This means that the embryo of the seed germinates and the seedling emerges from the seed coat, but remains enclosed within the fruit. Once the seeds fall from the trees and locate themselves in the substrate, the sprouting of the seeds will start, and a new mangrove tree will grow (Wiktionary: The free dictionary, 2024). Compared to propagules, these seeds survive shorter without soil.

Figure 2.4: White mangrove species (Florida Museum of Natural History, 2025)

Black Mangroves - Avicenna germinans

The black mangrove species appears in places where the tidal changes expose the roots to air, thus they can be found on a higher elevation than the red mangrove species. The black mangrove species is characterised by its long, horizontal roots. Compared to the white mangrove species, the black mangrove species also has pneumatophore roots that provide oxygen to its underground and submerged root systems (Florida Museum of Natural History, 2025). Black mangrove species reproduce in the same way as white mangrove species do.

Figure 2.5: Black mangrove species (Florida Museum of Natural History, 2025)

Growth cycle

The red mangrove (*Rhizophora mangle*) has an annual growth cycle that is influenced by both the species' characteristics and the local climate. Since the red mangrove is the most dominant species in the Biotopo Monterrico-Hawaii and is considered the most important by inhabitants, only the growth cycle of the *Rhizophora mangle* was focused upon. The cycle can be described as follows:

- *February to April*: During this period, propagules begin to grow on the mangrove trees (Thompson-Saud et al., 2024). Depending on the local climate, they develop until they reach a length of 15–30 cm (Van der Stocken et al., 2019).
- *May to June*: By this time, the propagules are fully mature and detach from their parent tree. The wet season also starts in May, resulting in a mangrove forest that remains largely submerged. Conducted research reveals that rainfall and propagule release are highly correlated with each other (T. Van der Stocken et al., 2017). These submerged conditions allow the propagules to float away from their parent trees and disperse throughout the mangrove ecosystem (Myrnamaría Galindo, personal communication).
- *July to October*: When the propagules encounter muddy soil, they begin to sprout and develop roots (Thompson-Saud et al., 2024). They establish best in soft, muddy soil covered by about 10 centimetres of water (Myrnamaría Galindo, personal communication).
- *November to May*: In November, the dry season begins, and water levels within the mangrove forest gradually fall. During this period, the young mangroves grow most rapidly (Thompson-Saud et al., 2024). They must grow tall enough to withstand the water levels of the next wet season. If they

remain shorter than the expected water depth, they become submerged and may die (Myrnamaría Galindo, personal communication).

A summarised visual representation of the annual growth cycle of the (*Rhizophora mangle*) is presented in figure 2.6. The wet-season phases (May-October) are highlighted in blue, while the dry-season phases (November-April) are shown in light yellow.

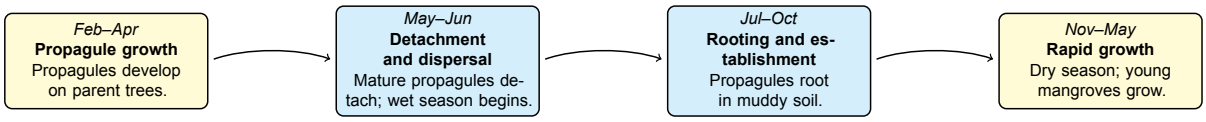

Figure 2.6: Schematic overview of the annual growth cycle of *Rhizophora mangle* based on field observations and literature; wet-season phases (May–Oct) are shown in blue and dry-season phases (Nov–Apr) in yellow (own image)

2.2. Healthy mangrove conditions

After a natural disaster or human-induced disturbance, a mangrove system will try to recover from the impact. However, stressors often arise that compromise mangrove regrowth (Rachel J. Harris & Bovard, n.d.). This subsection focuses on determining the most relevant stressors and explaining their impact.

Transport processes

One potential stressor is reduced tidal flushing (Rachel J. Harris & Bovard, n.d.). Tidal flushing is the natural process of water flowing in and out of a coastal water body due to the rise and fall of the tide. It is essential for renewing water, diluting pollutants, distributing nutrients and creating flow in a mangrove ecosystem (Fiveable, n.d.). Healthy tidal exchange maintains the balance of oxygen, nutrients and sediments in the system. In addition, rivers and groundwater supply nutrients that enhance mangrove productivity and promote subsurface expansion through root growth (Krauss et al., 2013; McKee, 2010). When this exchange is obstructed, nutrient replenishment and sediment transport decline, which can slow down recovery and lead to stagnation or shrinkage (Alongi, 2018).

Propagule dispersal is another key process that depends on tidal and flow dynamics. As explained in section 2.1, the red mangrove species releases buoyant propagules that are carried by the water to nestle in new areas. Effective dispersal promotes genetic connectivity between forest patches, maintaining diversity and resilience. If water movement between mangrove areas is reduced, fewer propagules reach suitable sites, and recovery after disturbance becomes slower (Van der Stocken et al., 2019).

Ground level and composition

Ground elevation plays a crucial role in the persistence of mangroves. When the ground level relative to its surroundings becomes higher, the water level decreases, and vice versa. Mangrove trees cannot tolerate prolonged inundation or increased water depths (Nurse et al., 2014; Waycott et al., 2011). When soil inputs exceed erosion, surface elevation may rise beyond the optimal range for mangrove growth, allowing terrestrial vegetation to outcompete them. Conversely, when soil inputs and losses are approximately balanced and the surface elevation remains relatively stable, mangroves can persist as the climax vegetation for many years (McIvor et al., 2013).

The key factors controlling surface elevation rates are external sediment inputs and subsurface root growth (McIvor et al., 2013). When estuarine mudbanks are covered by mangroves, sediment delivery is reduced, while strong protection against erosion promotes steady, long-term elevation gain. In contrast, bare estuarine mudbanks remain highly dynamic (Van Santen et al., 2006). The subsurface root growth is closely linked to the transport processes as mentioned in section 2.2.

Mangroves grow in a variety of soils, causing their composition and structure to vary across regions. These soils are formed from materials carried and deposited by rivers and the sea and consist of different mixes of sand, silt, and clay. Mud, a mixture of silt and clay, is typically rich in organic matter. The topsoil may be sandy or clayey, while deeper layers are waterlogged, poorly aerated, and high in organic content (Hossain & Nuruddin, 2016). Mangroves grow best in sheltered intertidal areas with soft muddy substrates rich in organic matter (Kathiresan & Bingham, 2001).

Physical-chemical conditions

Mangrove systems are highly sensitive to both physical and chemical environmental conditions. Under optimal conditions, mangroves show healthy growth, reproduction and efficient nutrient cycling. However, under stress, mangroves reallocate energy from growth and reproduction to survival mechanisms, such as salt exclusion or the use of aerial roots for oxygen uptake. Prolonged stress reduces forest productivity, increases vulnerability to climatic extremes and, in extreme cases, results in mortality.

Relevant parameters

Several parameters influence the process of mangrove regrowth. In this subsection, the focus will be on the key physical and chemical factors that regulate mangrove growth and ecological performance. Specifically, the following environmental factors will be considered:

1. Salinity
2. pH
3. Temperature
4. Dissolved oxygen
5. Redox potential

These five factors influence the mangrove regeneration rate according to (Radabaugh et al., 2021) and (Barik et al., 2017). The following subsections discuss their relevance and influence on the re-population of mangroves.

Salinity

Salinity refers to the concentration of dissolved salts in water or sediment and is typically expressed in parts per thousand [ppt]. Mangroves are halophytic plants, indicating that mangroves are capable of growing in saline environments (Puthiyapurayil Haseeba et al., 2025). The salinity gradient has long been recognised as a potential stressor and is acknowledged as an important factor that regulates physiological processes such as growth, height, survival, and zonation patterns in mangroves. Salinity tolerance differs quite strongly among mangrove species and even within the same mangrove families. Moreover, it is important to note that within a species, salt tolerance changes depending on its life stage, with seedlings being potentially more sensitive to salt stress than mature trees (Biber, 2006).

As explained in section 2.1, red mangroves are located in intertidal zones with a salt concentration between 0-60 ppt. As for the *Rhizophora Mangle*, one type of red mangrove, this matches its salinity tolerance, as this lies between 0-60 ppt. Seedlings cease to grow when salinity levels reach above 65 ppt (Biber, 2006). However, the optimal salinity range of the *Rhizophora Mangle* is lower than that. Based on two indicators (leaf stomatal conductance and chlorophyll fluorescence) that indicate the rate of photosynthesis in seedlings, the optimal salinity level lies between 0-35 ppt.

The *Avicenniacaeae* family (black mangroves) appears to be more tolerant to high salinity than the *Rhizophoraceae* (red mangroves). Generally, the black mangroves have a tolerance of 0 ppt up to saltwater, which is approximately 35 ppt and an optimal growth in salinity levels ranging from 17 ppt up to 28 ppt. The *Avicennia* species is suggested to tolerate even higher salinity levels up to 90 ppt (Turner et al., 2023). However, experimental studies specifically testing their upper salinity limits are limited compared to those available for the *Rhizophora* species.

The white mangrove species (*Laguncularia Racemosa*) inhabits environments with salinity levels ranging from 0 to 60 ppt, similar to those tolerated by the *Rhizophoraceae*. However, its optimal salinity range is lower, between 0 and 5 ppt, corresponding to only mildly saline conditions (Boletín del Centro de Investigaciones Biológicas, 2021). In laboratory experiments, 99% of healthy *Laguncularia Racemosa* seedlings died before the end of the study when exposed to salinity levels above 40 ppt. The same study reported that young seedlings grow best under low-salinity conditions, whereas adult individuals exhibit reduced growth at both high salinity and in the complete absence of dissolved salts. Generally, it can be said that *Laguncularia racemosa* is rarely dominant, except when salinity is low (Correa et al., 2021).

Figure 2.7 illustrates the survival range of different mangrove species in yellow, while the green area represents their optimal ranges.

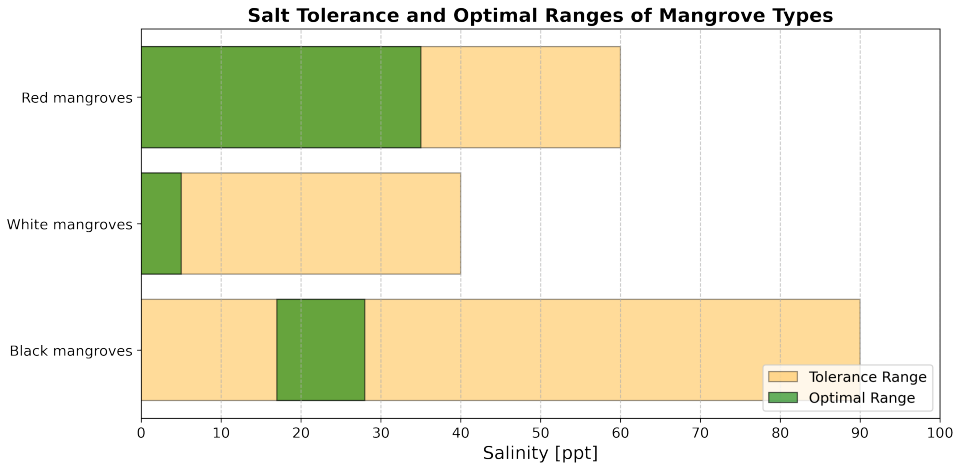

Figure 2.7: Salinity range for each of the mangrove species (yellow) and the range where they thrive (green) (Turner et al., 2023)

pH

The pH level measures acidity or alkalinity and typically ranges from 0 [−] (highly acidic) to 14 [−] (highly alkaline). Mangroves generally thrive in slightly acidic to neutral conditions, with a pH between 6.5 [−] and 8.5 [−] (Radabaugh et al., 2021). In figure 2.8, the range in which mangroves thrive is shown. Extreme acidity can lead to an accumulation of toxic nutrients, while extreme alkalinity may result in nutrient deficiencies. Both conditions also limit mangrove productivity. Mangrove productivity is assessed by quantifying the amount of organic matter they produce and sustain, such as propagules, roots, and other biomass. In figure 2.8 to figure 2.11, the red zone represents the stressed range, where the mangroves are in survival mode. The orange zone indicates conditions under which mangroves can function, but do not thrive, while the green zone represents the optimal range for mangrove growth and development.

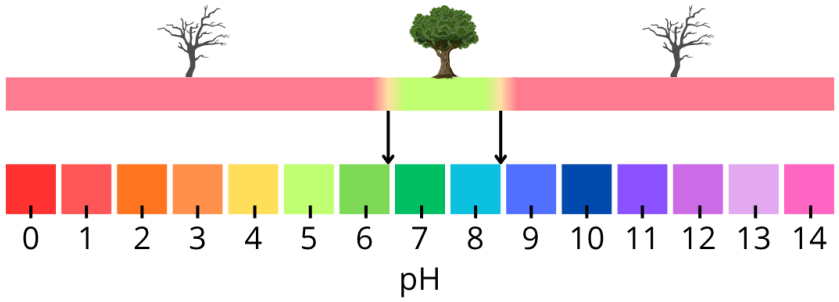

Figure 2.8: Range in which mangroves thrive (green) in relation to the pH value (own image)

Temperature

Temperature is a key factor controlling the global distribution of mangroves, restricting them to tropical and subtropical regions with consistently warm air and water. It influences both their reproduction and productivity. Freezing temperatures are lethal to mangrove growth, while forests typically thrive where mean temperatures range between 20 °C and 35 °C (Twilley, 1998). Optimal growth occurs between 26 °C and 32 °C (Radabaugh et al., 2021), see figure 2.9.

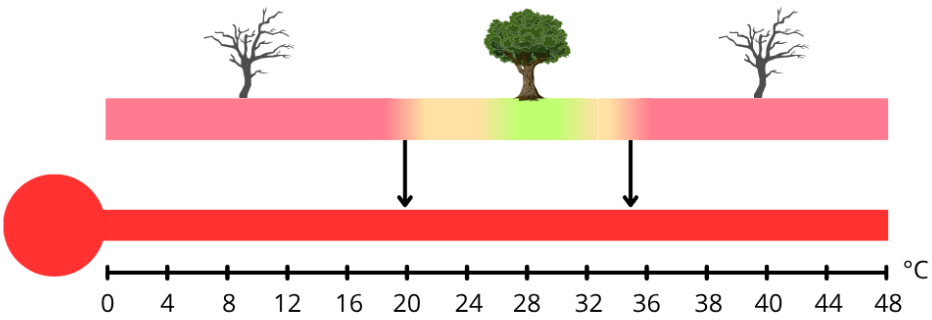

Figure 2.9: Range in which mangroves thrive (green) in relation to the temperature (own image)

Dissolved Oxygen (DO)

Dissolved oxygen indicates the amount of oxygen available in water or sediment and is measured in milligrams per litre (mg/L). Mangrove soils are frequently waterlogged and oxygen-poor; however, as explained in section 2.1, some mangrove species have pneumatophore roots that facilitate gas exchange and root respiration (Kathiresan & Bingham, 2005). Mangroves thrive when dissolved oxygen levels are above 4 mg/L, while values below 2 mg/L create conditions that stress the roots and reduce productivity, as shown in figure 2.10 (Radabaugh et al., 2021).

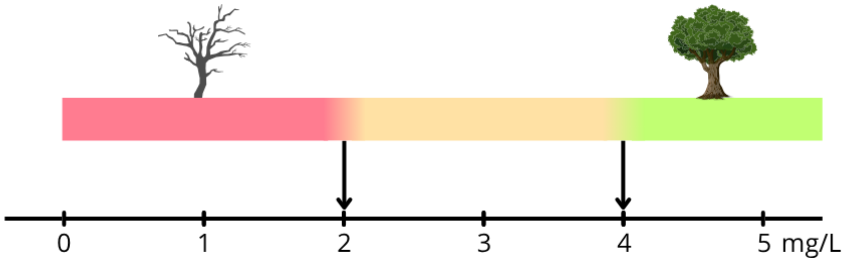

Figure 2.10: Range in which mangroves thrive (green) and survive (orange) in relation to the dissolved oxygen level (own image)

Redox Potential

Redox potential reflects the oxidation-reduction status of the sediments, and it is measured in millivolts $[mV]$. Positive values indicate oxidising conditions, whereas negative values indicate reducing conditions, characterised by the absence of oxygen and the predominance of anaerobic processes. Mangroves perform best under moderately reducing conditions with redox potentials between +100 and -100 mV (Radabaugh et al., 2021). In contrast, values below -300 mV indicate a strongly reducing environment that stresses root function and hinders growth, as illustrated in figure 2.11 (Holguin et al., 2001).

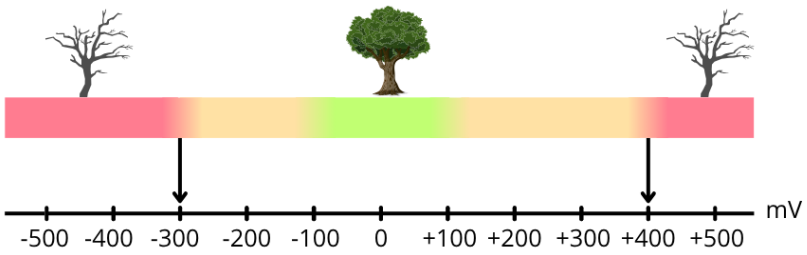

Figure 2.11: Range in which mangroves thrive (green) and survive (orange) in relation to the redox potential (own image)

Optimal vs. Stressed ranges

The preferred ranges corresponding to the optimal ecological performance of mangrove forests are summarised in table 2.1 (adapted from (Barik et al., 2017; Radabaugh et al., 2021)).

Parameters	Optimal conditions	Stressed conditions
Salinity [ppt]	Red: 0-35, White: 0-5, Black: 17-28	$>$35 (hypersalinity) or $<$5 (excess freshwater)
pH [$-$]	6.5–8.5	$<$6.5 (acidification) or $>$8.5 (alkalinization)
Temperature [C]	26–32	$>$34 (thermal stress, lower DO) or $<$20 (frost risk)
Dissolved oxygen [mg/L]	$>$4	$<$2
Redox potential [mV]	+100 to –100	$<$–300 (strongly reducing, sulfide accumulation)

Table 2.1: Comparison of optimal and stressed conditions for key physical-chemical parameters

3

Literature study of area: "Biotopo Monterrico-Hawaii"

This chapter provides an overview of the focus area of this research in various aspects. Firstly, the current situation is explained. Afterwards, the history and formation of the area, as well as restoration efforts, are discussed. Finally, the reference sites selected for parameter comparison are described and explained.

3.1. Current situation

This subsection describes the current situation of the area. First, a description of the geography and ecology of the area is given, followed by explaining the governmental organisation, the water system and the climate and precipitation.

Description of biotope

The Biotopo Monterrico-Hawaii has a total area of 1220.63 hectares (Galindo Lemus & Schönbeck, 2025). The total area can be seen in figure 3.1. The focus area in this research is a site of the biotope called *Las Brujas* (both visible in figure 3.1 and figure 3.2). It has a surface area of around 50 hectares and shows the least amount of natural regeneration. Other sites that have experienced great loss, but that recover faster are *El Dragado* and *El Barrigon* (figure 3.2). Biotopo Monterrico-Hawaii is partly protected, meaning that its land can only be used for personal purposes when permission from the government is granted. More information on the regulation of the biotope is provided in a later section.

Figure 3.1: Overview of multiple use areas in Biotopo Monterrico-Hawaii (own image)

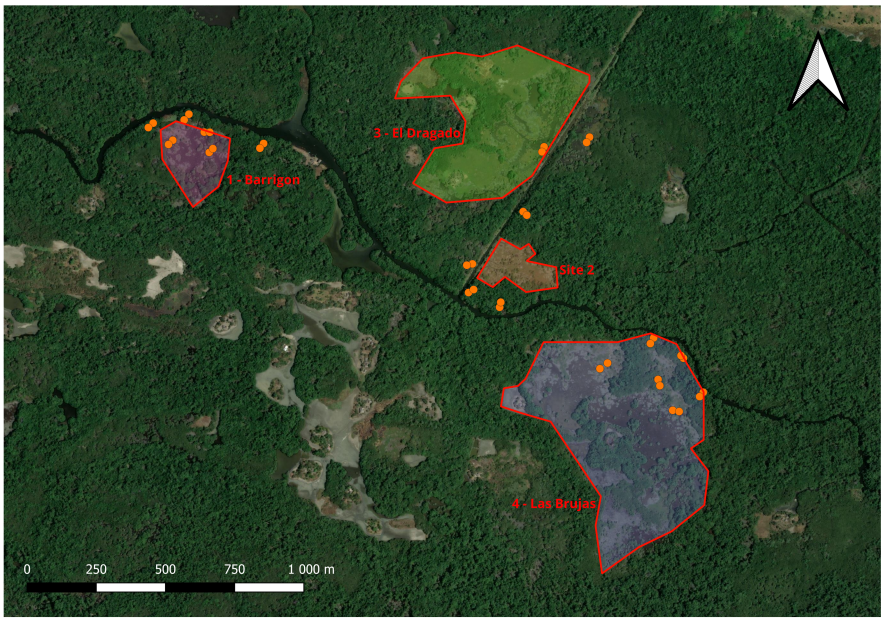

Figure 3.2: Overview of the different sites: El Barrigon, El Dragado, and Las Brujas. Site 2 is a subsite of El Dragado (own image)

Ecology

Red mangroves are the predominant species in the biotope, with white and black mangroves also occurring, but in lesser quantities. Red mangroves are slim in size and are considered the most valuable by the communities that live in and around the forest (section 3.1). Both for its practical use as firewood, for example, and its dominant appearance in the biotope. White mangroves are thicker in size and are used as construction material. Looking at Las Brujas, the southern part is more densely forested, where white mangrove trees are the dominant species. The northern and more accessible part has large areas of grasslands and swamps, where some mangrove trees grow sporadically. A general impression of the ecology of Las Brujas can be seen in figure 3.3.

(a) White mangroves in the southern part of Las Brujas (own image)

(b) Grassland and swamps in the northern part of Las Brujas (own image)

Figure 3.3: Different growth in Las Brujas

Invasive species

The channel hosts numerous plant species, several of which are invasive and hinder the passage. The main species present are:

- *Waterhyacinth*, also know as *Ninfa (Eichhornia crassipes)*.
- *Waterthyme* also know as *Horse tail (Hydrilla verticillata)*
- *Cabage* also known as *Lechuguilla (Pistia stratiotes)*
- *Watergrasses*

From these invasive species, ninfas have the greatest impact on the canal due to their extensive coverage and large size (Myrnamaría Galindo, personal communication). These floating plants obstruct channels and hinder the flow (see figure 3.4), leading to water quality deterioration and a reduction in biodiversity (Gunnarsson & Petersen, 2006).

Ninfas occur mainly during the rainy season (Myrnamaría Galindo, personal communication). Originally from tropical regions of South America, this invasive species does not tolerate brackish water; thus, high salinity levels can limit or alter its distribution ("Eichhornia crassipes," 2006). The growth of water hyacinth is greatly enhanced by nutrient-rich waters, particularly those with high concentrations of nitrogen, phosphorus, and potassium ("Eichhornia crassipes," 2006).

Figure 3.4: Nymphas obstructing the Chiqimulilla channel (own image)

Physical-chemical parameters in Las Brujas

Previous research by the Alas y Raíces Resilience project, which has not been published yet, has shown that the physical-chemical parameters salinity, pH, redox potential and temperature generally indicate stressed conditions in the Las Brujas area ("Schoenbeck et al, in prep." n.d.). Specifically, throughout the dry season, from December to April, these values are not optimal for mangrove growth or regrowth. More extensive research is necessary to verify whether this plays a crucial role in mangrove regrowth.

Communities

Altogether, six communities interact with the biotope, either through reliance on its resources or by residing nearby. These communities are the towns of El Pumpo, Monterrico, La Avellana and El Papaturro, and the communities "Agua Dulce" and "La Corbina" visible in figure 3.5 (Myrnamaría Galindo, personal communication). "Agua Dulce" is located within the mangrove forest, consisting of a village of 17 families that maintain a self-sustaining livelihood. They live off fishing and farming in the wet periods and maintain salt flats in the dry periods. They trade their crops and farm products with surrounding villages for petrol or money. Most of the children who live in Agua Dulce do

Figure 3.5: Overview of the location of communities (own image)

attend primary school, but often learn the trade from their parents (Noé Orantes Olivares, personal communication).

Governmental organisation of the Biotopo Monterrico-Hawaii

Understanding the governmental organisation responsible for managing Biotopo Monterrico-Hawaii is crucial for evaluating the current system and the factors contributing to its observed degradation. Changes are most likely to be effective if supported by the highest levels of authority (Myrnamaría Galindo, personal communication).

In Guatemala, in 1989, the Protected Areas Law was enacted, granting management of protected areas to the National Council on Protected Areas (CONAP) (Gonzalez-Bernat & Clifton, 2016). The Biotopo Monterrico-Hawaii is included under this law and has the mildest level of protection available for a marine protected area. Shrimp farmers, fishermen, agricultural workers, and sugarcane cultivators are required to obtain governmental permission before starting activities or clearing land. In practice, approvals are often granted if sufficient payments are made (Myrnamaría Galindo, personal communication).

Regional management of Biotopo Monterrico-Hawaii

On the 16th of December 1977, the biotope was established as a reserve area for the special protection of fauna, flora and the natural ecosystem (García, 2018). Locally, the Biotope Monterrico-Hawaii is situated within the department of Santa Rosa, which forms the focus of this section.

The Biotopo Monterrico-Hawaii is primarily governed by CONAP, which is responsible for all protected areas. CONAP manages, regulates, and enforces national laws (“Misión y Visión del CONAP,” n.d.).

CECON acts as the central coordinator for the area, managing new conservation projects and research, and serving as an academic link between the university and local communities. It ensures the implementation of laws (“MISIÓN – Centro de Estudios Conservacionistas – CECON –,” n.d.) and (Myrnamaría Galindo, personal communication).

FUNDAECO, a non-governmental organisation, supports CECON in implementing national laws, providing technical support for mangrove restoration and conservation projects. It also promotes ecotourism, environmental education, and sustainable development in collaboration with local communities (Myrnamaría Galindo, personal communication).

Alas y Raíces is a temporary supporting organisation with a cultural and educational focus. It strengthens cultural identity and traditions linked to ecosystems, promotes educational, artistic, and environmental awareness activities, and encourages youth and community participation in environmental protection (Myrnamaría Galindo, personal communication).

Further information on the governmental organisation, including its structure beyond the regional level, is provided in appendix A.

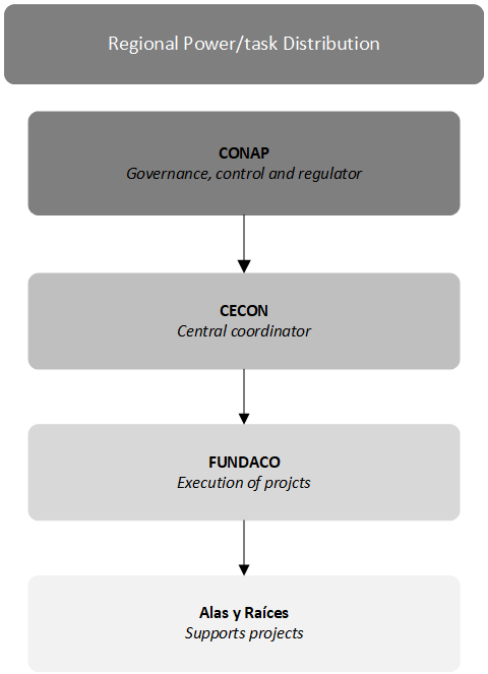

Figure 3.6: Regional stakeholders of Biotopo Monterrico-Hawaii (own image)

Water system

River system

In and around Biotopo Monterrico-Hawaii, various rivers and canals are present. Four main waterways are the river Maria Linda, the river Los Enclavos, the Chiquimulilla River and the Chiquimulilla canal. These are depicted in figure 3.7.

Figure 3.7: Overview of main waterways around research area, with light green representing the main rivers and canals, names of waterways included, and pink squares represent the river mouths. Multiple use areas are also depicted (own image).

Canal of Chiquimulilla

The Chiquimulilla canal crosses the biotope of Monterrico. This stream is a man-made canal that stretches 140 kilometres and was constructed around 1887 by inhabitants of the town of Chiquimulilla (Solórzano Vega, 2022). It is a branch of the Maria Linda River near the town of Iztapa, with its mouth located slightly east of the town of El Hawaii. Since the river is connected to the sea, it is a tidal river. The river was originally intended, and continues to serve, as a shipping route connecting towns along the Pacific coast, thereby facilitating trade for the local inhabitants.

Catchment area

A catchment area is the region from which surface run-off is collected and drained through a single river system (Agency, n.d.). The catchment area that includes Las Brujas is shown in figure 3.8, delineated by the dark blue line. All rainfall within this boundary is channelled through the rivers and canals represented by the light blue lines. The map was produced using data from the HydroSHEDS database (hydrosheds-2025), which provides detailed hydrographic and catchment information. The delineation was further validated in QGIS using the Strahler Order plugin, which conducts terrain analysis based on elevation data. The catchment area covers two departments of Escuintla and Santa Rosa.

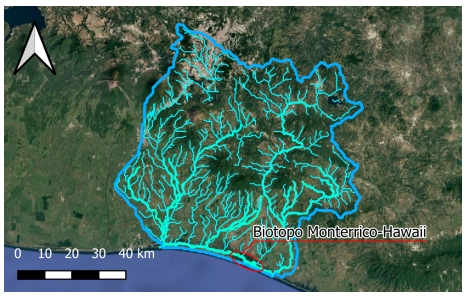

Figure 3.8: Catchment area of the study region (own image)

Tide

The tide at the coast of Monterrico has a tidal range, or water level variation between high and low tide, of 2 m during spring tide and 1 m during neap tide. The tide is mainly semidiurnal, which means that there are two high waters and two low waters during one day (Bosboom & Stive, 2023). Spring tide occurs at full moon and new moon and leads to a temporary increase in tidal range. A neap tide, however, occurs around the first and last quarter phases of the moon, leading to a reduced tidal range. The working of spring and neap tide is depicted in figure 3.9. In figure 3.10, the relative sea level of the tidal gauge near Acajutla, El Salvador, is depicted for September 2025. This station is the station closest to the Monterrico coast with a sea level similar to the level at Monterrico.

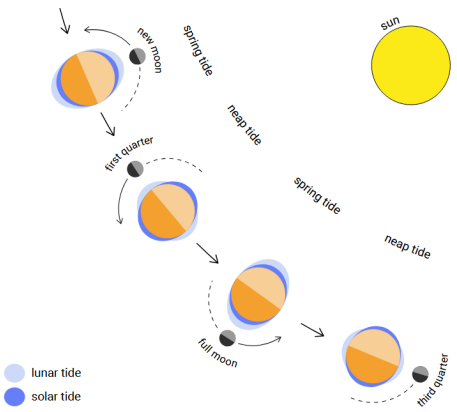

Figure 3.9: Illustration of spring and neap tides, adapted from (Bosboom & Stive, 2023).

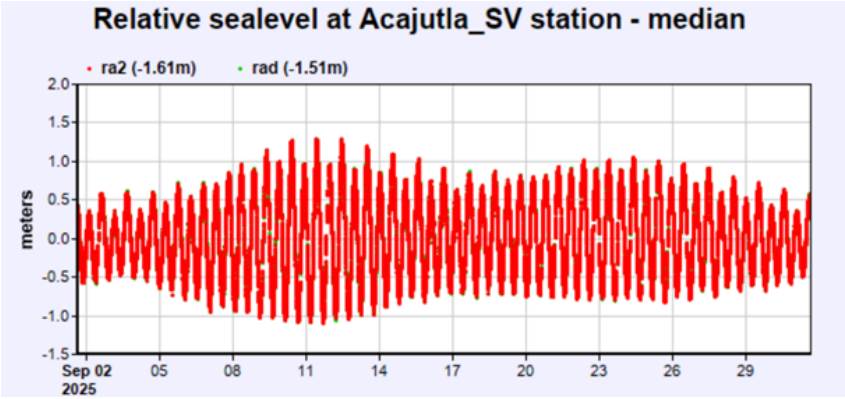

Figure 3.10: Relative sea level for September 2025 at the tidal gauge near Acajutla, El Salvador. The data is similar to the data at the coast of Monterrico (Unesco, 2025).

In figure 3.11, the three tidal inlets are shown, which are present in the circumference of the Biotope of Monterrico. Two are located downstream, and one is located upstream relative to the biotope. The two downstream river mouths near El Hawaii are depicted on the right-hand side of figure 3.11, and the upstream river mouth near Iztapa is shown on the left-hand side. At the river mouths, the influence of the tide is typically the strongest, gradually diminishing further upstream. The tidal inlets are relatively narrow (Deltares, n.d.), and the site of Las Brujas is located about 15 kilometres inland. Due to both its distance from the mouth and the narrow width of the inlet, the tidal range at Las Brujas is expected to be smaller than at the river mouth. Over the past 30 years, the tidal inlets have been periodically closed due to sediment deposition and reopened either during high-precipitation events leading to high fluvial discharge, or the efforts of local fishermen (Myrnamaría Galido, personal communication).

Figure 3.11: Recent satellite picture of the Chiquimulilla canal and Los Enclavos river mouths. The red squares depict tidal inlets (Google Earth, 2025).

Climate and precipitation

Biotopo Monterrico-Hawaii is located on the Pacific Plateau. This is the area between the Pacific coast and the volcanic highlands. Its climate is mostly steered by moist Pacific air, the wet and dry seasons, and orographic uplift along the volcanic chain. This means that warm, moist air is forced to rise over the volcanic chain, and as it rises, it condensates, forming clouds and causing precipitation on the windward side of the mountains (The Editors of Encyclopaedia Britannica, n.d.).

The location, combined with the tropical climate in Guatemala, makes for a strong seasonality difference between the dry season, which lasts from November until April and the wet season, which lasts from May until October. Figure 3.12 shows the mean monthly rainfall taken from datasets between 1981 and 2024 of the Escuintla and Santa Rosa departments (Climate Hazards Center, n.d.), as these are the departments that fall under the catchment area of the Biotopo Monterrico-Hawaii. In figure E.1 of appendix E, it can be observed that these regions follow a similar trajectory throughout the year regarding precipitation. Thus, the mean can be taken for the graphs.

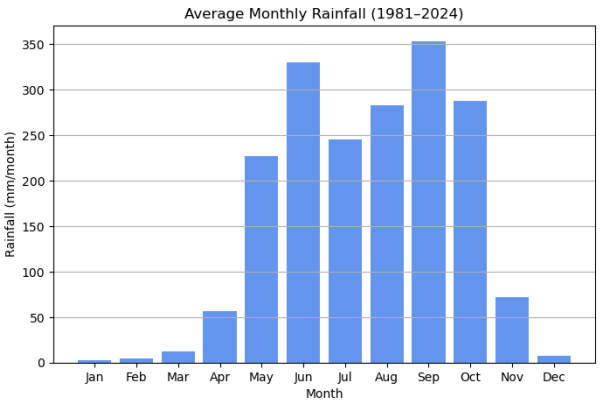

Figure 3.12: Average monthly rainfall (1981 - 2024) (Climate Hazards Center, n.d.) (own image)

In recent decades, Guatemala has begun to experience significant changes in precipitation patterns due to climate change. Multiple sources (e.g (Barban, 2021; Interactive Country Fiches, n.d.) and (Castellanos & Rivera, 2016)) and also people from the area (MyrnaMaría Galindo and Noé Orantes, personal communication) have indicated and said the following:

1. The precipitation amounts are increasing
2. The beginning and end of the wet and dry seasons are much more difficult to predict
3. That the precipitation amounts in the wet season are more extreme and concentrated in shorter times

3.2. History and area formation

During the existence of the biotope, events occurred that changed the morphology. The most significant events are highlighted below. No written records exist of these events; the dates are reconstructed from citizens' recollections (Myrnamaría Galindo, Noé Orantes Olivares and Marco Antonio, personal communication) and Google Earth imagery.

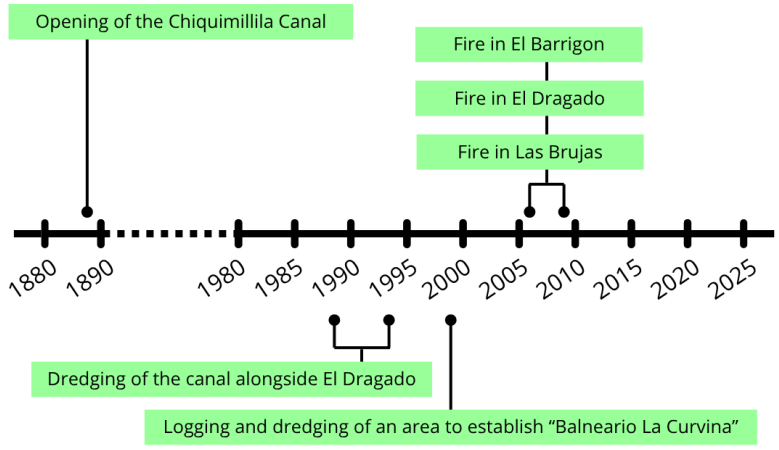

Figure 3.13: Timeline of events (Myrnamaría Galindo, Noé Orantes Olivares and Marco Antonio, personal communication) (own image)

In total, the biotope has experienced a loss of $182400\ m^2$ of mangrove forest, corresponding to 7,636 red mangroves and 12,405 white mangroves in the area (Castillo Cabrera et al., 2012).

Spit and lagoon formation

Over the last centuries, a spit and lagoon system has formed in which a mangrove forest can flourish. A spit is a land tongue extending into the sea (Bosboom & Stive, 2023), see figure 3.14. The coast near Monterrico is wave-dominated, meaning wave action plays a dominating role in the coast shape formation opposed to the role of rivers and tides. Waves at the coast generate a current parallel to the coast, named the longshore current. This current has a transport capacity, meaning it transports the sediment at the coast in the streamwise direction. A spit then develops when, for instance, a river interrupts the coast and thus decreases this longshore transport capacity. In this case, the María Linda river intersects the coast near the town of Iztapa, leading to the formation of a spit extending eastward toward the mouth of the Los Enclavos river. The development of this spit is depicted in a composition of old maps in figure 3.15. The lagoon in this case is the water body enclosed by the formed spit. Over the years, this water body has developed into a

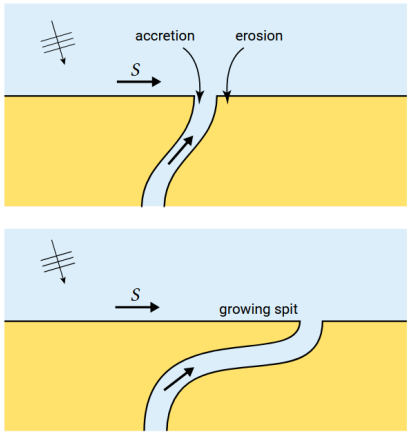

Figure 3.14: Textbook image of a growing spit (Bosboom & Stive, 2023).

mangrove forest, which is its current form.

Figure 3.15: Maps of developing spit at the same location. The maps are from the years 1823, 1837 and 1895, respectively. Lower maps are zoomed in. The yellow star represents a reference point at the mouth of river Maria Linda close to the town of Iztapa (Aubree, 1837; SAPPER, 1895; unknown, 1823).

3.3. Restoration efforts

Before 2025, there have been multiple initiatives to restore the mangrove forest. Most restoration efforts focus on establishing more red mangrove trees, as the success of such initiatives depends on the involvement of local communities, who prefer red mangroves (section 3.1). The biggest and most successful effort so far has been constructing chinampas. A chinampa is a bamboo box filled with soil in which approximately 8 red mangrove propagules are planted, as can be seen in figure 3.16. The soil level inside the box is higher than the water level to prevent the propagules from flooding in the wet season. To keep them from drying out when rain is scarce, local communities water the propagules when needed. In total, 600 chinampas have been placed in the biotope so far. They were constructed by 200 people in total from nearby communities. (Clima, 2023). Local communities are quite invested in this restoration effort and help in the dry season when the chinampas need additional water (Myrnamaría Galindo, personal communication).

Figure 3.16: Chinampa in el barrigon (own image)

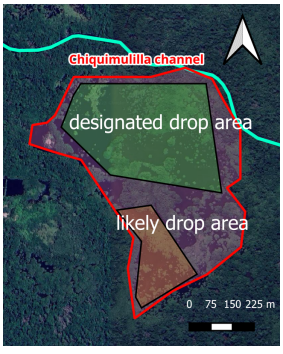

Figure 3.17: Designated vs likely real helicopter drop area (own image)

In other parts of the biotope, the construction of chinampas has facilitated mangrove restoration. In Las Brujas, however, the outcomes have been less successful: of the six chinampas constructed in this area, only one remains intact. Consequently, alternative restoration efforts have been initiated, largely based on the assumption that insufficient flow to Las Brujas limits the natural dispersal of propagules to the site. Therefore, in 2024, a new structure was implemented. Ropes bearing propagules of red mangroves at their ends were fastened to sticks to ensure their proper positioning. Moreover, in January 2025, 10,000 propagules were released from a helicopter (Coromac et al., 2025). At first, it was thought that the helicopter drop was not effective, since no sprouting propagules were spotted at the designated sites. However, during the fieldwork, some southern areas showed a re-

markable amount of juvenile red mangrove plants, as shown in figure 3.17. Many propagules are growing across a wide area, including in the centre of the lagoon. This pattern is unlikely to result from natural regeneration, as natural growth typically occurs in smaller numbers, in less clustered formations, and closer to the forest edge. Additionally, their developmental stage corresponds with the timing of the helicopter drop. Unlike typical conditions, where both white and red mangroves regenerate, only juvenile red mangroves were observed in this area. Therefore, it is plausible that these young individuals originated from the helicopter drop conducted at the beginning of 2025 (Myrnamaría Galindo, personal communication).

Lastly, in May 2025, some natural channels were dredged to stimulate the flow (figure 3.18). The outcome of this effort is still unknown (Myrnamaría Galindo, personal communication).

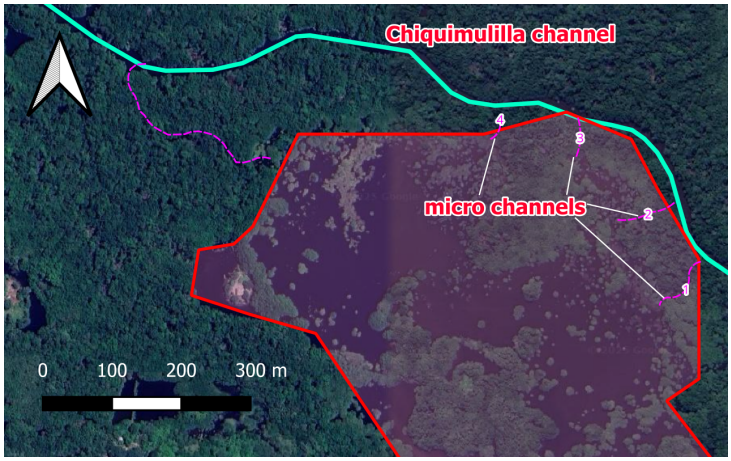

Figure 3.18: micro-channelsy connecting Las Brujas to the Chiquimulilla channel (own image)

3.4. Reference Sites: Selection and Characteristics

To assess the conditions in Las Brujas, two reference sites exhibiting healthy mangrove growth were selected for parameter comparison. One shows merely natural regeneration, the other shows primarily natural regeneration with some external intervention. This subchapter presents its selection and describes the sites' key characteristics. A comparative analysis with Las Brujas is presented in chapter 5.

Selection

Suitable reference sites were identified using *Google Earth*. Historical satellite images from 2006 to 2024 were analysed to locate areas with stable and healthy mangrove recovery. These findings were verified through field visits to potential sites. The two selected reference areas are shown in figure 3.19.

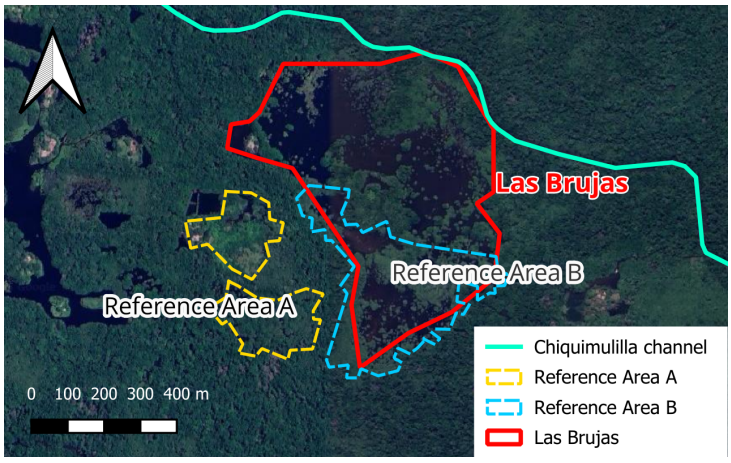

Figure 3.19: Overview of Las Brujas and the two reference areas (own image)

The selected areas both showed fire damage after the fires of 2006 and have shown decent regrowth

afterwards. The selection criteria were the density of the forest, the age of the juvenile mangrove trees and the type of mangroves in the area.

The two selected reference sites each represent different stages of natural mangrove regrowth. Reference Area A (RA-A), located near Las Brujas, exhibits relatively rapid recovery after the fire damage (Google Earth, 2025). The regeneration timeline is shown in figure 3.20.

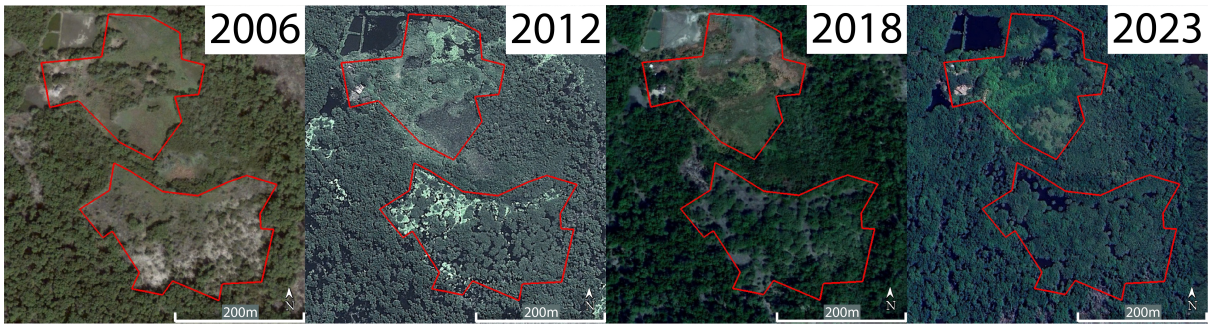

Figure 3.20: Reference Area A throughout the years (Google Earth, 2025)

The second site, Reference Area B (RA-B), is a southern subarea of Las Brujas. Its regeneration timeline is shown in figure 3.21. While RA-A exhibited nearly complete regeneration (approximately 100 %), RA-B showed approximately 60 % recovery. In appendix B an overview of the regrown areas in Reference Area B is shown.

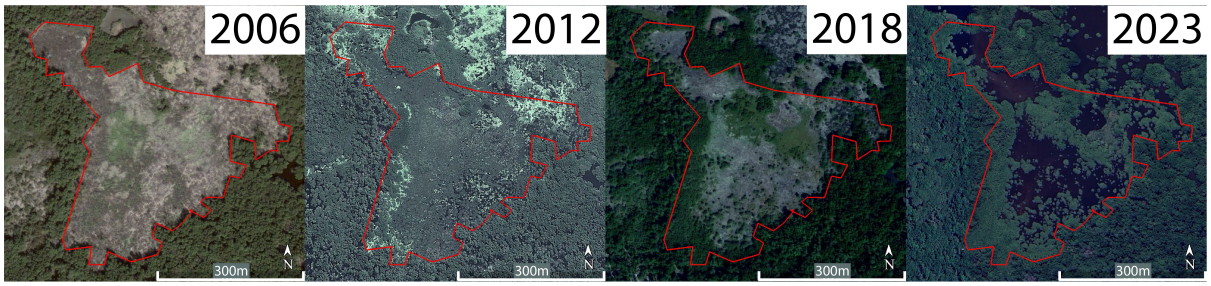

Figure 3.21: Reference Area B throughout the years (Google Earth, 2025)

Characteristics

Reference Area A

RA-A is characterised by a relatively dense mangrove forest dominated by red mangroves, with white mangroves present in smaller numbers. As shown in figure 3.20, natural regrowth in RA-A progressed rapidly, with substantial canopy closure already visible by 2012. Currently, the area exhibits a dense forest structure with mature red mangrove trees that appear healthy and produce abundant propagules, indicating ongoing natural regeneration (figure 3.22).

(a) Mature red mangrove trees in RA-A (own image)

(b) Natural regeneration occurring in RA-A (own image)

Figure 3.22: Different stages of regrowth visible in Reference Area A

Reference Area B

RA-B exhibits substantially less regrowth than RA-A. The area contains larger open patches and a more heterogeneous composition of red and white mangroves, as shown in figure 3.23. Most regeneration appears to have initiated along the outer margins of Las Brujas and gradually expanded inward. The reforested edge zones are dominated by red mangroves. Red mangrove saplings, likely originating from the helicopter propagule release (Myrnamaría Galindo, personal communication) (section 3.3), are dispersed across the open areas, with heights ranging from 70 to 110 cm in October 2025.

(a) Areal image of RA-B, showing open patches in the area (own image)

(b) High concentration of red mangrove saplings, likely originating from the helicopter drop (own image)

Figure 3.23: Different perspectives of Reference Area B

4

Methodology

This chapter outlines the research methodology. The first section presents the overall structure of the fieldwork approach, organised around five main pillars. Subsequent sections detail the objectives and data collection methods for each pillar, followed by a description of the fieldwork locations, the equipment employed, and the limitations identified before entering the field.

Subdivision of method

The main objective of the fieldwork was to identify the key factors contributing to the current ecological and hydrological problems of Las Brujas and its surroundings. Apart from the history and characteristics, as described in chapter 3, additional aspects play a vital role in the development of Biotopo Monterrico-Hawaii and require further examination. These aspects were grouped into the following main pillars:

1. **Precipitation patterns**
2. **Tidal influence**
3. **Flow**
4. **Ground level deformation**
5. **Physical-chemical parameters**

The next sections further elaborate on these main topics. Fieldwork that was performed that can be seen as additional to the main research can be found in appendix C. These methods include interviews, a bathymetry analysis with the *Chirp Sonar* and flow measurements with the *Geopacks Advanced Flow Meter*. The interview questions can be found in appendix D.

4.1. Precipitation patterns

Objectives

This pillar aims to identify how the precipitation patterns in the catchment area have influenced the water regime in the past and how they might affect the water regime in the future. The catchment area is depicted in figure 3.8 of section 3.1.

Methods

Precipitation data sets obtained from the Climate Hazards Center (Climate Hazards Center, n.d.) were analysed alongside the observations made by climatologists from various online sources (e.g. (Barban, 2021; Interactive Country Fiches, n.d.), and (Castellanos & Rivera, 2016)), as well as insights shared by local residents (Myrnamaría Galindo and Noé Orantes Olivares, personal communication). As explained in section 3.1, the precipitation datasets were scaled down to the two departments of Escuintla and Santa Rosa; the mean of both regions was taken into account for the observations. By plotting several figures and adding a trend through the data, the possible directions of change over time, and the possible long-term behaviour of precipitation patterns could be observed. These observations were related to a statistical analysis to see whether the conclusions were supported by the data and the trends available. The following statistical models were used:

1. Mann-Kendall: Checks whether there is a monotonic trend in a time series without assuming any particular shape or distribution of the data. It is determined by a P-value. If the $P<0.05$, the trend is statistically significant and if the $P>0.05$, there is no significant trend.
2. Sen's Slope: calculate the median rate of change per year for a trend based on the Mann-Kendall method
3. Ordinary Least Squares (OLS) linear regression: Fits a straight line through the data to estimate the trend direction. There are three output parameters: slope (how much the variable changes per year), the P-value (as explained above) and the R^2 (How much of the variability in the data is explained by the trend. 0 = none and 1 = perfect)

The code used to process the raw precipitation data can be found in appendix E.

4.2. Tidal influences

Objectives

The objective of this pillar is to assess the influence of tidal dynamics on the Las Brujas area, specifically examining whether tidal fluctuations affect surface water levels.

Methods

To map the tidal variations, a time-lapse recording of a full tidal cycle in the Las Brujas area was created. A measuring stick, marked at 10 cm intervals, was inserted into the ground within a micro-channel. Additional finer markings were added near the current water level to enhance measurement accuracy. A *GoPro* camera was positioned to capture the stick markings clearly and was programmed to take one photograph per minute over a 6-hour tidal cycle. Because the *GoPro* battery was insufficient for the duration of the recording, it was connected to an external power bank, secured in a waterproof phone case, and sealed with zip-lock bags and duct tape. The resulting images were compiled into a time-lapse video using the software *CapCut*, allowing visual determination of water level fluctuations throughout the tidal cycle.

To isolate the influence of tides, no rainfall was needed to occur during the experiment. Therefore, measurements were conducted during the day, when the likelihood of rain in the catchment area is lowest. Before the experiment, weather forecasts were reviewed to ensure dry conditions, and tidal data were consulted. The experiment was scheduled during the spring tide, when tidal influence is strongest, to maximise the observable effects of tidal variation. The experiment was conducted twice, once in micro-channel 1 and once in micro-channel 3 (see figure 3.18). These locations were selected because they are the main entrances for water transport in Las Brujas. The remaining micro-channels were obstructed by tall grasses and other invasive plants, which hindered water flow and access. The equipment used to measure tidal influence and its setup are shown in figure 4.1.

(a) GoPro 9 Black (own image)

(b) Measuring stick marked at 10 cm intervals (own image)

(c) Research setup up close (own image)

Figure 4.1: Equipment and setup used in the field research

4.3. Flow

Objectives

This pillar aims to gain information on the effect of the flow on transport processes within the biotope. The first step involves determining whether flow occurs and quantifying its magnitude, followed by assessing its direction and potential influence on the Las Brujas area.

Methods

Flow dynamics in Las Brujas were assessed at channels 2 and 4 (figure 3.18), which were selected for their relevance in quantifying water fluxes into and out of the area, as well as their accessibility during the measurements. To determine flow, velocity was estimated by measuring the time required for a floating object, such as a leaf, to travel a known distance. Flow velocity was then calculated by dividing this distance by the elapsed time. To improve reliability, the experiment was repeated three times at each measuring point, and the mean value was used. This method provided flow measurements only at the water surface.

4.4. Ground level deformation

Objectives

This pillar aims to identify ground level deformation within and around the Las Brujas area. It focuses on quantifying sediment flux and assessing the presence of sediment in the catchment area. Furthermore, it seeks to determine whether ground levels change over time and how these changes vary spatially.

Methods

Two techniques were used to quantify bottom height changes:

1. The first method entailed taking water samples and quantifying how much sediment was present in the samples. To improve reliability, two samples were taken at each sampling location.

   The sampling points in Las Brujas were selected based on the observed flow patterns and flow directions in the area. The sampling points are showcased in figure 4.2. The samples upstream were collected in the Canal de Chiquimulilla, between the towns of Papaturro and Madre Viedja, approximately 8 kilometres upstream from Biotopo Monterrico-Hawaii. The measuring points were chosen for their accessibility and position at river junctions, to capture differences between converging flows. These sampling points are portrayed in figure 4.3.

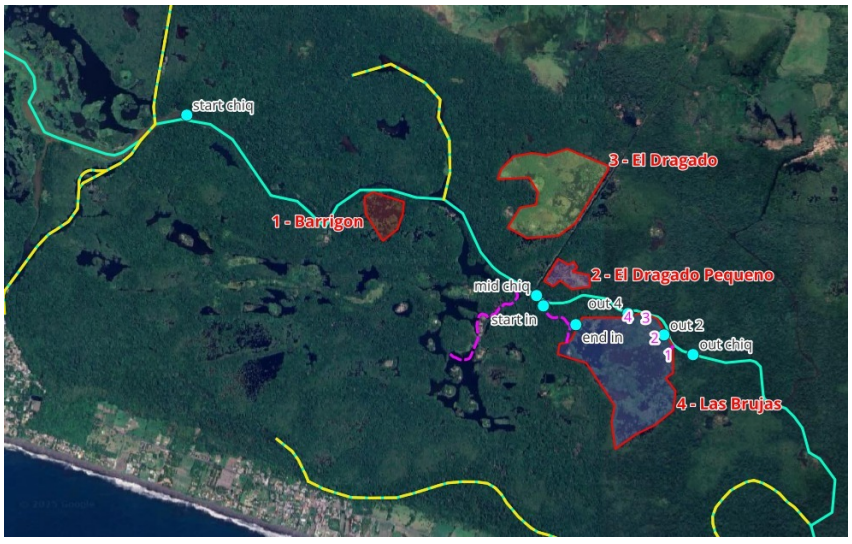

Figure 4.2: Las Brujas sampling points (experiment 1) (own image)

(a) Upstream area sampling location (experiment 2) (own image)

(b) Upstream area sample points (experiment 2) (own image)

Figure 4.3: (a) Las Brujas and (b) Upstream area measuring points of the sediment experiments, depicted in red.

Water samples were collected at the centre of the channel at a depth of approximately 10 cm, with the bottle oriented in the direction of the current so that water flowed directly into it. Each sampling bottle had a volume of 0.6 L and was labelled with its location using sports tape and a marker. After collection, the bottles were sealed tightly and stored in a cool, dark place for 12 hours. The following day, the samples were filtered using *Melitta* brand coffee filters to capture suspended sediment. The filters were placed on a labelled board and left to dry in the sun. Visual observations of the samples were recorded in a notebook. To protect the filters from rainfall, they were placed outside in the sun and taken indoors during rainfall, while spoons were used to prevent the wind from blowing them away. The drying setup is illustrated in figure 4.4b.

After three days of drying, the filters were weighed using a *WEIGHTMAN Premium Milligram Scale*. The amount of sediment was determined by calculating the difference between the mean weight of the clean filter and that of the dried filter containing sediment. To confirm complete drying and eliminate the influence of residual moisture, the filters were weighed again after eight days. Each weighing was repeated three times, and the mean value was recorded. Two control samples were included, consisting of filtered tap water only, to evaluate any potential influence of the water on filter weight.

The first sediment experiment was conducted in the Las Brujas area. Insights gained from this experiment were applied to improve the procedure for the second experiment, carried out in the upstream area. During the second experiment, only the operator remained in the room while weighing to minimise vibrations and noise, as the *WEIGHTMAN scale* proved extremely sensitive to disturbances. Additionally, although *Melitta* filters were chosen for their uniform weight, stated by the manufacturer as 1.500 g, this could not be verified before the first experiment due to the unavailability of the scale. Subsequent analysis revealed greater weight deviations than expected, suggesting that filter mass variability influenced the results. Therefore, in the second experiment, all filters were pre-weighed and their weights recorded both before and after filtration. Finally, the control samples were modified: instead of using tap water, which had produced noticeably different results, filtered mangrove water was used to ensure better comparability with the study conditions.

(a) Filtering the sediment out of the samples (own image)

(b) Set-up of filters drying (own image)

(c) Weighing the filters (own image)

Figure 4.4: Sediment experiment steps: (a) filtering the samples, (b) drying the filters, and (c) weighing the dried filters.

2. The second method used satellite data over time to quantify bottom-level differences. Data from the ASF Data search vertex was used ("ASF data search," n.d.). This is public data, collected by satellites from NASA. This data typically covers areas of 250 by 170 kilometres. A frame was chosen where the area of interest (Las Brujas) is centred. From this tile, the Sentinel-1 radar data were downloaded from the last 5 years. Due to laptop storage limitations, it was not possible to take a longer period of time into account. The data set runs from the first of January 2020 to the 15th of October 2025. Only ascending data, running from south to north, was considered. This choice was also made to limit storage.

   The data was downloaded using Small Baseline Subset (SBAS). This subset makes links between different radar images figure 4.5a. Next, *interferograms* were created using a process called Synthetic Aperture Radar Interferometry (InSAR). An interferogram is a radar-derived image that represents phase differences between two satellite acquisitions. These phase variations correspond to minute ground displacements, enabling the detection and measurement of surface deformation with centimetre-level accuracy. An example of an interferogram is shown in figure 4.5b. Each interferogram came with a number of files that could be used in deformation monitoring and time-series analysis. In this research, the line-of-sight (LOS) displacement files were used, which give the displacement of the ground between two radar passes. This was used to find the average LOS deformation velocity, by dividing the total displacement by time, and to create a time series. Data processing has been done with the help of notebooks obtained from *Github* (Jlmaurer, n.d.).

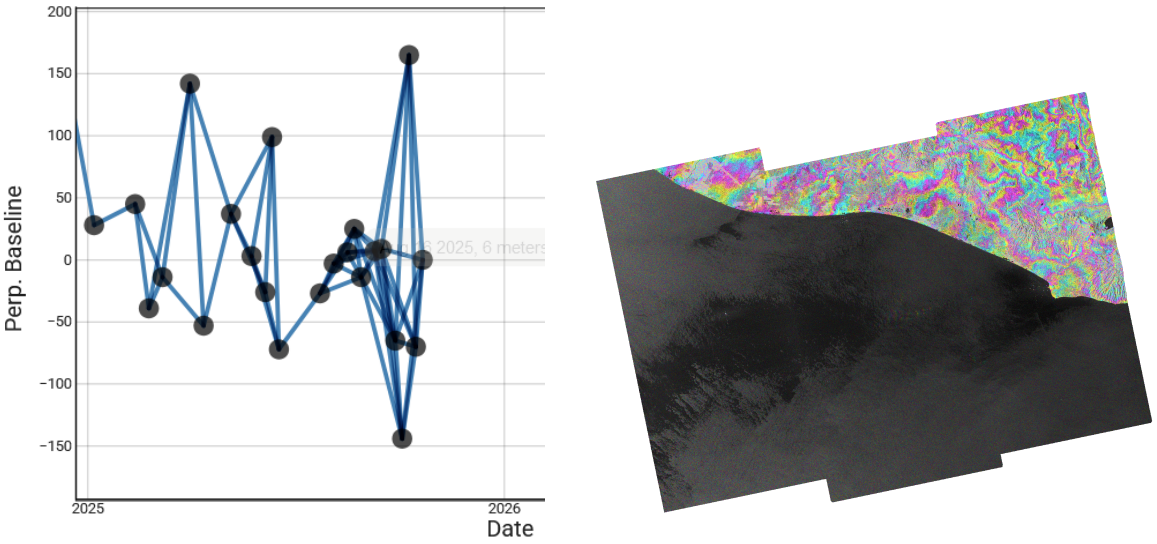

(a) SBAS data example

(b) Example of an interferogram, derived from ASF data

Figure 4.5: Comparison between SBAS time-series data (a) and an example interferogram (b) derived from ASF Sentinel-1 processing (“ASF data search,” n.d.)

4.5. Physical-chemical parameters

Objectives

This pillar focuses on the physical-chemical conditions mentioned in section 2.2. The goal of the pillar is to assess whether the physical-chemical conditions in Las Brujas comply with those of a healthy mangrove forest.

Methods

To assess the physical-chemical values in and around Las Brujas, sampling locations were selected where salinity, pH, temperature and redox potential were measured. These sampling locations are shown in figure 4.6 and figure 4.7. The locations were chosen such that each reference location (see section 3.4) contains measurement points. In the Las Brujas site, measurements were performed twice to improve the robustness of the results. After measuring, the physical-chemical values of the different reference sites were compared. Measurements were taken of superficial water, the water present at the surface.

Besides the samples in Las Brujas, 7 samples in the upstream river, about 8 kilometres upstream of the Las Brujas area, were taken. These sample locations are the same as where the sediment samples upstream were taken figure 4.3. The sampling in the upstream area had two goals. Firstly, to check the influence and intrusion of the tide in the area. Secondly, to check if the presence of shrimp farms and other types of farms upstream influenced the physical-chemical parameters.

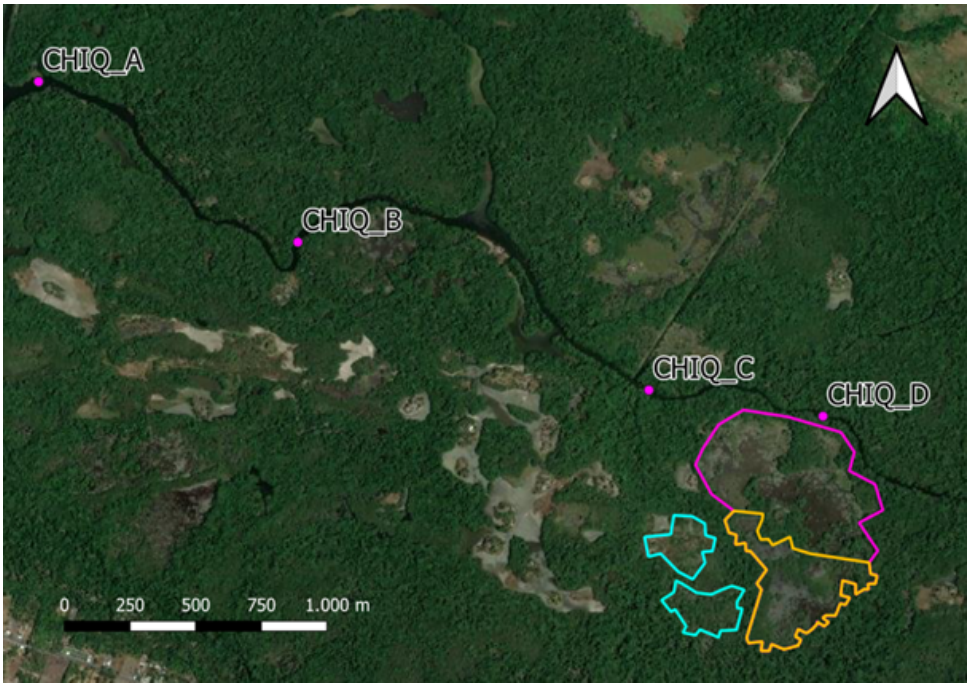

Figure 4.6: Chiquimulilla multimeter sampling points (own image)

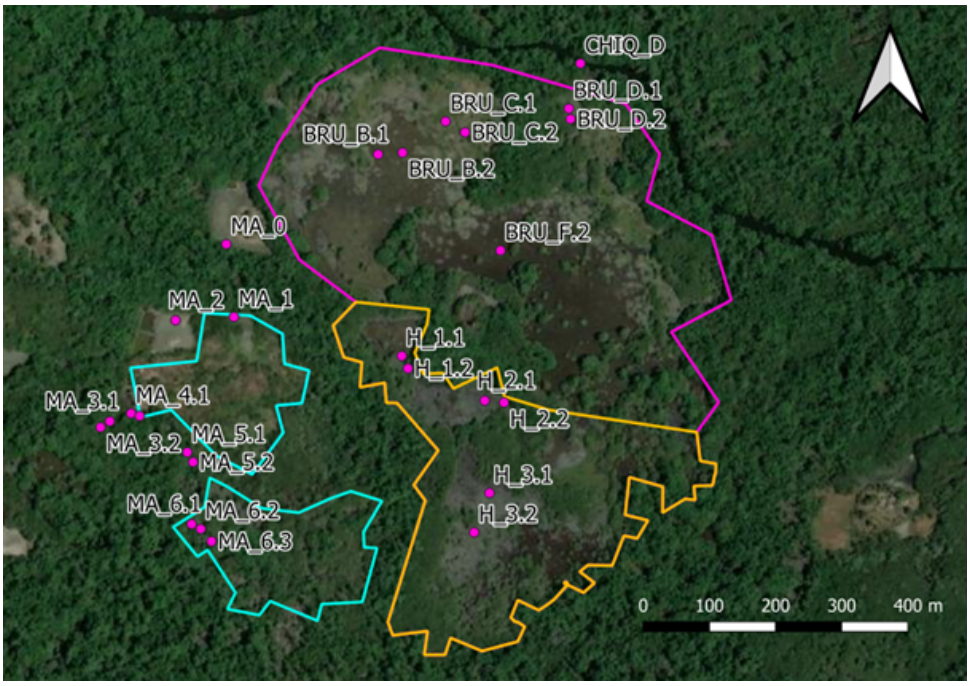

Figure 4.7: Las Brujas multimeter sampling points. Here, *BRU* points are located in the main Las Brujas area, inside the pink lines. *H* points are located in the Helicopter area, which corresponds to Reference area B, in the yellow lines. *MA* points are located in the area where Marco Antonio (interviewee) lives, corresponding to Reference area A, within the blue lines (own image).

To measure physical-chemical parameters, a *HI98194 Multi-Parameter Meter* (HANNA Instruments) was used (see figure 4.8). At each sampling point, the instrument's sampling cup was first rinsed with site water, then refilled and measured immediately. Samples were taken about ten centimetres below the water's surface. Measurements were considered complete once the pH reading stabilised (Myrnamaría Galindo, personal communication).

(a) HI98194 Multi-parameter from HANNA Instruments (HANNA Instruments Guatemala, 2025)

(b) Interface of the multi-parameter probe (own image)

Figure 4.8: Multi-parameter probe and its interface

After each measurement, a photograph of the instrument display was taken and labelled accordingly. After every 70 measurements, the multi-parameter probe was recalibrated, and at the end of each day, the pH meter was neutralised.

5

Results

5.1. Precipitation patterns

In this paragraph, the results of the data analysis of the precipitation data, as explained in section 3.1, are presented.

Total annual precipitation

As explained in section 3.1, between the late 1900s and the early 2000s, the mean annual precipitation has increased according to multiple sources and local residents. By plotting the total annual data throughout the years in figure 5.1, it can be observed when looking at the trend line that, for this catchment area, the change of the total mean annual precipitation has increased by almost 200 millimetres between 1981 and 2024.

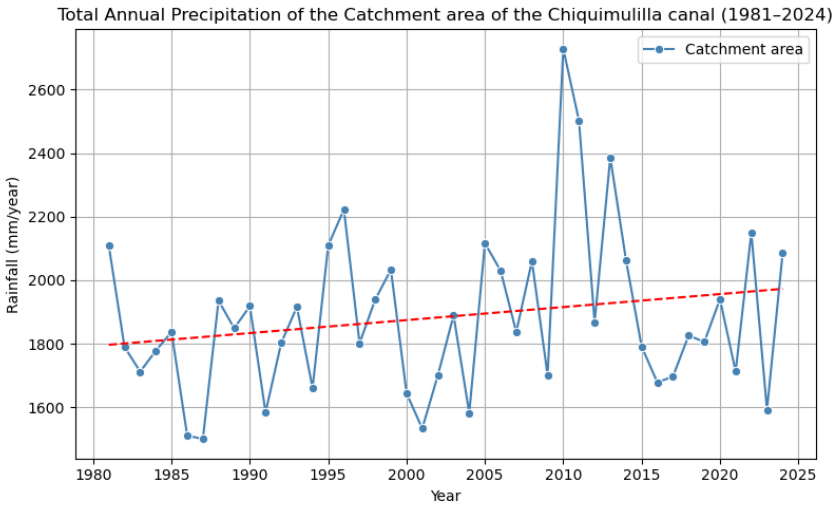

Figure 5.1: Total annual precipitation of the catchment area of the Biotopo Monterrico-Hawaii (Climate Hazards Center, n.d.) (own image)

From a statistical perspective, the Mann-Kendall trend test on the total annual precipitation shows no significant long-term trend over the period sketched with a P-value of 0.24. The Sen's slope estimate suggests a small positive change of about 3 millimetres per year, but this increase is not statistically significant. Similarly, the linear regression analysis indicates a weak upward slope of approximately 4.1 millimetres per year (P-value $= 0.19$ and $R^2 = 0.04$). Although the visual trend in figure 5.1 shows an apparent increase of around 200 millimetres between the observed time period. These statistical results imply that this rise is within the range of the natural variability rather than evidence of a long-term shift.

Changes in monthly precipitation

As explained in section 3.1, several sources have indicated that the global climate change has had, and will have an impact on the seasonal distribution in Guatemala and mainly the total monthly precipitation. It can be seen whether certain months became drier or wetter compared to a few decades ago. This is illustrated in figure 5.2.

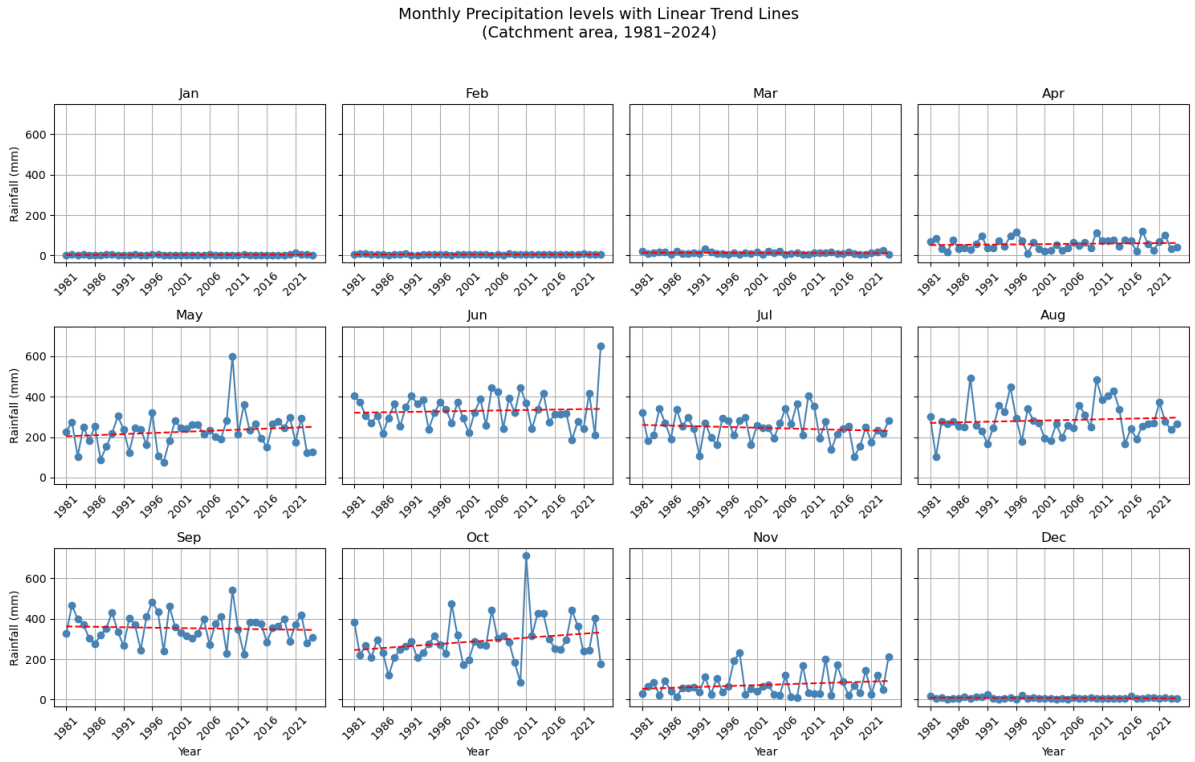

Figure 5.2: Monthly Precipitation levels with linear trend lines of the Catchment area (1981 - 2024) (Climate Hazards Center, n.d.) (own image)

As can be seen throughout the years, on average, May, June, August, October and November have become wetter, and July and September have, on average, become drier. As explained in section 3.1, the months December, January, February, March and April are part of the dry season, which makes it difficult to say whether there are any differences, as the amount of precipitation is already minimal. When looking at the decadal comparison, a similar observation can be made.

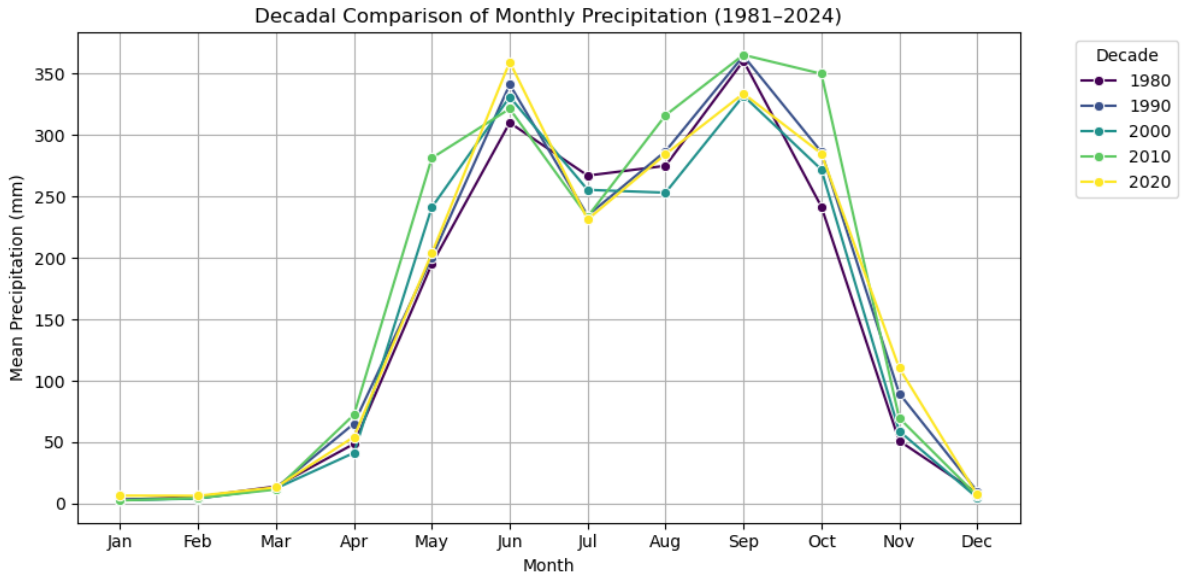

Figure 5.3: Decadal comparison of Monthly Precipitation (1981 - 2024) (Climate Hazards Center, n.d.) (own image)

Figure 5.3 shows the average monthly precipitation per decade. The darker blue curves indicate the decades of the late 1900s, and the lighter yellow curves indicate the early decades of the 2000s. It can be seen that the lighter curves are below the darker curves in July and September, indicating less precipitation. Figure 5.3 also indicates that the other months have become wetter as the lighter curves are above the darker curves, where the biggest differences can be seen in May, October and November.

When analysing the monthly precipitation patterns statistically, none of the individual months show a significant monotonic trend over the sketched time period according to the Mann-Kendall test, as all the P-values are above 0.05. However, the Sen's slope estimates indicate weak positive tendencies in May, June, August, October and November, consistent with the visual increase in those months and indicate weak negative slopes in July and September. These changes, however, are small in magnitude, typically less than 2 millimetres per year, suggesting that apparent differences are subtle rather than representing a strong pattern. The decadal comparison further supports this pattern: the 1980s and 1990s show slightly lower rainfall at the start and end of the rainy season and somewhat higher values in the middle, while the 2000s and 2010s exhibit a modest extension of rainfall into May and October. Overall, statistical tests confirm that the seasonal distribution has remained largely stable, with only minor shifts in the timing and intensity of rainfall peaks. Short-term deviations in precipitation can, however, be influenced by external climatic factors such as hurricanes, and the El Niño and La Niña phenomena, which periodically affect rainfall intensity and timing in the region.

Shifts in the rainy season

As explained in section 3.1, the traditional rainy season lasts between May and October. However, both online sources and the locals have indicated that this has changed throughout the last decades. Precipitation is less but more intense when it falls, but it also appears more often outside of the rainy season. When checking this with the data obtained, figure 5.4 can be illustrated.

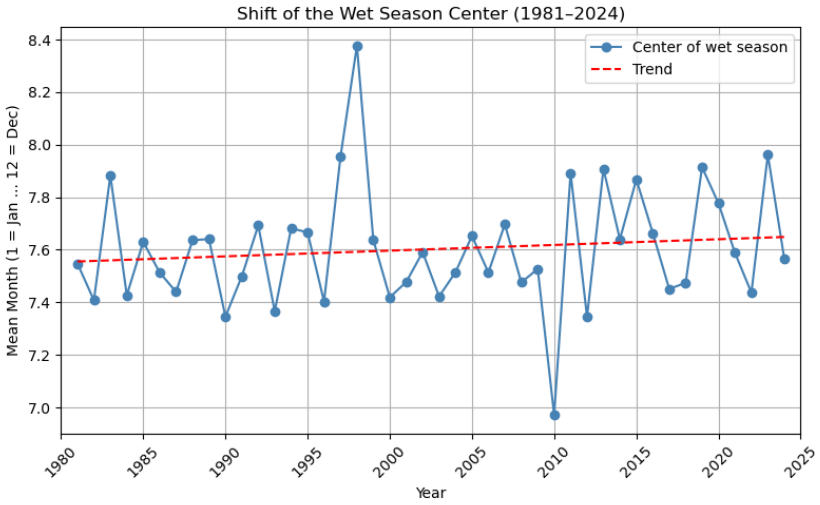

Figure 5.4: Shift of the rainy season (1981 - 2024) (Climate Hazards Center, n.d.) (own image)

Figure 5.4 shows the centre of the wet season throughout the years. On the vertical axis, the number of the month is depicted at the centre of the wet season. Every year since the measurements have started, the centre of the rainy season has been in July. There has only been one recording of the centre in August. When following the trend line, it does seem as if the centre is moving towards a later time in the year, albeit it being a relatively small change. This can also be satisfied when looking back at figure 5.3 as the months October and November show bigger differences in the current decades compared to the earlier, where currently, more precipitation is measured later in the year. Another takeaway from figure 5.3 and figure E.3 shown in appendix E is that more precipitation occurs outside of the wet season, as May and November have become wetter in recent years.

From a statistical standpoint, the Man-Kendall trend test on the centre of the wet season shows no significant long-term shift between the sketched time-frame, as the P-value is 0.23. The Sen's slope estimate of +0.003 months per year corresponds to a shift of less than one day per decade, indicating that the centre of the wet season has remained stable over the past decades. The mean centroid month remains close to 7.6, corresponding to mid-July, and a comparison between the earlier and later periods shows nearly identical averages (7.61 and 7.60, respectively). These results suggest that while October and November have become slightly wetter, the central timing of the rainy season itself has not shifted in a statistically meaningful way.

When looking at these results and relating them to mangrove growth, more precipitation occurs outside of the rainy season, and the period suitable for mangrove seedling establishment is delayed. As explained in section 2.1, propagules can float up for 15 days before dying or finding a suitable location to anchor. Persistently high and prolonged water levels can prevent them from settling in time, causing many seedlings to drown before they can establish.

5.2. Tidal influences

In this paragraph, the results of the tidal experiment (see section 4.2) are presented. In total, the tidal experiment was repeated twice. Once in micro-channel 1 and once in micro-channel 3 (see figure 3.18).

In figure 5.5, 5 pictures with an interval of 1.5 hours are shown of the first experiment in micro-channel 1. The experiment took place on the 6th of October during a spring tide with a tidal coefficient of 110. In appendix F, the monthly tidal cycle for October and the corresponding daily tidal coefficients are portrayed. In the time lapse, it can be seen that from minute 356, it started raining, so the cycle was not yet complete. However, these 4 minutes do not change the fact that there is no visible water level change in the 356 minutes that were correctly recorded. It is possible that a slight change did occur that is not visible in the time-lapse footage, but such a small variation would be insignificant to be considered as tidal influence. However, some flow was visible by leaves floating and a visible change in the direction of the horsetail grass that floated by during the time lapse.

Figure 5.5: Time lapse sequence channel 1 showing water level variation from 0 to 360 minutes (own image)

The second experiment took place on the 8th of October during a spring tide with a tidal coefficient of 104; more information is displayed in appendix F. In figure 5.6, 5 pictures with an interval of 1.5 hours are shown of the second experiment in micro-channel 3. The setup was positioned closer to the water than in the first experiment, as only minimal tidal effects were anticipated. This allowed the camera to be placed closer to the surface, enabling more accurate detection of small fluctuations. The camera fell down after 82 minutes, dangling on its cord to the power bank. However, the water remained in sight, and dark water lines on a tree nearby could be used as a reference level.

Likewise, as in experiment 1, no significant water level change because of tidal influence could be detected. Moreover, as in the first experiment, leaves and other floating materials did drift past.

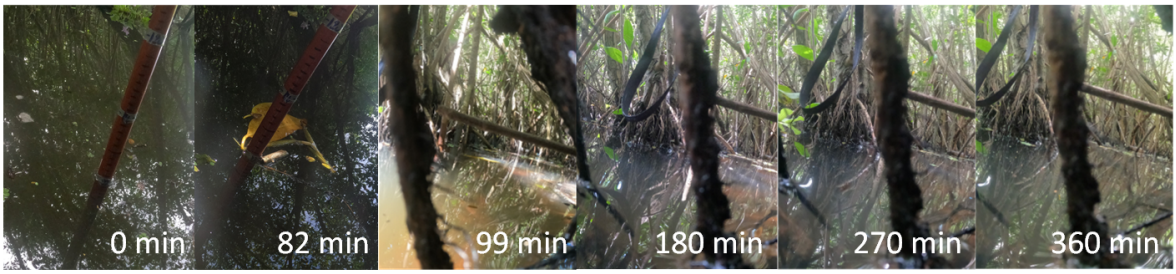

Figure 5.6: Time lapse sequence channel 3 showing water level variation from 0 to 360 minutes. (own image)

Inhabitants and experts were interviewed and asked whether tidal influence is visible in the area. Two of the interviewees have explained that they do see tide daily: Noé Orantes Olivares and Marco Antonio. Noé Orantes Olivares explained early on during the research that the tidal range is 5 centimetres each day and is in anti-phase in Las Brujas compared to the coast. However, we could not confirm either of these claims during our experiment. Marco Antonio stated that there is a daily tidal difference of 0.5 meters. Although his local knowledge provides useful insight into seasonal water-level variations, he was most likely confused with water fluctuations as a result of rainfall instead of tidal fluctuations.

5.3. Flow

Water flow plays a crucial role in transport processes within Las Brujas, including the movement of sediment, nutrients, and propagules. As discussed in section 5.2, tidal effects in the study area during the wet season were found to be negligible. This excludes the possibility of a tidal-driven flow within the wet season. However, field observations and stakeholder interviews revealed noticeable water movement. Possible flow drivers include wind, river discharge, and river gradient (Pérez-Ceballos et al., 2020). Given the minimal river gradient, it is most likely that flow during the wet season is primarily driven by wind and/or fluvial discharge. Furthermore, to enable flow in the mangrove forest, it must not be obstructed in its path.

The mean flow velocities at each measurement point are presented in table 5.1 and table 5.2.

Location	Flow velocity [m/s]	Distance to previous m.p. [m]
1	0.06	-
2	<0.03	5
3	0.06	10
4	0.12	10
5	0.09	10
6	0.15	10

Table 5.1: Flow velocity per measuring point (m.p.) in micro-channel 2

Location	Flow velocity [m/s]	Distance to previous m.p. [m]
1	0.04	-
2	0.06	5
3	0.09	5
4	0.12	5
5	0.12	5
6	0.10	5

Table 5.2: Flow velocity per measuring point in micro-channel 4

River discharge

A potential driver of flow is river discharge. However, discharge data for the Chiquimulilla Canal are not readily available, and time constraints did not allow for field measurements. Due to high amounts of precipitation in the wet season, it is plausible that river discharge makes a significant contribution to the observed flow.

Wind

Local actors emphasised the strong influence of wind on the area's hydrodynamics (Noé Orantes Olivares, personal communication), which was visually confirmed as the water consistently flowed in the direction of the prevailing wind. As flow velocity decreases due to other drivers, the relative influence of wind on surface water movement increases (Roh & Choi, 2023). The maximum flow measured equals 0.15 m/s as illustrated in table 5.1 and table 5.2. Common values for flow velocity of calm rivers equal 0.2 to 0.5 m/s (Fain, 2025), supporting the observed effect.

The wind rose for Monterrico (section 5.3) shows the annual distribution of wind directions based on 30 years of hourly model simulations ("Simulated historical climate and weather data for Monterrico - meteoblue," n.d.). Dominant winds come from the NNE, WSW, and SW, suggesting that surface flow generally follows these directions.

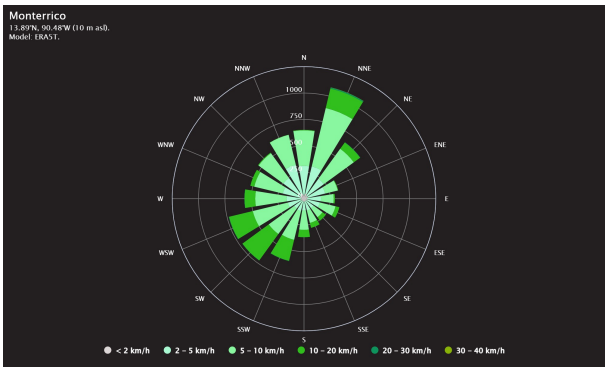

Figure 5.7: Wind rose of Monterrico ("Simulated historical climate and weather data for Monterrico - meteoblue," n.d.)

Obstruction of channel

The final driver influencing flow is the degree of channel obstruction. As discussed in section 3.1, invasive plant species block the channel, hindering water movement and seedling transport. Propagules often become trapped, which restricts their dispersal and subsequent growth. The presence of ninfas has increased in recent years, likely not due to accelerated growth but to reduced removal efforts (Myrnamaría Galindo, personal communication).

Micro-channels

section 3.3 states that natural micro-channels were dug as an attempt to restore natural flow. Since this has been done recently, the effect is still unknown. However, in the interview with Marco Antonio, he stated that the area behind his house, also referred to as reference area A, has a lot of micro-channels that induce flow within this area. This area has shown strong mangrove regrowth in recent years, suggesting that the presence of micro-channels effectively enhances the favourable flow conditions for regeneration.

5.4. Ground level deformation

Both sediment transport and ground level deformation affect surface elevation, which in turn influences water depth. Prolonged water levels above mangrove seedlings can lead to their submersion and eventual mortality. The next subchapters focus on these ground level changes.

First experiment: Las Brujas area

The first sediment experiment consisted of an analysis of the water samples near and in the area of Las Brujas. The method used can be seen section 4.4. The filters were weighed after 3 and 8 days and showed a lower weight after 8 days. This indicates continued moisture loss beyond the initial drying period. Therefore, the weights recorded after 8 days were used in the final analysis. The results of the first experiment are shown in table 5.3. The raw data of this experiment and additional measurements can be found in appendix G.

Location	Mean weight filter+sediment	Unit	Remarks
1.1	1.475	g	Cloudy water
1.2	1.488	g	Cloudy water
2.1	1.478	g	Much visible sediment
2.2	1.476	g	Filter broke during experiment
3.1	1.473	g	No remarks during experiment
3.2	1.462	g	Filter broke during experiment
4.1	1.478	g	No remarks during experiment
4.2	1.482	g	No remarks during experiment
5.1	1.471	g	Much visible sediment
5.2	1.468	g	Much visible sediment
6.1	1.461	g	Much visible sediment
6.2	1.463	g	Some visible sediment
7.1	1.483	g	No remarks during experiment
7.2	1.476	g	No remarks during experiment
C1	1.480	g	No remarks during experiment
C2	1.481	g	No remarks during experiment

Table 5.3: Mean values of samples experiment 1 after 8 days

The recorded weights differed more than the sediments were expected to differ. It was expected that the filters were not uniformly weighted, as was assumed initially. Therefore, 10 empty filters were weighed to analyse the difference between individual filters. The results are illustrated in appendix G.

The filters did vary in weight more than anticipated. This factor was not considered before the start of the experiment and made it difficult to isolate the weight of the sediment using this data alone. This means that quantification of the sediment is not possible. However, qualitative observations were made regarding the samples, their locations, and the visible sediment residues remaining in the filters. In section 5.4, all remarks made during the experiment are noted. The comment ”No remark during experiment” means that no extraordinary things were noticed during the experiment, but it does not mean that there was no sediment present in the samples.

Location 1 showed very cloudy, sediment-filled water during sample collection. Additionally, in samples 2.1, 5.1, 5.2, and 6.1, a noticeable amount of sediment in the filter was visible after filtration. This means that it can be qualitatively concluded that sediment is present in the Las Brujas area, but this could, however, not be quantified.

Second experiment: Upstream area

The second experiment was conducted with sediment samples taken from the upstream area between the towns of Papaturro and Madre Vieja, see figure 4.3. Some lessons were learned from the first experiment, and the method of experiment 2 was slightly adapted compared to the first experiment (see section 4.4). Therefore, before the second experiment, all filters were weighted before they were used to filter. This provides the following results, visible in table 5.4.

Sample	Weight filter	Weight filter+sediment	Difference	Unit	Remark
1.1	1.500	1.500	0.000	g	Much visible sediment in filter
1.2	1.480	1.477	-0.003	g	Much visible sediment in filter
2.1	1.495	1.493	-0.002	g	No remarks during experiment
2.2	1.481	1.475	-0.006	g	No remarks during experiment
3.1	1.492	1.482	-0.010	g	No remarks during experiment
3.2	1.513	1.508	-0.007	g	Much visible sediment in filter
4.1	1.480	1.476	-0.004	g	No remarks during experiment
4.2	1.471	1.461	-0.010	g	No remarks during experiment
5.1	1.505	1.487	-0.018	g	Some visible sediment in filter
5.2	1.525	1.510	-0.015	g	No remarks during experiment
6.1	1.507	1.497	-0.010	g	No remarks during experiment
6.2	1.481	1.470	-0.011	g	Some visible sediment in filter
7.1	1.499	1.484	-0.015	g	No remarks during experiment
7.2	1.508	1.496	-0.012	g	Much visible sediment in filter
C1	1.483	1.467	-0.016	g	No remarks during experiment
C2	1.501	1.489	-0.012	g	No remarks during experiment
Mean	**1.497**	**1.486**	**-0.011**	**g**	

Table 5.4: Mean filter weight before the filtration process and the weight of the sediment and filter after the filtration process of experiment 2, after 3 days.

Despite the measures taken after the first experiment, it appears that this method remains unsuitable under current conditions. Except for the first filter, after 3 days, all filters weighed less than before filtration, even though they were expected to gain weight due to the accumulation of sediment. However, after 8 days, they appeared to have gained weight again. This data is visible in appendix G. Why this happens is unknown; it might be that the weight of the filters depends on the humidity. Nevertheless, the measurements are unreliable, which only leaves the qualitative observations for this experiment. The qualitative observations are added within table 5.4 similarly to experiment 2. These observations are similar to the first experiment, namely that sediment has been visually determined but cannot be quantified.

Overall, the data from both experiments does not allow for a quantitative assessment of sediment levels. However, with the help of visual observations, the result is that sediment is present in both the upstream area of Las Brujas as well as in the Las Brujas area itself.

Ground level deformation through satellite data

Satellite data from January 2020 to October 2025 were analysed to assess ground level deformation. The observed deformation was compared across different time periods and geographic locations to identify spatial and temporal patterns.

When looking at the line-of-sight (LOS) displacement velocity at the location of the Biotopo Monterrico-Hawaii (figure 5.8), it seems that Las Brujas has become lower during the selected period with a difference of -0.53 cm/yr. The rest of the biotope, on average, seems to stay constant or even rise with +0.15 cm/yr, and 0,79 cm/yr for Monterrico and El Hawaii, respectively.

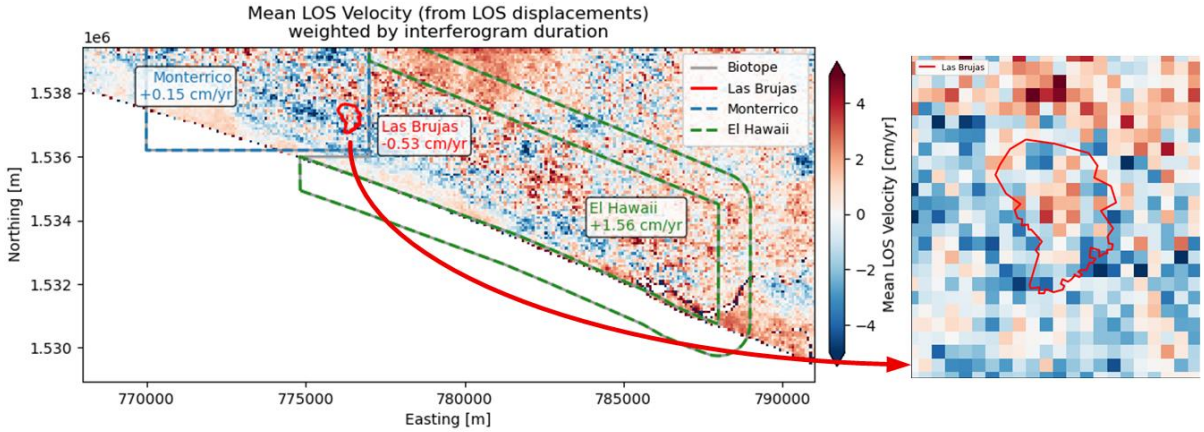

Figure 5.8: Velocity of ground deformation in Biotopo Monterrico-Hawaii and zoomed in to Las Brujas (own image)

To validate if the velocities are significantly distinguishable from zero, the 95% confidence intervals are used (table 5.5). By comparing them with the mean LOS velocity, it can be seen that for all three areas, the 95 % confidence interval does not include zero ($|Mean| > 95\%CI$). This indicates that it is significantly distinguishable from zero, though only marginally so, especially for Las Brujas and Monterrico. It also seems that there is a lot of noise, which is likely due to atmospheric variance. When looking at Las Brujas specifically, it can be seen that the size of the pixels is relatively large compared to the pixel size. Taking all this into account, it is not possible to state the differences in velocity with complete certainty.

Table 5.5: Mean Line-of-Sight (LOS) velocity and 95% confidence intervals for each area of interest.

Area	Mean LOS Velocity [cm/yr]	95% Confidence Interval [cm/yr]
Las Brujas	-0.53	± 0.46
Monterrico	$+0.15$	± 0.11
El Hawaii	$+0.79$	± 0.49

A time-series analysis has been conducted for the same time period. Looking at this time series, it can be seen that there is actually no sinking trend, but the ground level is fluctuating over the years.

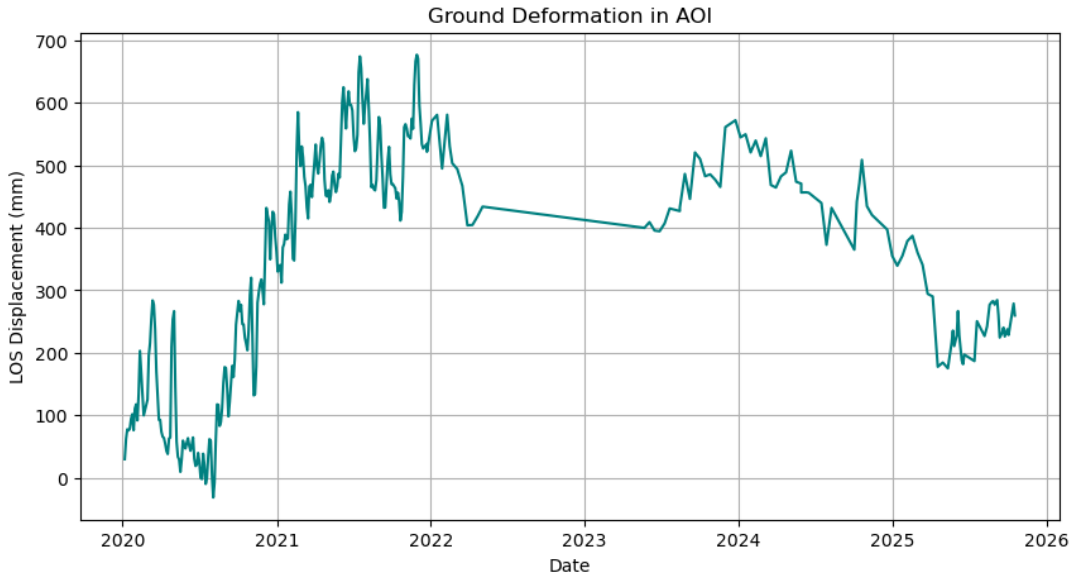

Figure 5.9: Displacement over time (own image)

Interviews with local stakeholders

Qualitative insights into ground level deformation were obtained through interviews with local stakeholders. According to Marco Antonio, a community member from Agua Dulce, the Chiquimulilla Canal has become shallower over the years, suggesting increased sediment accumulation and transport. He also reported that sediment frequently washes ashore on the island where he lives (Marco Antonio, personal communication). In addition, dredging activities have been carried out in the canal, further confirming the presence of sedimentation (Myrnamaría Galindo, personal communication).

Altogether, the sediment present might result in locally higher ground levels, which is also confirmed by interviews with local stakeholders. The satellite data shows big fluctuations over time, but no significant trend. It is also not possible to distinguish Las Brujas from nearby areas, considering ground level deformation.

5.5. Physical-chemical parameters

In this subchapter, results for the physical-chemical parameters experiments are depicted. When performing the measurements, initially, the dissolved oxygen was also tested. However, in the applied method for measuring the physical-chemical parameters, air is scooped into the sampling jar, making the dissolved oxygen values unreliable. Therefore, these values were not taken into account.

Looking at the obtained results, figure 5.10 shows the results of all measured parameters in the Las Brujas area taken on 2 October 2025 and 8 October 2025.

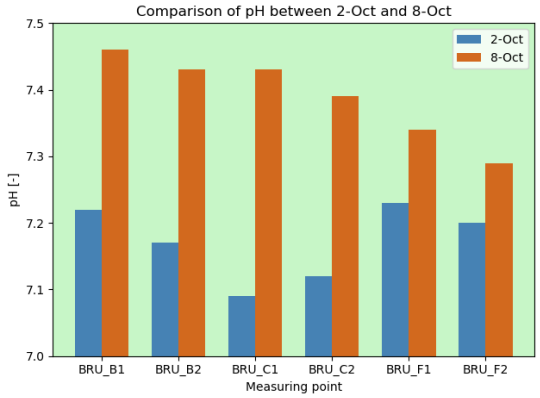

(a) Comparison of pH values in Las Brujas area between October 2nd and 8th

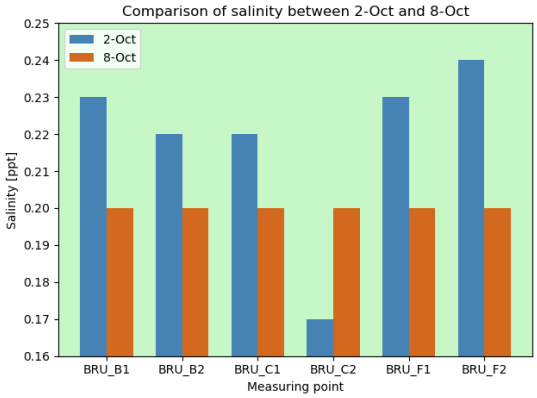

(b) Comparison of salinity values in Las Brujas area between October 2nd and 8th

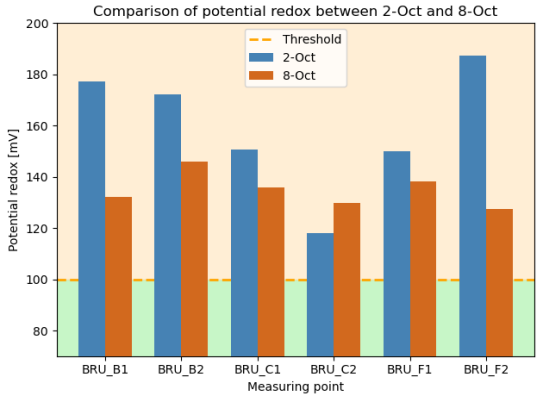

(c) Comparison of redox values in Las Brujas area between October 2nd and 8th

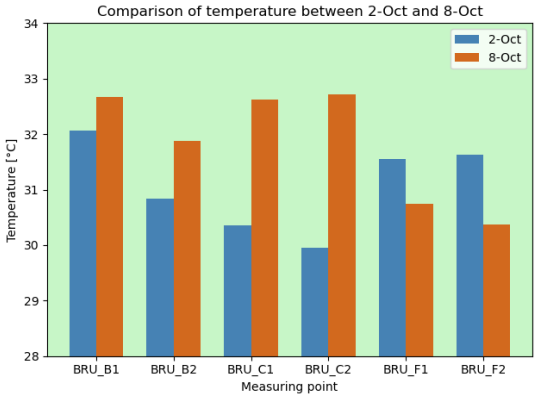

(d) Comparison of temperature values in Las Brujas area between October 2nd and 8th

Figure 5.10: Comparison of physical-chemical values of Las Brujas area, measured on October 2nd and 8th. Measured values are pH levels (a), salinity (b), potential redox (c) and temperature (d). Blue bars represent measurements on October 2nd, brown bars represent measurements on October 8th. The graphs' backgrounds depict the healthy (green) and acceptable range (orange) for red mangroves to grow (own image).

In general, it can be observed that almost all measured physical-chemical parameters lie within the optimal range as described in section 2.2. Solely the measured potential redox values lie in the acceptable range as they exceed +100 mV. In appendix H, the potential redox values can be found for the reference areas. Here, it can be observed that the potential redox values are slightly less in the stressed range than in the Las Brujas area. Furthermore, it can be seen that the values between the measurements differ in time. Generally, the mean pH level increased from approximately 7.16 to 7.36. The mean salinity levels reduced from 0.25 to 0.22 PSU. This could be the result of the heavy rainfall that has accumulated during the time between the two measurement days. To confirm this hypothesis, rainwater was measured using the multi-parameter probe. These rainwater measurements indicated a mean pH level of 7.95 and a mean salinity level of 0.185 PSU. In figure 5.11, the weather forecast has been added for the two weeks at the location of the biotope, and this indeed indicates significant rainfall. The comparison between the different measurement days for the physical-chemical values for all areas can be found in appendix H. All measurement data can be found in appendix I.

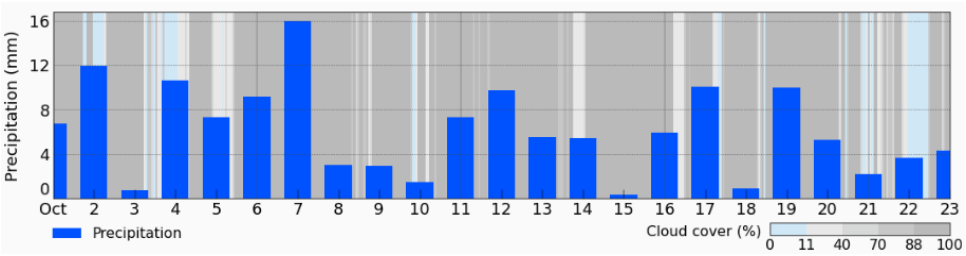

Figure 5.11: Precipitation of the month october 2025 ("Weather Archive Monterrico - meteoblue," n.d.)

Comparison of Las Brujas area to reference areas

The next analysis compares the different research areas with each other. For this analysis, only the set of measurements on the 8th of October will be taken into account, as this dataset contains more measurements and excludes the changes over time induced by rainfall.

Figure 5.12 shows the salinity values for both the Las Brujas area and the reference areas. These areas are described in section 3.4.

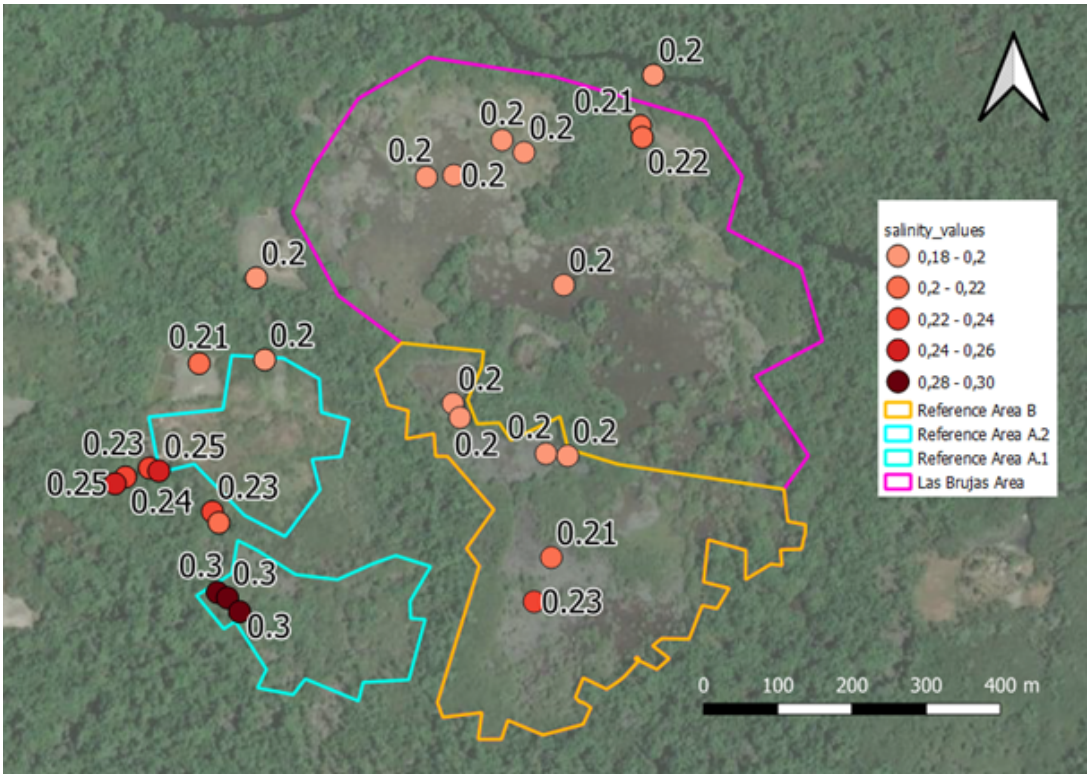

Figure 5.12: Point map showing salinity values in different areas around Las Brujas. All measurements are taken on October 8th, 2025 (own image).

In general can be observed that the difference in salinity values between the different areas is small, being 0.2 PSU at minimum and 0.3 PSU at maximum. The values in the south of Reference Area A are thus 0.1 PSU higher, but this difference is not significant. The observation that there is no significant difference between the reference areas and the Las Brujas area holds as well for the other researched physical-chemical parameters, as can be seen in appendix H. Next to that in appendix H, the point maps for the pH, potential redox and temperature can be found.

Upstream area

Next, upstream measurements were conducted with the multi-parameter probe. These results are shown in appendix H. It can be concluded that the water is similar to the area of Las Brujas, but it does contain a lower salinity level. Next to that, no outlier values, pH or salinity values are measured in the upstream river area. From this can be concluded that there is little influence from various types of farms on the river water. These farms might influence the physical-chemical state of the water, causing for instance, eutrophication. However, a local inhabitant stated that these types of farms are usually located in private areas, which are inaccessible and even dangerous for unauthorised persons. The actual influence of these farms on water quality and quantity is therefore difficult to measure (Max Lopéz, personal communication).

6

Conclusions

Precipitation patterns

Analysis of the precipitation datasets (1981 - 2024) shows considerable year-to-year variation, with a clear wet season from May to October and a dry season from November to April. Annual totals indicate a slight increase in rainfall of approximately 3-4 millimetres per year, while the plotted monthly data reveal notable variation between the years and within the wet season itself. The months May, June, August, October and November likely have become wetter, and July and September likely have become drier. This variability suggests changes in how rainfall is distributed over the course of a year, rather than a consistent seasonal pattern, as precipitation is also influenced by factors such as hurricanes and the El Niño and La Niña phenomena. The centre of the wet season remains stable around mid-July, with no significant shift detected. However, a slight increase in precipitation at the beginning and end of the wet season (increase of precipitation in May and November) may indicate a modest extension of rainfall beyond the traditional boundaries of the rainy period. Although these changes in rainfall distribution seem relatively small, they may still influence mangrove regeneration dynamics, as the process depends on the precise timing and duration of seasonal precipitation to prevent seedlings from remaining afloat or drowning under extended high water conditions.

The three statistical checks performed all show that the correlation values are low. This means that the trends are not statistically significant for a long-term conclusion, though the dataset is sufficiently reliable to describe general variability.

Tidal influence

During the tidal experiment, it was discovered that no tidal influence is present within the wet season near the Las Brujas. Some community members have stated that tidal influence is present in the dry season, but the legitimacy of this information and if this effect is significant has not been confirmed by research yet.

The reduced or absence of tidal influence can negatively affect the regrowth of the mangrove system. Limited (tidal) flow leads to a reduced supply of nutrients, decreased propagule dispersal, and less sediment transport. Specifically, the absence of tidal flow during the dry season would result in very limited water in the biotopes system. This interrupts both nutrient and sediment exchange, results in parched soil, and creates overall stress on vegetation. Such stress would affect both mature trees and young saplings. Consequently, the overall regrowth capacity of the mangrove ecosystem would be substantially reduced (Rachel J. Harris & Bovard, n.d.).

Flow

Flow measurements in micro-channel 2 and 4 show low velocities, ranging between 0.03 and 0.15 m/s. These results confirm that water movement in Las Brujas is limited. In chapter 6, it was also concluded that the tide is not present during the wet season when flow was measured. This means that the flow during the wet season is not driven by tidal action. Field observations and stakeholder interviews indicate that flow during the wet season is mainly influenced by wind and by river discharge,

with the dominant wind directions being southwest, west-southwest and north-northeast. Lastly, channel obstruction by invasive plant species further reduces water movement and restricts the distribution of propagules, contributing to the overall stagnation in the natural growth of the mangroves.

Flow plays a crucial role in mangrove ecosystems, as it facilitates the transport of nutrients, sediments, and propagules throughout the biotope. These transport processes contribute to the healthy growth of seedlings, saplings, and mature trees. When this flow is restricted, either due to weak hydrodynamic forcing or obstruction by invasive species, like ninfas, it can negatively affect the growth and vitality of both adult trees and young saplings. This overall stress limits mangrove regrowth. As indicated by Marco Antonio during the interview, the construction of micro-channels within the area may promote the desired hydrological flow.

Ground level deformation

The experiment on the qualification and quantification of sediment was repeated twice: once in the Las Brujas area and once in the upstream area. Qualitatively, it was discovered that sediment is present in both the upstream area and in the Las Brujas area itself. Considering the low flow velocities in the area, sediment is likely to settle over time, leading to gradual ground level elevation, as also reported by local stakeholders. However, this process has not yet been quantified.

The analysis of ground deformation using satellite data shows that it is not possible to find a significant trend in ground level deformation, but it is possible to see that there are strong fluctuations in ground level. Las Brujas seems to be sinking more in the last five years than the rest of the biotope, but the difference is not significant.

The fluctuating ground levels due to sediment, as observed by satellite data, influence mangrove growth. Currently, the water level seems to be too high for many young saplings during the wet season, causing them to drown. However, when ground levels rise (naturally) due to sediment settling, water height decreases, which could prevent seedlings from drowning and encourage mangrove regrowth.

Physical-chemical parameters

In conclusion, the measured physical-chemical parameters — salinity, pH, redox potential, and temperature — remained within acceptable ranges during the wet season. Salinity, pH, and temperature values can all be considered optimal. Redox potential values were either within the optimal or acceptable range. This indicates that mangrove seedlings and trees can occasionally experience stress. Their overall conditions remain healthy and stable.

Furthermore, there appears to be no significant variation in physical-chemical parameter values between areas with different mangrove regrowth rates around Las Brujas. This suggests that the measured environmental conditions are suitable for natural regeneration within the studied mangrove ecosystem, within the wet season.

Final conclusion

The conclusions indicate that the limited regrowth of mangroves in Las Brujas is primarily controlled by hydrological factors. The most limiting parameters for natural regeneration during the wet season appear to be water depth and flow dynamics. The submergence of saplings for more than 15 days results in high mortality due to oxygen deprivation, while reduced flow conditions limit propagule dispersal and restrict nutrient exchange in the water column.

In addition, the findings suggest that while hydrological limitations persist, the water quality remains favourable for mangrove growth. Moreover, the presence of sediment and the absence of significant ground level variation indicate strong potential for natural elevation processes, which could help reduce water levels. However, limited flow and tidal connectivity still restrict consistent mangrove regeneration; enhancing these hydrological conditions would significantly support long-term recovery in Las Brujas.

7

Discussions

Precipitation patterns

The analysis of the catchment area was primarily based on the CHIRPS satellite precipitation dataset from the Climate Hazard Centre (Climate Hazards Center, n.d.). This dataset provided long-term data coverage essential for identifying general rainfall patterns. However, the spatial resolution of this dataset, which is approximately 10 km, limits its precision for representing rainfall variability in smaller areas such as the Biotopo Monterrico-Hawaii. On top of this, the only datasets used were the monthly, global precipitation sets, meaning a lot of data was discarded after scaling the set down to the desired region, while the dataset itself was of proportional size and taking up space on the hard drive, which could have been used for more useful data relevant to this research. The absence of local weather station data or rain gauge records within the biotope reduced the ability to validate the satellite data. Consequently, while the data allowed for a reliable overview of regional precipitation patterns, microclimatic differences within the catchment area may not have been fully captured.

Furthermore, the statistical analysis applied was appropriate for identifying trends but proved to be insensitive given the large variability throughout the year and the limited number of observations, which were only monthly. This explains why visual patterns suggested slight changes while the statistical results found no significant trends.

Another limitation is that the dataset does not directly account for short-term climatic anomalies such as hurricanes or El Niño and La Niña events, which can locally distort rainfall totals.

Tidal influence

The assessment of tidal influence in the Las Brujas area faced several limitations that affected how the tidal effects could be identified. The study relied mainly on observations based on a time-lapse to detect changes in water level. Although this method was practical and straightforward to implement, it provided only visual evidence and lacked the precision needed to capture subtle variations in water level elevation that are not discernible to the naked eye. Additionally, both experiments encountered minor issues that affected data quality. During the first experiment, it had started raining in the last 3 minutes of the tidal cycle. In the second experiment, the camera was displaced after 80 minutes, which disturbed the time lapse and reduced the visibility.

Moreover, the observation period was limited to only a part of the wet season, so potential seasonal fluctuations in water level may not have been fully captured. Another limitation was the small number of measurement sites, which may not fully represent how local conditions like channel shape or density of vegetation affect water movement.

Flow

Measuring flow in the Las Brujas area was one of the most challenging parts of the fieldwork, and several limitations affected the accuracy and characteristics of the results. Neither of the methods used was optimal; the electronic flow meter did not work because of the high temperatures and the humidity. The flow speed of the canal was also close to the detection limit of the flow meter, making it difficult to

measure extremely low velocities. Fieldwork was carried out during a short period in the wet season, so possible differences in flow during the dry season could not be assessed. In addition, there were no discharge data available for the Chiquimulilla canal, which limited the availability to relocate possible local flow. Dense vegetation, including invasive aquatic plants, also made some areas difficult to access and may have slowed water movement locally.

Ground level deformation

The sediment transport study faced several practical limitations that influenced the level of detail and certainty in the results. The samples contained only 0.6 litres, which is relatively small. Additionally, the method worked well for measuring fine suspended sediments, but did not capture coarser materials that moved along the channel bed, as only superficial samples were taken.

The number of samples collected was limited because of time constraints and difficult field access at certain events, which made the spatial coverage of the area relatively small. In addition, sampling was only done once during the wet season, meaning that possible differences between wet and dry conditions could not be examined. The short sampling period also made it impossible to capture temporary changes that might occur after heavy rainfall or discharge events. Environmental factors such as vegetation cover and wind may also have affected sediment movement, but were not measured directly.

Moreover, the current sediment method did not perform well under the specific conditions in which the project was conducted. As a result, it was not possible to quantify the sediment, and the assessment remained qualitative. Alternative methods may therefore yield more reliable or detailed results.

During the ground level deformation analysis using satellite data, there were some additional limitations that need to be considered. First of all, it was only possible to download a relatively small dataset due to storage limitations. This means that the time interval was really small. This small data set results in the growing possibility that the differences in deformation found are due to atmospheric effects, noise, or a specific event that occurred in this time interval. With few interferograms, the atmospheric noise might cause phase differences that are not due to ground level differences, which could lead to incorrect conclusions. Using a bigger dataset would give the opportunity to find significant trends and isolate real deformation.

Second of all, no atmospheric correction has been applied, which also results in increased noise. As the area is close to the coast, the chance of atmospheric disturbance is high.

Thirdly, the Sentinel-1 data that is used has pixels of 10 meters, which may be too coarse when looking at an area of only 50 hectares (Las Brujas), or even multiple kilometres (the entire biotope). This makes the analysis very sensitive to outliers and inaccurate pixels.

Lastly, there is a data gap around 2023. This has a negative impact on the accuracy of the data.

Physical-chemical parameters

The measurement of physical-chemical parameters presented several limitations that influenced the precision and reliability of the data. The main constraint was that the research period took place solely during October, which is part of the wet season. Therefore, no measurements could be made during dry season. However, various physical-chemical parameters seem to be critical during the dry season. For instance, salinity can reach stressed values during the dry season (“Schoenbeck et al, in prep.” n.d.).

All measurements were taken approximately 5 to 10 centimetres below the water surface. This approach gives a good indication of the conditions experienced by floating propagules, but does not fully reflect the environment near and in the soil where seedlings are settling. Physical-chemical parameters such as salinity, oxygen and redox potential vary with depth, meaning that conditions near the bottom may differ from the values recorded at the surface.

Measurements were performed on separate days to see how the water quality changes over time. However, heavy rainfall between the measurement days caused large differences in water quality, making it difficult to compare results measured on different days directly. This rainwater influenced parameters such as salinity and pH. Some areas were difficult to access due to dense vegetation, so most measurements were taken in more open locations. Dissolved oxygen was not included in the analysis because air entered the sample jars during collection, making these readings unreliable.

Furthermore, the influence of agricultural farms has not been extensively investigated in this research. This is due to the inaccessibility of these farms. However, these farms possibly have significant impacts, such as eutrophication.

8

Recommendations

Precipitation patterns

To gain a more accurate and detailed understanding of precipitation patterns in the catchment area, it is recommended to use higher-resolution precipitation datasets in future research. This would allow for a more precise analysis of local precipitation and also better identification of shifts in the timing and intensity of the wet season on a smaller spatial scale. Where possible, satellite-based data should be compared and validated with local measurements from rain gauges or weather stations to improve reliability. In addition, it is recommended to develop a local drainage model as this would further enhance the understanding of the origin, flow and distribution of water within the catchment area. Such a model could also support improved water management, flood prevention, and accessibility planning for the mangrove forests. Finally, future studies should explore the influence of short-term climatic anomalies, including hurricanes and El Niño or La Niña events, to better understand how these phenomena affect rainfall distribution and seasonal dynamics. Such research would contribute to more effective management and conservation strategies for the biotope and provide valuable guidance for local adaptation measures.

Tidal influence

It is recommended to repeat the tidal experiment during the dry season to determine whether seasonal variations influence the observed tidal effects. This could be done using the same method, including a time-lapse or with a more accurate method if available. Additionally, future measurements should be conducted closer to the river mouth and at several alternative sites between the river mouth and Las Brujas to better understand the extent of tidal intrusion and identify where it diminishes. This would be interesting in both the dry and wet seasons. Finally, it is advised to investigate the current pathways of salt intrusion, which can be both through groundwater and via seawater inflow, to gain a more comprehensive understanding of the salinisation processes in the area.

Flow

Future studies on water flow should look at the main flow drivers more closely to gain a clearer understanding of the hydrological system. Complementary research should also measure the influence of river discharge, during both the dry and wet seasons, as this will help explain seasonal differences in flow behaviour. In addition, it is recommended to study flow directions and patterns, particularly during the dry season, to identify possible stagnation zones. This could include research on the presence of ninfas and on the role of micro-channels in local water movement. Such studies would help clarify small-scale flow pathways and identify areas where stagnation occurs. Finally, examining how flow conditions affect the movement and dispersal of propagules, could provide valuable insights into vegetation establishment and how stagnations can be resolved.

Ground level deformation

During the conducted sediment experiment, it appeared that the ground level likely plays an important role in the survival of the young saplings. However, the data collected was insufficient to quantify ground

level differences. Therefore, it is recommended to do more research on the ground levels in and around Las Brujas and on how they deform. During the dry season, visual observations can be made to view the differences between areas and to identify micro-channels. In addition, investigations are needed on the influence of ground levels and, therefore, water levels on sapling survival.

To quantify the amount of sediment present, it is recommended to repeat the sediment experiment and investigate how much sediment is present and how it is distributed across the biotope.

Soil properties within the biotope are very important. However, researching these properties is challenging during the wet season. Therefore, it would be beneficial to carry out soil studies during the dry season, when conditions are more stable and accessible. In addition, it is recommended to systematically observe the types of mangrove species that appear as saplings in different regrowth areas. This will help determine which species regenerate most successfully under natural conditions. Finally, conducting a mud test to examine how mangrove seeds grow under the current soil conditions would provide valuable insights into soil suitability and support more effective restoration efforts.

Valid conclusions of the ground level deformation over a long time, obtained by looking at satellite data, can only be drawn by using the support of a larger dataset. Therefore, it is recommended to use a dataset, of at least 30 years, so that significant trends can be found. For this, a computer with very large storage is needed, with a high calculating capacity. It is also recommended to do the analysis using Mintpy to reduce atmospheric noise.

Physical-chemical parameters

The main recommendation for the investigation of physical-chemical values is to measure these values in the same reference areas as in this research during the dry season. Specifically, salinity values are expected to be outside of the optimal range (“Schoenbeck et al, in prep.” n.d.). Ideally, field observations should complement the measurement of physical-chemical parameters to assess the survival of mangrove seedlings during this critical period. In addition, interstitial measurements of physical-chemical parameters should be conducted, as mangrove roots absorb essential nutrients from the surrounding soil. These measurements in the Las Brujas area should be compared with those from reference sites to identify any critical differences. It is further recommended to include the concentration of dissolved oxygen in the groundwater analysis, as this is a key indicator of a healthy mangrove system (Radabaugh et al., 2021).

Furthermore, it is recommended to measure physical-chemical parameter values in various river sections surrounding the Las Brujas area, where accessibility allows. Obtaining these measurements would make it possible to assess the influence of nearby agricultural activities on the mangrove system, such as potential eutrophication. These findings could then be related to the presence and abundance of invasive species in the area, such as ninfas.

Community engagement

In addition to the research-specific recommendations, it is advised to study mangrove reference projects as is done in appendix J. A necessary factor for mangrove restoration is to engage the communities living in and around the mangrove system. By looking at other successful projects, much could be learned and applied in the mangrove restoration in Las Brujas.

References

Agency, E. E. (n.d.). Catchment area. https://www.eea.europa.eu/archived/archived-content-water-topic/wise-help-centre/glossary-definitions/catchment-area

Alongi, D. M. (2018). Impact of global change on nutrient dynamics in mangrove forests. *Forests*, *9*(10), 596. https://doi.org/10.3390/f9100596

American Museum of Natural History. (n.d.). *What's a mangrove? and how does it work?* https://www.amnh.org/explore/videos/biodiversity/mangroves/what-is-a-mangrove

ASF data search. (n.d.). https://search.asf.alaska.edu/#/

Aubree, A. (1837). Republique des etats unis du mexique. guatemala ou provinces unies de l'amerique centrale. https://www.davidrumsey.com/luna/servlet/detail/RUMSEY~8~1~34913~1180526

Barban, M. (2021, November). *Climate change in guatemala* [Accessed: 2025-10-16]. https://www.pionerophilanthropy.org/2021/11/climate-change-in-guatemala/

Barik, J., Mukhopadhyay, A., Chowdhury, S. M., Chowdhury, R., Bhattacharya, S., & Hazra, S. (2017). Mangrove species distribution and water salinity: An ecological study from indian sundarbans. *Journal of Coastal Conservation*, *21*, 127–138. https://doi.org/10.1007/s11852-016-0469-0

Biber, P., University of Southern Mississippi. (2006, September). *Measuring the effects of salinity stress in the red mangrove, Rhizophora mangle L* (tech. rep.). University of Southern Mississipi. African Journal of Agricultural Research. https://www.researchgate.net/publication/228340196_Measuring_the_effects_of_salinity_stress_in_the_red_mangrove_Rhizophora_mangle_L

Boletín del Centro de Investigaciones Biológicas. (2021). Vista de laguncularia racemosa (l.) gaertn. más que halofita es una especie halotolerante. https://produccioncientificaluz.org/index.php/boletin/article/view/44303

Bosboom, J., & Stive, M. J. (2023). *Coastal dynamics*. TU Delft OPEN Publishing.

Castellanos, D. E., & Rivera, P. (2016, March). *Water and climate change in guatemala according to the experts* [Accessed: 2025-10-16]. https://www.entremundos.org/revista/economy/water-and-climate-change-in-guatemala-according-to-the-experts/?lang=en

Castillo Cabrera, F. J., Davila Perez, C. V., Morales, A. S., de San Carlos de Guatemala, U., de Investigación –DIGI-, D. G., & de Investigación en Recursos Naturales –PUIRNA-, P. U. (2012). *Actualización del Plan Maestro de la Reserva de Usos Múltiples Monterrico: el levantamiento detallado de la vegetación y la cartografía botánica* (tech. rep.).

Clima, L. (2023, October). Restauración de manglares en Guatemala brinda esperanza frente a los impactos del cambio climático. https://ojoalclima.com/articles/restauracion-de-manglares-en-guatemala-brinda-esperanza-frente-a-los-impactos-del-cambio-climatico

Climate Hazards Center, U. S. B. (n.d.). *Chirps: Rainfall estimates from rain gauge and satellite observations* [Accessed: 2025-10-16]. https://www.chc.ucsb.edu/data/chirps

CONRED. (2013, February). Boletín Informativo No. 3084 – INCENDIOS FORESTALES ACTIVOS EN SANTA ROSA y ZACAPA » CONRED. https://conred.gob.gt/boletin-informativo-no-3084-incendios-forestales-activos-en-santa-rosa-y-zacapa/

Coromac, D., Coromac, D., & Coromac, D. (2024, October). Entregan oficialmente el libramiento de Chiquimulilla para mejorar la transitabilidad. https://agn.gt/entregan-oficialmente-el-libramiento-de-chiquimulilla-para-mejorar-la-transitabilidad/

Coromac, D., Coromac, D., & Coromac, D. (2025, February). Ejército esparce propágulos de mangle en zonas de difícil acceso. https://agn.gt/ejercito-esparce-propagulos-de-mangle-en-zonas-de-dificil-acceso/

Correa, J. N., Federal University of Maranhão, de Jesus Azevedo, J. W., Federal University of Alagoas, de Oliveira, A. R., Federal University of Maranhão, & Mochel, F., Federal University of Maranhão. (2021, October). *Salinity assessment in the germination of Laguncularia racemosa (L.) C. F. Gaerth for selecting mangrove restoring sites* (tech. rep.). Atena. https://www.researchgate.net/publication/355325047_Salinity_assessment_in_the_germination_of_Laguncularia_racemosa_L_C_F_Gaerth_for_selecting_mangrove_restoring_sites

Credits, C. (2025, September). The Ultimate Guide to Understanding Carbon Credits. https://carboncredits.com/the-ultimate-guide-to-understanding-carbon-credits/

DeeperSonar. (2025). Deeper smart sonar chirp 2 [Accessed: 2025-09-29].

Deltares. (n.d.). Aqua Monitor - monitoring surface water changes from space. https://aqua-monitor.appspot.com/

Duke, N. (2017, November). Mangrove floristics and biogeography revisited: Further deductions from biodiversity hot spots, ancestral discontinuities, and common evolutionary processes. https://doi.org/10.1007/978-3-319-62206-4_2

Eichhornia crassipes. (2006, August). https://www.iucngisd.org/gisd/species.php?sc=70#:~:text=Control%20strategies%20must%20address%20both,be%20a%20pest%20(Pacific).

Ellison, A., Farnsworth, E., & Moore, G. (2000). White mangrove - laguncularia racemosa. *The IUCN Red List of Threatened Species 2010*. https://doi.org/https://dx.doi.org/10.2305/IUCN.UK.2010-2.RLTS.T178798A7609219.en.

Enschedé, M., van Looij, Z., van der Meer, R., van Oorschot, H., Oudshoorn, R., & Stevens, T. (2017, March). *Coastal protection of the Bac Lièu province by rehabilitationof the mangrove forest* (tech. rep.). TU Delft.

Fain, J. (2025, September). Understanding surface water speed in rivers: why it matters and how it's measured. https://bwi.earth/understanding-surface-water-speed-in-rivers-why-it-matters-and-how-its-measured/

File:Mangrove ecosystem in the coastal intertidal zone.png - Wikimedia Commons. (2020, May). https://commons.wikimedia.org/wiki/File:Mangrove_ecosystem_in_the_coastal_intertidal_zone.png

Fiveable. (n.d.). Tidal flushing - (marine biology) - vocab, definition, explanations. https://fiveable.me/key-terms/marine-biology/tidal-flushing

Florida Museum of Natural History. (2025, July). https://www.floridamuseum.ufl.edu/southflorida/habitats/mangroves/species/

Geopacks. (2025). Image of geopacks advanced flow meter. https://www.geopacks.com/products/new-advanced-flowmeter-with-temperature-gauge-and-improved-screen

GFS. (2025). Image of flow meter display. https://www.gpsforestry-suppliers.com/Geopacks-Advanced-Flowmeter

Food and Agriculture organization of the United Nations. (2025). *Mangrove management*. https://www.fao.org/forestry/mangrove/ecology/

Friess, D. A. (2016). Mangrove forests. *Current Biology*, *26*(1). https://www.cell.com/current-biology/fulltext/S0960-9822(16)30321-9

Friess, D. A., Rogers, K., Lovelock, C. E., Krauss, K. W., Hamilton, S. E., Lee, S. Y., Lucas, R., Primavera, J., Rajkaran, A., & Shi, S. (2019). The state of the world's mangrove forests: past, present, and future. *Annual Review of Environment and Resources*, *44*(1), 89–115. https://doi.org/10.1146/annurev-environ-101718-033302

Galindo Lemus, M., & Schönbeck, M. (2025). *Caracterización fisicoquímica en agua del ecosistema manglar de la reserva natural de usos múltiples monterrico: Una mirada hacia la restauración* [Presentation at the Simposio Manglares, FUNDAECO and Universidad de Cornell, Monterrico, Guatemala, February 2025].

García, G. (2018, July). Reserva natural de Monterrico, Santa Rosa | Aprende guatemala.com. https://aprende.guatemala.com/historia/geografia/reserva-natural-monterrico-santa-rosa/?utm_source=chatgpt.com

Geopacks. (2025). Advanced flowmeter with temperature gauge [Accessed: 2025-09-29].

González, C., Graham, A., & Jaramillo, C. (2023). The rise and fall of caribbean mangroves [Preprint]. *Preprints*, *2023010380*. https://doi.org/10.20944/preprints202301.0380.v1

Gonzalez-Bernat, M. J., & Clifton, J. (2016). *"Living with our backs to the sea": A critical analysis of marine and coastal governance in Guatemala* (tech. rep.). Elsevier Ltd.

Google Earth. (2025). Satellite image of river mouth. https://earth.google.com/web/@13.84380711,-90.35248151,9.54749524a,8151.30507245d,35y,0h,0t,0r/data=CgRCAggBMikKJwolCiExNzdjTUtCZTZtNFRmTEs2Wk1RS09wY2M4Wmw3dVRjVU8gAToDCgEwQgIIAEoICL3ExfgDEAE

Gunnarsson, C. C., & Petersen, C. M. (2006). Water hyacinths as a resource in agriculture and energy production: A literature review. *Waste Management*, *27*(1), 117–129. https://doi.org/10.1016/j.wasman.2005.12.011

HANNA Instruments Guatemala. (2025). Medidor multiparamétrico de ph / orp / ce / tds / salinidad / od / presión / temperatura (10 m cable) [Accessed: 2025-09-29].

Hiller, D. (1998). *Environmental soil physics*.

Holguin, G., Vazquez, P., & Bashan, Y. (2001). The role of sediment microorganisms in the productivity, conservation, and rehabilitation of mangrove ecosystems: An overview. *Biology and Fertility of Soils*, *33*, 265–278. https://doi.org/10.1007/s003740100373

Hossain, M., & Nuruddin, A. (2016). Soil and Mangrove: A Review. *Journal of Environmental Science and Technology*, *9*(2), 198–207. https://doi.org/10.3923/jest.2016.198.207

Interactive Country Fiches, U. G. (n.d.). *Climate change / guatemala* [Accessed: 2025-10-16]. https://dicf.unepgrid.ch/guatemala/climate-change

Jlmaurer. (n.d.). GE6146/notebooks/Lab4$_{I}nSAR.ipynbatmasterjlmaurer/GE6146$. https://github.com/jlmaurer/GE6146/blob/master/notebooks/Lab4_InSAR.ipynb

Kathiresan, K., & Bingham, B. L. (2005). Biology of mangroves and mangrove ecosystems. *Advances in Marine Biology*, *40*, 81–251. https://doi.org/10.1016/S0065-2881(05)40002-6

Kathiresan, K., & Bingham, B. (2001, January). *Biology of mangroves and mangrove Ecosystems*. https://doi.org/10.1016/s0065-2881(01)40003-4

Komiyama, A., Eong Ong, J., & Poungparn, S. (2008). Allometry, biomass, and productivity of mangrove forests: A review [Mangrove Ecology – Applications in Forestry and Costal Zone Management]. *Aquatic Botany*, *89*(2), 128–137. https://doi.org/https://doi.org/10.1016/j.aquabot.2007.12.006

Krauss, K. W., McKee, K. L., Lovelock, C. E., Cahoon, D. R., Saintilan, N., Reef, R., & Chen, L. (2013). How mangrove forests adjust to rising sea level. *New Phytologist*, *202*(1), 19–34. https://doi.org/10.1111/nph.12605

Lopéz, M. (2025).

Massel, S., Furukawa, K., & Brinkman, R. (1999). Surface wave propagation in mangrove forests. *Fluid Dynamics Research*, *24*(4), 219–249. https://doi.org/https://doi.org/10.1016/S0169-5983(98)00024-0

McIvor, A., Spencer, T., Möller, I., & Spalding, M. (2013, July). *The response of mangrove soil surface elevation to sea level rise* (tech. rep.). The Nature Conservancy; Wetlands International. http://coastalresilience.org/science/mangroves/surface-elevation-and-sea-level-rise

McKee, K. L. (2010). Biophysical controls on accretion and elevation change in Caribbean mangrove ecosystems. *Estuarine Coastal and Shelf Science*, *91*(4), 475–483. https://doi.org/10.1016/j.ecss.2010.05.001

Mikoko pamoja. (n.d.). https://mikokopamoja.org/

MISIÓN – Centro de Estudios Conservacionistas – CECON –. (n.d.). https://cecon-ccqqfar.usac.edu.gt/nosotros/mision/

Misión y Visión del CONAP. (n.d.). https://conap.gob.gt/

National Geographic Society. (n.d.). Intertidal zone [Accessed: 2025-09-30].

National Oceanic and Atmospheric Administration. (2024). What is a ”mangrove” forest? [Accessed: 2025-09-25]. https://oceanservice.noaa.gov/facts/mangroves.html

Nurse, L., Mclean, R., Agard, J., Briguglio, L., Duvat-Magnan, V., Pelesikoti, N., Tompkins, E., & Webb, A. (2014). *Small islands*. https://hal.science/hal-01090732

Pérez-Ceballos, R., Zaldívar-Jiménez, A., Canales-Delgadillo, J., López-Adame, H., López-Portillo, J., & Merino-Ibarra, M. (2020). Determining hydrological flow paths to enhance restoration in impaired mangrove wetlands. *PLoS ONE*, *15*(1), e0227665. https://doi.org/10.1371/journal.pone.0227665

Project, M. A. (2019, March). Restoring the natural mangrove forest. https://www.youtube.com/watch?v=Vh7CoPBLQa8

Project, M. A. (2023, November). Restoring aquaculture ponds in Thailand - Mangrove Action Project. https://mangroveactionproject.org/case-study/restoring-aquaculture-ponds-in-thailand/

Puthiyapurayil Haseeba, K., Mohammed Aboobacker, V., Vethamony, P., & Abdulla Al-Khayat, J. (2025, July). *Water and sediment characteristics in the Avicennia Marina environment of the Arabian Gulf: a review* (tech. rep.). Elsevier. https://www.sciencedirect.com/science/article/pii/S0025326X25004382

Rachel J. Harris, E. M. E. I., Eric C. Milbrandt, & Bovard, B. D. (n.d.). *The Effects of Reduced Tidal Flushing on Mangrove Structure and Function Across a Disturbance Gradient* (tech. rep.). Springer Nature.

Radabaugh, K. R., Moyer, R. P., Chappel, A. R., Joyse, K. M., Russo, C. E., Mangubhai, S., & Alongi, D. M. (2021). Mangrove restoration and conservation in a changing climate. *Estuaries and Coasts*, *44*, 1321–1335. https://doi.org/10.1007/s12237-020-00835-5

Roh, Y., & Choi, K. (2023). Study on the influence of wind speed on the measurement of surface velocity. *19th Annual Meeting of the Asia Oceania Geosciences Society*, 80–82. https://doi.org/10.1142/9789811275449_0027

SAPPER, K. T. (1895). As nördliche mittel-amerika, nebst einem ausflug nach dem hochland von anahuac. reisen und studien aus den jahren 1888-1895 ... mit ... karten. https://commons.wikimedia.org/wiki/File:457_of_%27Das_n%C3%B6rdliche_Mittel-Amerika,_nebst_einem_Ausflug_nach_dem_Hochland_von_Anahuac._Reisen_und_Studien_aus_den_Jahren_1888-1895_..._Mit_.._Karten%27_(11239649155).jpg

Schoenbeck et al, in prep. (n.d.).

Simulated historical climate and weather data for Monterrico - meteoblue. (n.d.). https://www.meteoblue.com/en/weather/historyclimate/climatemodelled/monterrico_guatemala_3592390

Solórzano Vega, A. I. (2022). *Origins and organization of las lisas', chiquimulilla fishermen* (Bolet in de Tradiciones Populares No. 12) (Accessed on 2025-11-04). Centro de Estudios de las Culturas en Guatemala (CECEG), Universidad de San Carlos. https://ceceg.usac.edu.gt/wp-content/uploads/2025/09/268-traduccion.pdf

The Editors of Encyclopaedia Britannica. (n.d.). *Orographic precipitation* [Accessed: 2025-10-16]. https://www.britannica.com/science/orographic-precipitation

Thompson-Saud, G., Robertson, A., Choukroun, S., Ospina-Alvarez, A., Logan, M., van der Mheen, M., & Grech, A. (2024, December). *Factors influencing the early growth and dispersal potential of mangrove propagules* (tech. rep.).

Tide times and charts for Monterrico, Santa Rosa and weather forecast for fishing in Monterrico in 2025. (n.d.). https://tides4fishing.com/gt/santa-rosa/monterrico

Unesco. (2025). Tide near acajutla, el salvador. https://www.ioc-sealevelmonitoring.org/station.php?code=acaj

Turner, R. E., Lee, S. Y., & McKee, K. L. (2023). Mangrove ecosystem services: A global perspective. *Biological Conservation*, *265*, 109398. https://doi.org/10.1016/j.biocon.2022.109398

Twilley, R. R. (1998). Mangrove ecology: A review of physiology, structure, and function. *Trees*, *12*, 100–112. https://doi.org/10.1007/s004680050114

unknown. (1823). 1823 map of central america from a statistical and commercial history of the kingdom of guatemala. https://commons.wikimedia.org/wiki/File:1823_map_of_Central_America_from_A_statistical_and_commercial_history_of_the_Kingdom_of_Guatemala.jpg

Van der Stocken, T., Carroll, D., Menemenlis, D., Simard, M., & Koedam, N. (2019). A general framework for propagule dispersal in mangroves. *Biological Reviews*, *94*(2), 824–845. https://doi.org/10.1111/brv.12473

Van der Stocken, T., Vrije Universiteit Brussel, López-Portillo, J., Institute of Ecology INECOL, & Koedam, N., Vrije Universiteit Brussel. (2017, February). *Seasonal release of propagules in mangroves*

– *Assessment of current data* (tech. rep.). Vrije Universiteit Brussel. Aquatic Botany. https://doi.org/10.1016/j.aquabot.2017.02.001

Van Santen, P., Augustinus, P., Janssen-Stelder, B., Quartel, S., & Tri, N. (2006). Sedimentation in an estuarine mangrove system. *Journal of Asian Earth Sciences*, *29*(4), 566–575. https://doi.org/10.1016/j.jseaes.2006.05.011

Waters, H. (2016). Mangrove restoration: Letting mother nature do the work. *OCEAN FIND YOUR BLUE*.

Waycott, M., McKenzie, L., Mellors, J. E., Ellison, J. C., Sheaves, M. T., Collier, C., Schwarz, A.-M., Webb, A., Johnson, J. E., & Payri, C. E. (2011, January). *Vulnerability of mangroves, seagrasses and intertidal flats in the tropical Pacific to climate change*. http://pubs.iclarm.net/resource_centre/WF_3028.pdf

Weather Archive Monterrico - meteoblue. (n.d.). https://www.meteoblue.com/en/weather/historyclimate/weatherarchive/monterrico_guatemala_3592390

Wiktionary: The free dictionary. (2024). *Cryptovivipary*. https://en.wiktionary.org/wiki/cryptovivipary#English

A

Governmental organisation of the Biotopo Monterrico-Hawaii

This section outlines the distribution of power and management responsibilities, focusing on the roles of the Marine Protected Area and the regional authorities in relation to the Biotopo Monterrico-Hawaii.

Marine Protected Areas

The coastal and maritime conservation efforts of the Guatemalan government have started since 1956 when maritime and coastal protection laws were implemented and have been quite inconsistent since. Notable for the Biotopo Monterrico-Hawaii is the Protected Areas Law, which was enacted in 1989, and introduced the Guatemalan System of Protected Areas (SIGAP). This law grants the management of protected areas to the National Council on Protected Areas (CONAP). By the Protected Areas Law, a total of 32 % of national Guatemalan territory is protected by law, of which 2 % is a Maritime Protected Area (MPA) (Gonzalez-Bernat & Clifton, 2016).

The Biotopo Monterrico-Hawaii is one of the 7 Maritime Protected Areas (MPA) within Guatemala. An MPA status (referred to as Marine Parks in the Protected Areas Law) designates a legally recognised management category of protected areas, specifically applied to marine and coastal regions (Gonzalez-Bernat & Clifton, 2016). Of the 7 MPAs, 4 are managed by the state of Guatemala, 2 are co-managed by non-governmental organisations (NGO's), and one is privately owned (Gonzalez-Bernat & Clifton, 2016). The level of protectiveness differs from very well protected to mildly protected. This means that, dependent on the gradation of the protection level, some industries are still allowed within a protected area. The Biotopo Monterrico-Hawaii has the mildest level of protection an MPA can be provided with. This means that shrimp farmers, fishermen, agricultural workers, and sugarcane cultivators must obtain government permission before starting their activities or clearing land for their projects. In practice, however, this often translates to widespread approval, provided that sufficient payments are made (Myrnamaría Galindo, personal communication).

Governmental management of conserved areas

In Figure A.1, the governmental power distribution concerning MPAs is provided on both a general governmental level (Figure A.1a) and a more regional level (Figure A.1b). The MPAs in Guatemala are governed through a multi-level structure involving national, regional, and local authorities, supported by academic, non-governmental, and international organisations (Gonzalez-Bernat & Clifton, 2016).

Within the executive power, the highest power is held by the president and vice-president which both have supporting secretariats (SEGEPLAN and SENACYT). CONAP is an authority that helps to manage biodiversity projects and governs protected areas. They are supported by the CONAP Council, which includes academic representatives, government ministries, and NGO members. Advisory support comes from universities, NGOs, and international organisations such as UNDP, USAID, IUCN, WWF, TNC, and GIZ. The local implementation is carried out by departmental and municipal governments in coordination with UGAM (Municipal Environmental Units) and local communities. The Development councils

at national (CONADUR), regional (CODEDE), departmental (CODEDE), and municipal (COMUDE) levels ensure that national policies are translated into local action (Gonzalez-Bernat & Clifton, 2016). The enforcement of regulations is limited, which results in little compliance with the laws and more environmental harm than desired (Myrnamaría Galindo, personal communication).

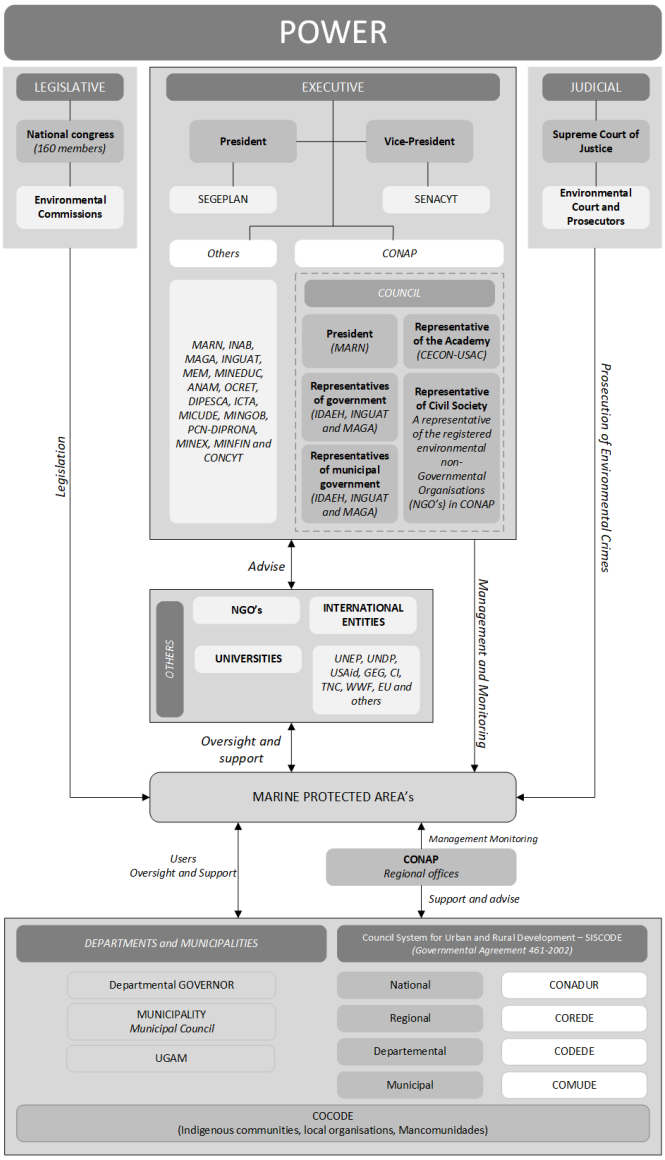

Current governance structure for MPAs. Key: SEGEPLAN – Secretary of Planning and Programming of the Presidency; SENACYT – National Secretary of Science and Technology; CONAP – National Council of Protected Areas; MARN – Ministry of Natural Resources and Environment; CECON-USAC – Centre for Conservation Studies of the State University of San Carlos; IDAEH – Institute of Anthropology and History, MAGA – Ministry of Agriculture, Livestock and Food; ANAM – National Association of Municipalities, INAB – National Forest Institute; INGUAT – Guatemalan Institute of Tourisms; MEM – Ministry of Energy and Mining; MINEDUC – Ministry of Education; OCRET – Bureau of State Land Reserves; DIPESCA – Fisheries and Aquaculture Unit; ICTA – Institute of Science and Technology; MICUDE – Ministry of Culture and Sport; MINGOB – Ministry of Interior; PNC-DIPRONA – National Police through the Division for Environmental Protection; MINEX – Ministry of Foreign Affairs; MINFIN – Ministry of Finance; CONCYT – National Council of Science and Technology, UGAM – Municipal Environmental Management Unit; CONADUR – National and Urban Development Council; COREDE – Regional Development Council; CODEDE – Departmental Development Council; COMUDE – Municipal Development Council; COCODE – Community Development Council.

(a) Role and power relations in Guatemala concerning mangrove conservation (Gonzalez-Bernat & Clifton, 2016)

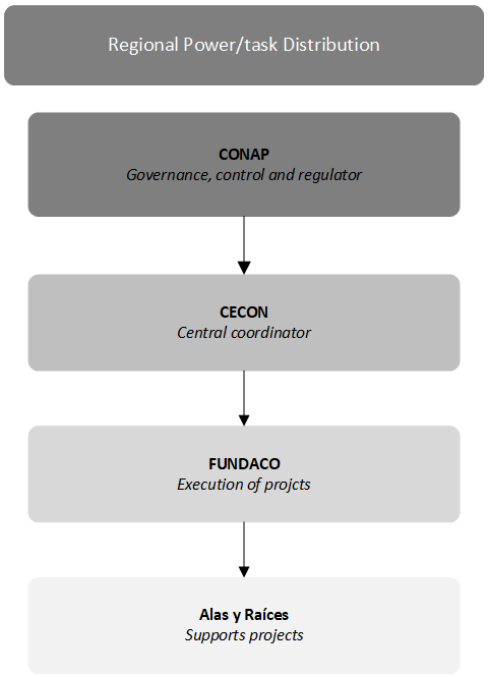

(b) Regional role and power relations in Guatemala concerning the Biotopo Monterrico-Hawaii (Myrnamaría Galindo, personal communication) (own image)

Figure A.1: Stakeholder power relations in Guatemala (general and regional level)

Regional management of Biotopo Monterrico-Hawaii

On the 16th of december 1977, the biotopo was established as a reserve area for the special protection of fauna, flora and the natural ecosystem (García, 2018). Locally, the Biotopo Monterrico-Hawaii is located in two so called departments: departemento de Chiquimula and departemento de Santa Rosa. This entails that the biotopo is split in two parts each managed by a different department. The research area Las Brujas lies in the department of Chiquimula. Therefore, this section focuses on the organization of the department of Chiquimula.

The Biotopo Monterrico-El Hawaii is primarily governed by CONAP, which is responsible for all protected areas. CONAP manages, regulates, and enforces national laws ("Misión y Visión del CONAP," n.d.).

CECON serves as the central coordinator of the area. Their organisation is responsible for managing new conservation projects and research, and acts as an academic link between the university and the local inhabitants. Therefore, CECON makes sure laws are implemented ("MISIÓN – Centro de Estudios Conservacionistas – CECON –," n.d.) and (Myrnamaría Galindo, personal communication).

FUNDAECO is a non-governmental organisation that supports CECON with the implementation of national laws. They provide technical support during activities like mangrove restoration projects and conservation projects. Moreover, they promote ecotourism and environmental education, supporting sustainable development programs and collaborating with the local communities directly (Myrnamaría Galindo, personal communication).

Alas y Raíces is a temporary supporting organisation with a cultural and educational focus. Its responsibilities include strengthening cultural identity and traditions linked to ecosystems, promoting educational, artistic, and environmental awareness activities, and encouraging youth and community participation in environmental protection (Myrnamaría Galindo, personal communication).

B

Reference area

Figure B.1 shows Reference Area B. The map clearly shows which patches of Area B are regrown (yet).

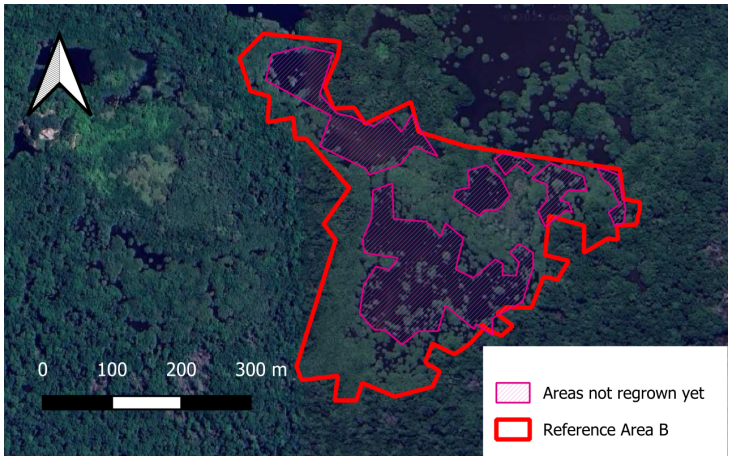

Figure B.1: Reference Area B and the area that has or has not regrown (yet) (own image)

C

Additional fieldwork

In addition to the quantitative data collected during fieldwork, qualitative insights were obtained through interviews with local stakeholders. Furthermore, CHIRP sonar was used to complement these efforts by providing high-resolution bathymetric data.

Interviews

During the fieldwork period, the following people were interviewed:

1. **Members of the Agua Dulce community**: Agua Dulce, comprising approximately twenty households, which have lived within the biotope for around 200 years (see section 3.1), maintain a close connection to the project. Their livelihoods are closely intertwined with the mangrove ecosystem, upon which they depend for sustenance and daily life. Two inhabitants were interviewed.
2. **Employees of FUNDAECO**: As described in section 3.1, FUNDAECO is a non-governmental organization that provides technical support for mangrove restoration and conservation. Two of its employees, Noé Orantes Olivares and Myrnamaría Galindo, are closely involved in the project and have extensive knowledge of its objectives and progress.
3. **A ranger from CECON**: Rangers are responsible for protecting the entire habitat. Their duties include monitoring the area, addressing inappropriate or harmful activities, and supporting organizations such as FUNDAECO in efforts to improve local environmental conditions. Many rangers, such as Samuel García Cristales, have extensive knowledge of the area, as they grew up there and have a long-standing connection to the ecosystem.

All interview questions are displayed in appendix D.

Sonar Chirp measurements

The *Deeper Smart Sonar Chirp+2* was used to measure the water levels at multiple locations in Las Brujas during the period fieldwork was done (DeeperSonar, 2025). During this period a lot of rainfall has fallen and therefore water levels fluctuate a lot on a daily basis. Therefore, it is important to note that water levels at the same location vary from day to day. During this period, water levels generally increased, as the fieldwork took place in the wet season.

The *Deeper Smart Sonar Chirp+2* is shown in figure C.1a. Figure C.1b shows the interface of the *Fish Deeper app*. This app monitors the bathymetry of the area and saves the data, which can be manipulated in *QGIS* to obtain the water heights and create an insight in the bathymetry of the area. The stick, as described in section 5.2 and depicted in figure 4.1b, was used to validate the water depth measured by the sonar measuring device.

(a) Deeper Smart Sonar Chirp+2 (own image)

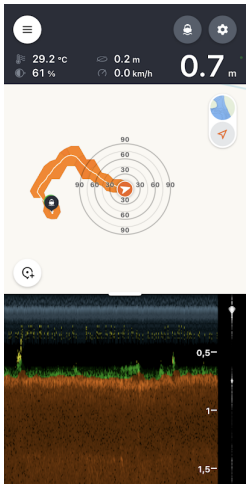

(b) Interface of the Fish Deeper app to measure bathymetry (own image)

Figure C.1: Deeper Smart Sonar Chirp+2 and its user interface

Because of the great daily water fluctuations and the fact that it was deemed impossible to map the entire area of Las Brujas in one day, this bathrymetry data was not used directly to obtain results. However, it did give some insight in the ground level of the Las brujas area and the importance of the daily water fluctuations in the wet season.

Geopacks Advanced Flow Meter

The *Geopacks Advanced Flow Meter* was used to try to measure the flow velocities (Geopacks, 2025). The instrument measures flow by placing a propeller sensor at the desired depth in the water column. A photograph of the display was taken and labeled according to the corresponding measurement location. The flowmeter is illustrated in figure C.2. However, since flow speeds in the area were too low in order to use the *Geopacks Advanced Flow Meter*, the instrument was not used any further and other methods for measuring flow were used.

(a) Geopacks Advanced Flow Meter (Geopacks, 2025)

(b) Display of the flow meter (GFS, 2025)

Figure C.2: Geopacks Advanced Flow Meter and its display

D

Interviews

Questions interview Marco Antonio (Inhabitant Agua Dulce)

1. What is your name?
2. Where are we right now? Can you describe the area (*generally*)?
3. What is your background (*Think: where did you grow up, how did you end up what you do to this day, etcetera*)?
4. How long have you been living in Agua Dulce?
5. What does your daily life look like?
   (a) What do you do to get water/food/other necessities
   (b) How often do you go out of Agua Dulce?
6. What do you know about mangroves?
7. What is your/the communities' relation with the mangrove forest (*positive/negative/neutral*)?
   (a) What 'use' is the mangrove for you?
8. What do you think of the state of the mangroves at the moment?
   (a) Did you see any changes over the years, and if yes, what changed
   (b) What do you think is the reason for this change?
9. Did you notice a change in the water quality over the years? (*Think of: Different smell, color, amount of fish, etcetera*)
10. Have there always been this many invasive species? (*Think of nymphas, etcetera*)
    (a) If yes, how did this change over the years?
    (b) What do you notice about the effect of the nympas? (*Think of: How do they influence your daily life, does the flow in the biotope change, etcetera*)
11. Do you think good maintenance of mangroves is important?
    (a) Do you take the health of the mangrove forest into account in your daily life?
    (b) Have you ever participated in a restoration effort? (*for example building chinampas*), can you explain?
12. Some forest fires occurred at the start of this century, what do you know about these fires?
    (a) What was the impact on Agua dulce?
    (b) What was the impact on the biotope?
13. Did you see the biotope change over the years, and if yes, what has changed related to the following factors? (*Think of mangrove growth, mangrove cover, invasive species, water flow, boats, tourism etcetera*)

14. What do you think is the future of the mangrove forest?

15. Do you experience tidal differences during the day? (*Changes in water height that occur due to oceanic tides*)
    (a) Are there differences in wet and dry season?
16. Did you experience any changes in the amount of rainfall over the years? (*Think of extremes and an overall trend*)
17. Which parts of the biotopo are still wet during the dry season? (*Think of the channel, different sites, can you still use the boat, etcetera*)
    (a) Do you also experience areas that are sometimes wet (*for example with high tide*) and sometimes are dry (*for example with low tide*)?
18. Do you notice at which places new mangroves start to grow?
    (a) Can these places be linked to similar tide, flow or topographical resemblance?
19. Do you know where fresh water is coming from? Are there rivers coming from upstream that fill the lagoon? Or is it mainly rainwater?
20. Around 1870 the Chiquimilia channel was constructed. Do you know what were the major changes in the biotope due to this construction?
    (a) If not, is there anyone that still knows something about the time before the canal?
21. Have you ever noticed, in the biotope, water washing soil away or instead that sediment is added? In other words, did you notice the ground level change (*over the years*)?
22. What happens to waste and wastewater from the citizens of Agua Dulce?

Questions interview Adriana (Inhabitant Agua Dulce)

1. What is your name?
2. Where are we right now? Can you describe the area (*generally*)?
3. What is your background (*Think of: where did you grow up, how did you end up what you do to this day, etcetera*)?
4. What does your daily life look like?
5. How long have you been living in Agua Dulce?
6. What does your daily life look like?
7. What do you know about mangroves?
8. What is your relation with the mangrove forest (*positive/negative/neutral*)?
9. What do you think of the state of the mangroves at the moment?
   (a) Did you see any changes over the years, and if yes, what changed
10. Do you think good maintenance of mangroves is important?
11. Some forest fires occurred at the start of this century, what do you know about these fires?
    (a) What was the impact on Agua Dulce?
12. Did you see the biotope change over the years, and if yes, what has changed related to the following factors? (*Think of mangrove growth, mangrove cover, invasive species, water flow, boats, tourism etc.*)

Questions interview Myrnamaría Galindo (FUNDAECO)

1. What is your name and what is your study/work background?
2. What do you do for a living?
   (a) What do you do on a daily basis at work? (*different activities on a day*)
   (b) What is your exact function title?
3. Where are we right now? Can you describe the area (*generally*)?
4. How would you explain what mangroves are (*to someone that doesn't know anything about it*)?
5. What is your relation to mangroves?
6. What is the importance of good maintenance of the mangroves?
7. How important are mangroves for the ecosystem (*flora and fauna*)?
   (a) Do mangroves have any other purposes/values? Can you give examples? (*Think of:communities, flood protection, etcetera?*)
8. What do you think of the state of the mangroves at the moment?
9. What are the problems that are present in Biotopo Monterrico-Hawaii?
   (a) and what are the problems specifically in Las Brujas?
   (b) When and how did these problems start? (*Think of: fires, etcetera*)
10. Is there a difference in regrowth of the mangrove trees between dry and wet season?
11. What are the current efforts that have been taken to restore the mangroves?
    (a) What was the most effective in general (*Think of: chinampas, microcanals, dredging, etcetera*)?
    (b) Why do you think those efforts are less effective in Las Brujas?
12. What do you think is the future of the mangrove forest?
13. What do you want for the mangroves in the future?
14. What is the difference between interstitial and superficial water when we look at salinity?

Questions interview Noé Orantes Olivares (FUNDAECO)

1. What is your name?
2. What is your background (*Think: where did you grow up, how long have you been living here, how did you end up what you do to this day, etcetera*)?
3. What do you do on a daily basis at work?
   (a) How would you describe the title of your job?
4. Where are we right now? Can you describe the area (generally)?
5. How would you explain what mangroves are (*to someone that doesn't know anything about it*)?
6. What is your relation to mangroves?
7. Why are mangroves important?
8. What is the importance of good maintenance of the mangroves?
9. What do you think of the state of the mangroves here at the moment?
10. Is there a difference in regrowth of the mangrove trees between dry and wet season?
11. Did you see the biotope change over the years, and if yes, what has changed related to the following factors? (*Think of mangrove growth, mangrove cover, invasive species, water flow, boats, tourism etc.*)
    (a) What do you think might be the reason for these changes?
12. Can you tell something about the invasive species present in the mangrove forest and its influence?
    (a) How did this change over the years?
13. What people live in/around the mangrove forest?
    (a) What is the interaction of the communities with the mangroves?
    (b) Do you think people take better care of the mangroves now, compared to in the past?
14. What do you think is the future of the mangrove forest?
15. What do you want for the mangroves in the future?

Questions interview Samuel García Cristales (CECON)

1. What is your name and what is your study/work background?
2. What do you do for a living?
   (a) What do you do on a daily basis at work? (*different activities on a day*)
   (b) What is your exact function title?
3. Where are we right now? Can you describe the area (*generally*)?
4. Where does CECON stand for, and how do those goals translate to your job?
5. How many rangers are working for CECON (*If not described previously: and how would you describe their role?*)
6. How would you explain what mangroves are (*to someone that doesn't know anything about it*)?
7. What is your relation to mangroves?
8. Why are mangroves important?
9. What is the importance of good maintenance of the mangroves?
10. What do you think of the state of the mangroves here, at the moment?
11. Are you also involved in other mangrove projects across the coast?
    (a) If yes, are there differences in how the mangrove forests react in the different areas?
12. Do you notice a difference in regrowth of the mangrove trees between the dry and wet season?
13. Did you see the biotope change over the years, and if yes, what has changed related to the following factors? (*Think of mangrove growth, mangrove cover, invasive species, water flow, boats, tourism etc.*)
    (a) What do you think might be the reason for these changes?
14. Can you tell something about the invasive species present in the mangrove forest and its influence?
    (a) How did this change over the years?
    (b) How often do you remove these species and how do you do it?
15. What do you think could be a cause that mangroves struggle to regenerate naturally? (*Think of forest fires, pollution, obstructed flow, etcetera*)
16. What do you think is the future of the mangrove forest?
17. What do you want for the mangroves in the future?

18. Do you know why only six chinampas were built in Las Brujas?
19. Did you ever notice any tidal influences in Las Brujas?
20. Did you notice that some areas of Las Brujas weren't completely dry during the dry season?
    (a) Does this change with the tide?
21. During the dry season, do you notice microcreeks (*small ridges in the ground level that can transport water*) in the ground?
    (a) Was there still water in these microcreeks?

E

Precipitation patterns

Below, the code is given to load the CHIRPS datasets obtained from the Climate Hazard Center (Climate Hazards Center, n.d.). Most of the figures are shown in the main report in section 5.1. However, some figures provide support but are not necessary to understand the research done in the main report. Those are therefore shown in this appendix.

Loading in the datasets from 1981 - 2024 and cropping them to the relevant scale

```
import xarray as xr
import geopandas as gpd
import rioxarray
import matplotlib.pyplot as plt
import pandas as pd
import glob

files = sorted(glob.glob("chirps-v2.0.*.monthly.nc"))
print(f"Found␣{len(files)}␣files:", files)

try:
    import dask
    print("␣Dask␣detected,␣using␣open_mfdataset␣...")
    ds = xr.open_mfdataset(files, combine="by_coords")
except (ImportError, ValueError) as e:
    print("␣Dask␣not␣found␣or␣failed␣-␣using␣manual␣merge␣instead.")
    datasets = [xr.open_dataset(f) for f in files]
    ds = xr.concat(datasets, dim="time")

precip = ds['precip']
precip.rio.write_crs("EPSG:4326", inplace=True)

adm1 = gpd.read_file("gadm41_GTM_1.shp")
depts = ['Escuintla', 'Santa␣Rosa']

all_results = []
for dept in depts:
    geom = adm1[adm1['NAME_1'] == dept].to_crs("EPSG:4326")
    dept_precip = precip.rio.clip(geom.geometry, geom.crs)
    dept_mean = dept_precip.mean(dim=['latitude','longitude'])
    df = dept_mean.to_dataframe().reset_index()
    df['Department'] = dept
    all_results.append(df)

rain_df = pd.concat(all_results)

plt.figure(figsize=(10,6))
for dept in depts:
    subset = rain_df[rain_df['Department'] == dept]
    subset.groupby('time')['precip'].mean().plot(label=dept)
plt.title("Monthly␣Rainfall␣-␣Escuintla␣vs␣Santa␣Rosa␣-(19812024)")
```

```
plt.ylabel("Rainfall (mm/month)")
plt.xlabel("Year")
plt.legend()
plt.grid(True)
plt.show()

rain_df['Year'] = pd.to_datetime(rain_df['time']).dt.year
annual = rain_df.groupby(['Year','Department'])['precip'].sum().reset_index()

plt.figure(figsize=(8,5))
for dept in depts:
    sub = annual[annual['Department']==dept]
    plt.plot(sub['Year'], sub['precip'], marker='o', label=dept)
plt.title("Annual Rainfall Totals -(19812024)")
plt.ylabel("Rainfall (mm/year)")
plt.xlabel("Year")
plt.legend()
plt.grid(True)
plt.savefig('C:/Users/Robin Bruins/Pictures/AnnualprecipESSANROS.png')
plt.show()
```

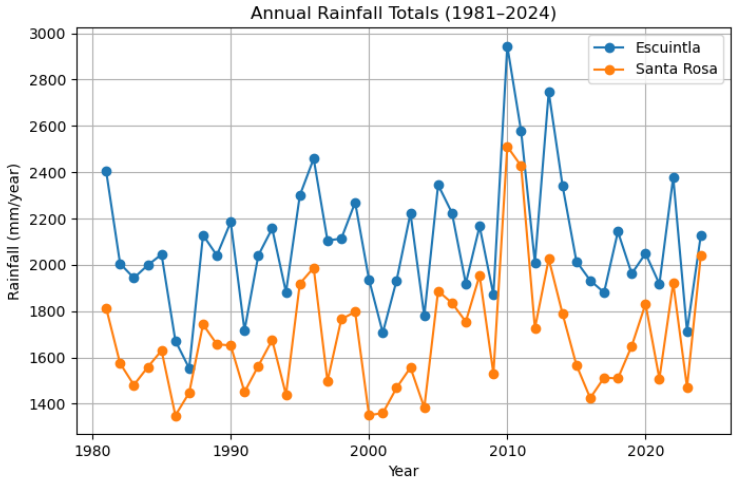

Figure E.1: Annual Rainfall total of the Escuintla, Chiquimula and the Santa Rosa departments (Climate Hazards Center, n.d.) (own image)

Average monthly rainfall plot

This figure can be seen in the main report: figure 3.12

```
monthly_mean = rain_avg.groupby('Month')['precip'].mean().reset_index()
plt.figure(figsize=(8,5))
plt.bar(monthly_mean['Month'], monthly_mean['precip'], color='cornflowerblue')
plt.xticks(range(1,13), ['Jan','Feb','Mar','Apr','May','Jun','Jul','Aug','Sep','Oct','Nov','
    Dec'])
plt.title('Average Monthly Rainfall -(19812024)')
plt.ylabel('Rainfall (mm/month)')
plt.xlabel('Month')
plt.grid(True, axis='y')
plt.savefig('C:/Users/Robin Bruins/Pictures/MonthlyAverage.png')
plt.show()
```

Total annual precipitation of the catchment area plot

This figure can be seen in the main report: figure 5.1

```
rain_df['time']  = pd.to_datetime(rain_df['time'])
rain_df['Year']  = rain_df['time'].dt.year
```

```
rain_df['Month'] = rain_df['time'].dt.month
rain_avg = (
    rain_df.groupby(['Year','Month'])['precip']
    .mean()
    .reset_index()
)

rain_avg = rain_avg[rain_avg['Year'].between(1981, 2024)]
```

Monthly precipitation levels with linear trend lines plot

This figure can be seen in the main report: figure 5.2

```
rain_df['Year'] = pd.to_datetime(rain_df['time']).dt.year
rain_df['Month'] = pd.to_datetime(rain_df['time']).dt.month
combined = (rain_df
            .groupby(['Year','Month'])['precip']
            .mean()
            .reset_index())

fig, axes = plt.subplots(3, 4, figsize=(15,10), sharey=True)
axes = axes.flatten()
month_names = ['Jan','Feb','Mar','Apr','May','Jun','Jul','Aug','Sep','Oct','Nov','Dec']

for i, month in enumerate(range(1,13)):
    ax = axes[i]
    sub = combined[combined['Month'] == month]
    ax.plot(sub['Year'], sub['precip'], marker='o', color='steelblue', label='Rainfall')

    if len(sub) > 1:
        z = np.polyfit(sub['Year'], sub['precip'], 1)
        p = np.poly1d(z)
        ax.plot(sub['Year'], p(sub['Year']), color='red', linestyle='--', label='Trend')

    ax.set_title(month_names[i])
    ax.grid(True)

    ax.xaxis.set_major_locator(mticker.MultipleLocator(5))
    ax.set_xticks(sub['Year'][::5])  # tick every 5 years
    ax.set_xticklabels(sub['Year'][::5], rotation=45)

    if i % 4 == 0:
        ax.set_ylabel('Rainfall (mm)')
    if i >= 8:
        ax.set_xlabel('Year')

plt.suptitle('Monthly Precipitation levels with Linear Trend Lines\n(Catchment area, -
    19812024)', fontsize=14)
plt.tight_layout(rect=[0, 0.03, 1, 0.95])

plt.savefig('C:/Users/Robin Bruins/Pictures/MonthlyPrecipitationtrend.png')
plt.show()
```

Three wettest months plot

Figure E.2 can be used to understand what the wettest months have been throughout the years. On the horizontal axis, all the years are plotted, and on the vertical axis, all the months are plotted. For each year, the three wettest months have been plotted with dots that range in the blue colour scheme. The darker the blue colour is, the wetter this month has been. As can be seen, both June and September have been among the wettest months for most of the year, indicating the peaks of the traditional wet season. It can also be seen that in the later decades, October has appeared more often.

```
import matplotlib.pyplot as plt
import seaborn as sns
import numpy as np

top3 = (combined.sort_values(['Year','precip'], ascending=[True, False])
               .groupby('Year')
               .head(3)
```

```
                .reset_index(drop=True))

plt.figure(figsize=(10,6))
sc = plt.scatter(
    top3['Year'], top3['Month'],
    c=top3['precip'], cmap='Blues', s=80, edgecolor='k', alpha=0.8
)
plt.colorbar(sc, label='Rainfall (mm)')
plt.yticks(range(1,13), ['Jan','Feb','Mar','Apr','May','Jun','Jul','Aug','Sep','Oct','Nov','
    Dec'])
plt.title("3 Wettest Months per Year (19812024)\nCatchment area")
plt.xlabel("Year"); plt.ylabel("Month")
plt.grid(True, linestyle=':')
plt.tight_layout()

plt.savefig('C:/Users/Robin Bruins/Pictures/wettestmonths.png')
plt.show()
```

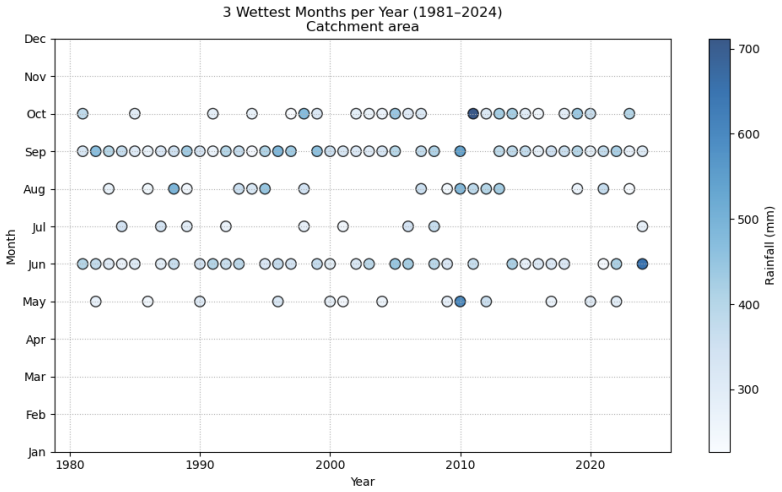

Figure E.2: 3 wettest months per year (1981 - 2024) for the catchment area (Climate Hazards Center, n.d.) (own image)

Shift of the wet season center plot

Figure 5.4 shows the location of the wet season for each year between 1981 and 2024. On the horizontal axis, all the years have been plotted against the number of the month on the vertical axis, where the number 7 indicates the month of July and the number 8 indicates the month of August. Throughout the years, the center of the wet season is located most of the times located in July, with only one occasion where it was located in August. This graph shows there is a tiny shift towards later in July; however, this is not big enough to say that there is a trend.

```
rain_df['time'] = pd.to_datetime(rain_df['time'])
rain_df['Year'] = rain_df['time'].dt.year
rain_df['Month'] = rain_df['time'].dt.month
def rainfall_centroid(group):
    months = group['Month']
    weights = group['precip']
    return (months * weights).sum() / weights.sum()

centroid = (
    rain_df.groupby(['Year', 'Department'])
    .apply(rainfall_centroid)
    .reset_index(name='Rainfall_Centroid')
)

centroid_avg = (
    centroid.groupby('Year')['Rainfall_Centroid']
    .mean()
    .reset_index()
)
```

```

plt.figure(figsize=(8,5))
plt.plot(
    centroid_avg['Year'], centroid_avg['Rainfall_Centroid'],
    marker='o', color='steelblue', label='Center of wet season'
)

if len(centroid_avg) > 1:
    z = np.polyfit(centroid_avg['Year'], centroid_avg['Rainfall_Centroid'], 1)
    p = np.poly1d(z)
    plt.plot(
        centroid_avg['Year'], p(centroid_avg['Year']),
        linestyle='--', color='red', label='Trend'
    )

plt.title("Shift of the Wet Season Center -(19812024)")
plt.ylabel("Mean Month (1 = Jan ... 12 = Dec)")
plt.xlabel("Year")
plt.legend()
plt.grid(True)

plt.gca().xaxis.set_major_locator(mticker.MultipleLocator(5))
plt.xlim(1980, 2025)
plt.xticks(rotation=45)

plt.tight_layout()

plt.savefig('C:/Users/Robin Bruins/Pictures/Shiftofwetseason.png')

plt.show()
```

Percentage of annual rainfall in wet season plot

figure E.3 Shows the percentage of the total annual rainfall measured in the traditional wet season lasting from May until October. This graph shows that throughout the decades, there is a small increase in the occurrence of precipitation outside of the traditional wet season. However, it cannot be said that this is a trend throughout the years, but rather a result of seasonal variability.

```
rainy = rain_avg[rain_avg['Month'].between(5,10)]
rainy_sum = rainy.groupby('Year')['precip'].sum()
total_sum = rain_avg.groupby('Year')['precip'].sum()
ratio = ((rainy_sum / total_sum) * 100).reset_index(name='RainySeasonFraction')
plt.figure(figsize=(8,5))
plt.plot(ratio['Year'], ratio['RainySeasonFraction'], marker='o', color='steelblue')
z = np.polyfit(ratio['Year'], ratio['RainySeasonFraction'], 1)
p = np.poly1d(z)
plt.plot(ratio['Year'], p(ratio['Year']), '--', color='red')
plt.title('Percentage of Annual Rainfall in the Wet Season (-MayOct)')
plt.ylabel('Percentage of total rainfall')
plt.xlabel('Year')
plt.grid(True)
plt.gca().xaxis.set_major_locator(mticker.MultipleLocator(5))
plt.tight_layout()
plt.savefig('C:/Users/Robin Bruins/Pictures/Precipitationpercentage.png')
plt.show()
```

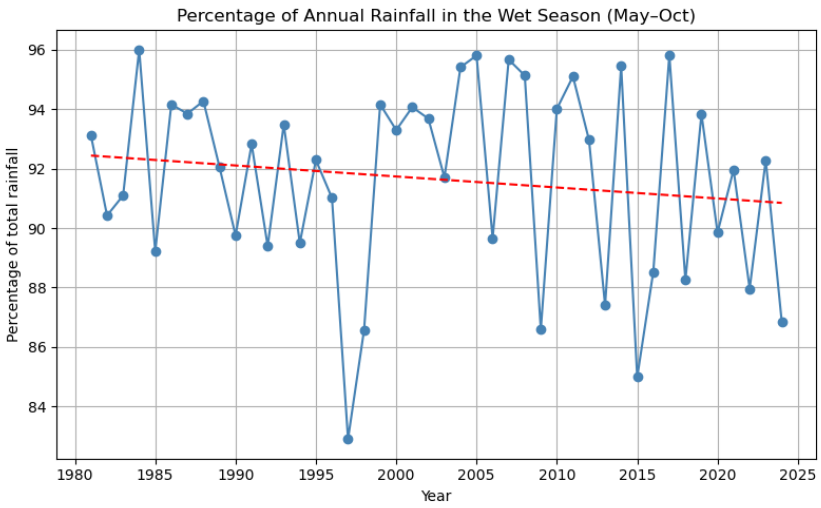

Figure E.3: Percentage of precipitation in the wet season (Climate Hazards Center, n.d.) (own image)

Decadal comparison of monthly precipitation plot

This figure can be seen in the main report: figure 5.3

```
rain_avg['Decade'] = (rain_avg['Year']//10)*10
decadal = rain_avg.groupby(['Decade','Month'])['precip'].mean().reset_index()

plt.figure(figsize=(10,5))
sns.lineplot(
    data=decadal, x='Month', y='precip',
    hue='Decade', marker='o', palette='viridis'
)

plt.xticks(
    ticks=np.arange(1,13),
    labels=['Jan','Feb','Mar','Apr','May','Jun','Jul','Aug','Sep','Oct','Nov','Dec']
)

plt.title('Decadal Comparison of Monthly Precipitation (19812024)')
plt.ylabel('Mean Precipitation (mm)')
plt.xlabel('Month')
plt.legend(title='Decade', bbox_to_anchor=(1.05,1), loc='upper left')
plt.grid(True)
plt.tight_layout()
plt.savefig('C:/Users/Robin Bruins/Pictures/Decadalchange.png')
plt.show()
```

Code relevant for the statistical checks

Below, the relevant code for the statistical checks is posted. In chapter 4, the relevance of these checks and what checks have been done is explained.

```
    import numpy as np
import pandas as pd
import matplotlib.pyplot as plt

rain_df['time']  = pd.to_datetime(rain_df['time'])
rain_df['Year']  = rain_df['time'].dt.year
rain_df['Month'] = rain_df['time'].dt.month


combined = (
    rain_df.groupby(['Year','Month'])['precip']
    .mean()
    .reset_index()
```

```
)

annual_totals = combined.groupby('Year')['precip'].sum().reset_index(name='Annual_mm')

rainy = combined[combined['Month'].between(5,10)]
rainy_totals = rainy.groupby('Year')['precip'].sum().reset_index(name='Rainy_mm')
annual_for_ratio = annual_totals.merge(rainy_totals, on='Year', how='left').fillna(0.0)
annual_for_ratio['RainyShare_pct'] = (annual_for_ratio['Rainy_mm']/annual_for_ratio['Annual_mm
    ']*100)

    m = group['Month'].values.astype(float)
    w = group['precip'].values.astype(float)
    return (m*w).sum()/w.sum() if w.sum() > 0 else np.nan

centroid_by_dept = (
    rain_df.groupby(['Year','Department'])
    .apply(rainfall_centroid)
    .reset_index(name='Rainfall_Centroid')
)

centroid_avg = (
    centroid_by_dept.groupby('Year')['Rainfall_Centroid']
    .mean()
    .reset_index()
)

def mk_summary(y, label):
    y = y.dropna()
    res = original_test(y.values)  # trend, h, p, Tau, s, var_s, z, slope, intercept
    print(f"\n=== {label} ===")
    print(f"Trend: {res.trend} | p={res.p:.4f} | Sen slope={res.slope:.4f} per year | Tau={res
        .Tau:.3f}")
    return res

mk_summary(annual_totals.set_index('Year')['Annual_mm'], "Annual rainfall (mm)")

mk_summary(annual_for_ratio.set_index('Year')['RainyShare_pct'], "Rainy-season share (%)")

mk_summary(centroid_avg.set_index('Year')['Rainfall_Centroid'], "Center of wet season (month)"
    )

def ols_with_ci(df, ycol):
    d = df.dropna().copy()
    X = sm.add_constant(d['Year'])
    model = sm.OLS(d[ycol], X).fit()
    print(f"\nOLS for {ycol}:\nSlope={model.params['Year']:.3f}  (p={model.pvalues['Year']:.4f
        })  R²={model.rsquared:.3f}")

    ci = model.conf_int().loc['Year']
    print(f"95% CI for slope: [{ci[0]:.3f}, {ci[1]:.3f}]")
    return model

ols_with_ci(annual_totals, 'Annual_mm')
ols_with_ci(annual_for_ratio, 'RainyShare_pct')
ols_with_ci(centroid_avg, 'Rainfall_Centroid')


def two_period_tests(series, early=(1981,2000), late=(2001,2024), label=""):
    s = series.dropna()
    s_early = s.loc[(s.index>=early[0]) & (s.index<=early[1])]
    s_late  = s.loc[(s.index>=late[0])  & (s.index<=late[1])]
    print(f"\n=== {label} | {early[0]}{early[1]} vs {late[0]}{late[1]} ===")
    print(f"Means: early={s_early.mean():.2f}, late={s_late.mean():.2f}")

    t,p = stats.ttest_ind(s_early, s_late, equal_var=False, nan_policy='omit')
    print(f"Welch t-test: t={t:.2f}, p={p:.4f}")

    u,p2 = stats.mannwhitneyu(s_early, s_late, alternative='two-sided')
    print(f"-MannWhitney U: U={u:.0f}, p={p2:.4f}")


two_period_tests(annual_totals.set_index('Year')['Annual_mm'], label="Annual rainfall (mm)")

```

```
two_period_tests(annual_for_ratio.set_index('Year')['RainyShare_pct'], label="Rainy-season share (%)")

two_period_tests(centroid_avg.set_index('Year')['Rainfall_Centroid'], label="Center of wet season (month)")

rng = np.random.default_rng(42)

def bootstrap_mean_ci(x, B=10000, alpha=0.05):
    x = np.asarray(x, float)
    boots = rng.choice(x, size=(B, x.size), replace=True).mean(axis=1)
    lo, hi = np.quantile(boots, [alpha/2, 1-alpha/2])
    return boots.mean(), lo, hi

def bootstrap_diff_ci(x, y, B=10000, alpha=0.05):
    x = np.asarray(x, float); y = np.asarray(y, float)
    xb = rng.choice(x, size=(B, x.size), replace=True).mean(axis=1)
    yb = rng.choice(y, size=(B, y.size), replace=True).mean(axis=1)
    diff = yb - xb
    dmean = diff.mean()
    lo, hi = np.quantile(diff, [alpha/2, 1-alpha/2])
    return dmean, lo, hi

early = (1981,2000)
late  = (2001,2024)

centroid_series = centroid_avg.set_index('Year')['Rainfall_Centroid'].dropna()
early_vals = centroid_series.loc[early[0]:early[1]].values
late_vals  = centroid_series.loc[late[0]:late[1]].values

mE, loE, hiE = bootstrap_mean_ci(early_vals)
mL, loL, hiL = bootstrap_mean_ci(late_vals)
d, loD, hiD  = bootstrap_diff_ci(early_vals, late_vals)

print("\n=== Bootstrap CIs (wet-season center, in month units) ===")
print(f"Early {early-[0]}{early[1]}:  mean={mE:.2f}  95% CI [{loE:.2f}, {hiE:.2f}]")
print(f"Late  {late-[0]}{late[1]}:  mean={mL:.2f}  95% CI [{loL:.2f}, {hiL:.2f}]")
print(f"Difference (Late - Early):  Δ={d:.2f}  95% CI [{loD:.2f}, {hiD:.2f}]")

annual_max = (combined.groupby('Year')['precip']
              .max().reset_index(name='MaxMonth_mm'))

mk = original_test(annual_max['MaxMonth_mm'].values)
print(f"[Max monthly mm] trend={mk.trend}, p={mk.p:.4f}, Sen slope={mk.slope:.2f}/yr, Tau={mk.Tau:.3f}")

X = sm.add_constant(annual_max['Year'])
model = sm.OLS(annual_max['MaxMonth_mm'], X).fit()
print(f"OLS slope={model.params['Year']:.2f}, p={model.pvalues['Year']:.4f}, R²={model.rsquared:.3f}")
print("95% CI for slope:", model.conf_int().loc['Year'].tolist())

annual_sd = (combined.groupby('Year')['precip']
             .std().reset_index(name='IntraAnnualSD'))
mk_sd = original_test(annual_sd['IntraAnnualSD'].values)
print(f"[Intra-annual SD] trend={mk_sd.trend}, p={mk_sd.p:.4f}, Sen slope={mk_sd.slope:.3f}/yr")

early, late = (1981,2000), (2001,2024)
sd_series = annual_sd.set_index('Year')['IntraAnnualSD']
sd_early = sd_series.loc[early[0]:early[1]].dropna()
sd_late  = sd_series.loc[late[0]:late[1]].dropna()

W, p_levene = stats.levene(sd_early, sd_late, center='median')
print(f"Levene variance test: W={W:.2f}, p={p_levene:.4f} (diff in variability between periods?)")

year_tot = combined.groupby('Year')['precip'].sum().rename('YearTotal')
mshare = combined.join(year_tot, on='Year')
mshare['share'] = mshare['precip'] / mshare['YearTotal']

hhi = (mshare.assign(sq=lambda d: d['share']**2)
       .groupby('Year')['sq'].sum().reset_index(name='HHI'))
```

```

ent = (mshare.assign(term=lambda d: d['share']*np.log(d['share'].replace(0,np.nan))))
ent = ent.groupby('Year')['term'].sum().reset_index()
ent['Shannon'] = -ent['term']

mk_hhi = original_test(hhi['HHI'].values)
mk_ent = original_test(ent['Shannon'].values)
print(f"[HHI] trend={mk_hhi.trend}, p={mk_hhi.p:.4f}, slope={mk_hhi.slope:.5f}/yr")
print(f"[Shannon] trend={mk_ent.trend}, p={mk_ent.p:.4f}, slope={mk_ent.slope:.5f}/yr")

annual_by_dept = (rain_df.groupby(['Department','Year'])['precip']
                  .sum().reset_index())

for dept in annual_by_dept['Department'].unique():
    series = annual_by_dept[annual_by_dept['Department']==dept]['precip'].values
    mkd = original_test(series)
    print(f"[{dept}] Annual mm trend={mkd.trend}, p={mkd.p:.4f}, slope={mkd.slope:.2f}/yr, Tau
        ={mkd.Tau:.3f}")
```

F

Tidal cyclus

This appendix presents the tidal height and coefficient data used to assess the tidal conditions around the observation period. The figures illustrate the daily tidal variations and the corresponding tidal coefficients of the 6th and 8th of October 2025.

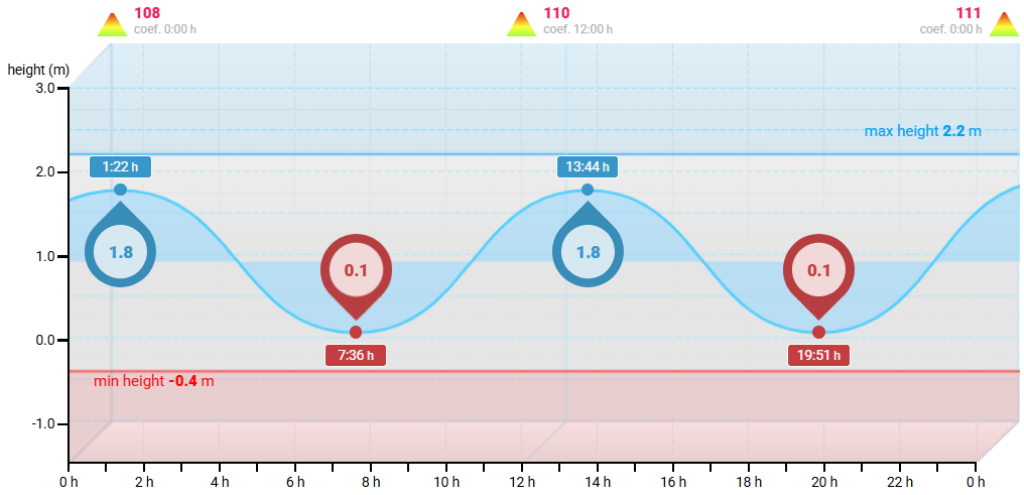

Figure F.1: Tidal height variations and tidal coefficient on 6 October 2025, indicating strong tidal range near spring tide conditions ("Tide times and charts for Monterrico, Santa Rosa and weather forecast for fishing in Monterrico in 2025," n.d.).

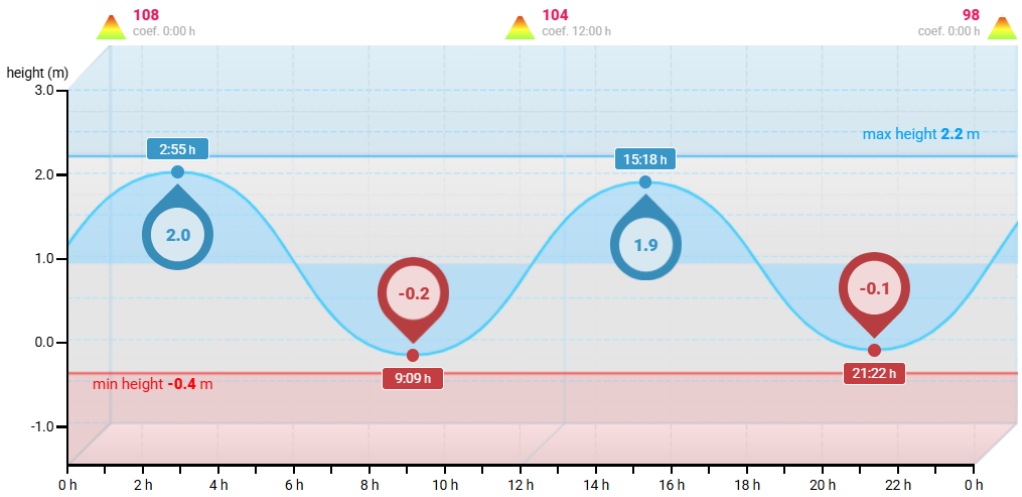

Figure F.2: Tidal height variations and tidal coefficient on 8 October 2025, indicating strong tidal range near spring tide conditions ("Tide times and charts for Monterrico, Santa Rosa and weather forecast for fishing in Monterrico in 2025," n.d.).

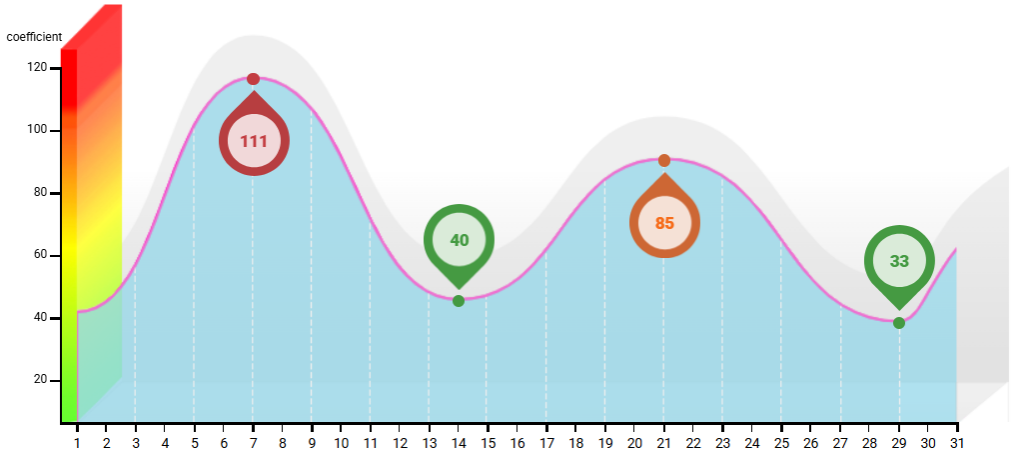

Figure F.3: Tidal coefficient variation over the month, showing peaks corresponding to spring tides and lows corresponding to neap tides ("Tide times and charts for Monterrico, Santa Rosa and weather forecast for fishing in Monterrico in 2025," n.d.).

G

Sediment measurements

In this appendix, weights of the sediment experiment are shown.

Location	Mean weight	Unit	Location	Mean weight	Unit
1.1	1.531	g	1.2	1.541	g
2.1	1.528	g	2.2	1.529	g
3.1	1.521	g	3.2	1.510	g
4.1	1.527	g	4.2	1.526	g
5.1	1.516	g	5.2	1.515	g
6.1	1.506	g	6.2	1.514	g
7.1	1.529	g	7.2	1.547	g
C1	1.535	g	C2	1.535	g

Table G.1: Mean values of the filter and sediment of samples in experiment 1 after 3 days

Location	Mean weight	Unit	Location	Mean weight	Unit
1.1	1.475	g	1.2	1.488	g
2.1	1.478	g	2.2	1.476	g
3.1	1.473	g	3.2	1.462	g
4.1	1.478	g	4.2	1.482	g
5.1	1.471	g	5.2	1.468	g
6.1	1.461	g	6.2	1.464	g
7.1	1.483	g	7.2	1.476	g
C1	1.480	g	C2	1.481	g

Table G.2: Mean values of the filter and sediment of samples in experiment 1 after 8 days

Location	Measurement 1 (g)	Measurement 2 (g)	Measurement 3 (g)	Mean (g)
1.1	1.532	1.532	1.528	1.531
1.2	1.541	1.541	1.541	1.541
2.1	1.529	1.526	1.529	1.528
2.2	1.529	1.529	1.529	1.529
3.1	1.522	1.521	1.521	1.522
3.2	1.510	1.511	1.510	1.510
4.1	1.528	1.526	1.526	1.527
4.2	1.525	1.527	1.527	1.526
5.1	1.515	1.517	1.515	1.516
5.2	1.515	1.514	1.517	1.515
6.1	1.507	1.506	1.506	1.506
6.2	1.513	1.514	1.514	1.514
7.1	1.530	1.527	1.530	1.529
7.2	1.548	1.546	1.548	1.547
C1	1.534	1.534	1.536	1.535
C2	1.537	1.534	1.535	1.535

Table G.3: Raw data used to calculate the mean of the filter and sediment weight of experiment 1 after 3 days

Location	Measurement 1 (g)	Measurement 2 (g)	Measurement 3 (g)	Mean (g)
1.1	1.476	1.473	1.476	1.475
1.2	1.488	1.486	1.490	1.488
2.1	1.475	1.479	1.480	1.478
2.2	1.478	1.475	1.475	1.476
3.1	1.475	1.473	1.470	1.473
3.2	1.463	1.460	1.464	1.462
4.1	1.478	1.478	1.478	1.478
4.2	1.483	1.480	1.482	1.482
5.1	1.469	1.472	1.471	1.471
5.2	1.466	1.468	1.470	1.468
6.1	1.462	1.462	1.459	1.461
6.2	1.462	1.462	1.469	1.464
7.1	1.486	1.482	1.482	1.483
7.2	1.497	1.490	1.500	1.476
C1	1.481	1.478	1.478	1.480
C2	1.481	1.480	1.483	1.481

Table G.4: Raw data used to calculate the mean of the filter and sediment weight of experiment 1 after 3 days

Baseline filter	Weight	Unit
1	1.463	g
2	1.493	g
3	1.495	g
4	1.481	g
5	1.500	g
6	1.485	g
7	1.490	g
8	1.512	g
9	1.481	g
10	1.492	g
Mean	**1.489**	**g**

Table G.5: Baseline measurements for a single filter

Filter	Measurement 1 (g)	Measurement 2 (g)	Measurement 3 (g)	Mean	Used for sample
1	1.500	1.500	1.500	1.500	1.1
2	1.480	1.480	1.480	1.480	1.2
3	1.490	1.500	1.495	1.495	2.1
4	1.480	1.481	1.481	1.481	2.2
5	1.494	1.493	1.490	1.492	3.1
6	1.513	1.514	1.512	1.513	3.2
7	1.482	1.479	1.480	1.480	4.1
8	1.472	1.471	1.471	1.471	4.2
9	1.500	1.500	1.500	1.500	5.1
10	1.526	1.526	1.524	1.525	6.2
11	1.508	1.509	1.505	1.507	6.1
12	1.483	1.481	1.479	1.481	5.2
13	1.500	1.496	1.500	1.499	7.1
14	1.505	1.504	1.506	1.505	7.2
15	1.484	1.483	1.483	1.483	C1
16	1.503	1.500	1.500	1.501	C2

Table G.6: Raw data to calculate mean weight of filters prior to filtration

Location	Weight filter	Weight filter+sediment	Difference	Unit
1.1	1.500	1.500	0.000	g
1.2	1.480	1.477	-0.003	g
2.1	1.495	1.493	-0.002	g
2.2	1.481	1.475	-0.006	g
3.1	1.492	1.482	-0.010	g
3.2	1.513	1.508	-0.007	g
4.1	1.480	1.476	-0.004	g
4.2	1.471	1.461	-0.010	g
5.1	1.500	1.487	-0.013	g
5.2	1.525	1.510	-0.015	g
6.1	1.507	1.497	-0.010	g
6.2	1.481	1.471	-0.010	g
7.1	1.499	1.484	-0.015	g
7.2	1.505	1.493	-0.012	g
C1	1.483	1.467	-0.016	g
C2	1.501	1.489	-0.012	g
Mean	**1.496**	**1.486**	**-0.010**	**g**

Table G.7: Mean values of samples experiment 2 after 3 days

Location	Weight filter	Weight filter+sediment	Difference	Unit
1.1	1.500	1.526	+0.026	g
1.2	1.480	1.504	+0.024	g
2.1	1.495	1.522	+0.027	g
2.2	1.481	1.500	+0.019	g
3.1	1.492	1.509	+0.017	g
3.2	1.513	1.530	+0.017	g
4.1	1.480	1.500	+0.020	g
4.2	1.471	1.491	+0.020	g
5.1	1.500	1.519	+0.019	g
5.2	1.525	1.535	+0.012	g
6.1	1.507	1.521	+0.014	g
6.2	1.481	1.500	+0.019	g
7.1	1.499	1.508	+0.009	g
7.2	1.505	1.518	+0.013	g
C1	1.483	1.500	+0.017	g
C2	1.501	1.516	+0.015	g
Mean	**1.495**	**1.512**	**+0.017**	**g**

Table G.8: Mean values of samples experiment 2 after 8 days

Location	Measurement 1 (g)	Measurement 2 (g)	Measurement 3 (g)	Mean (g)
1.1	1.500	1.500	1.500	1.500
1.2	1.479	1.477	1.475	1.477
2.1	1.494	1.494	1.492	1.493
2.2	1.475	1.475	1.475	1.475
3.1	1.483	1.480	1.483	1.482
3.2	1.507	1.509	1.508	1.508
4.1	1.476	1.476	1.477	1.476
4.2	1.462	1.462	1.459	1.461
5.1	1.488	1.484	1.490	1.487
5.2	1.511	1.509	1.511	1.510
6.1	1.500	1.495	1.497	1.497
6.2	1.470	1.470	1.472	1.471
7.1	1.484	1.484	1.484	1.484
7.2	1.492	1.493	1.495	1.493
C1	1.467	1.466	1.469	1.467
C2	1.489	1.488	1.489	1.489

Table G.9: Raw data used to calculate the mean of the filter and sediment weight of experiment 2 after 3 days

Location	Measurement 1 (g)	Measurement 2 (g)	Measurement 3 (g)	Mean (g)
1.1	1.526	1.526	1.526	1.526
1.2	1.504	1.503	1.506	1.504
2.1	1.524	1.520	1.522	1.522
2.2	1.500	1.500	1.500	1.500
3.1	1.508	1.509	1.510	1.509
3.2	1.529	1.531	1.529	1.530
4.1	1.500	1.500	1.500	1.500
4.2	1.491	1.492	1.491	1.491
5.1	1.520	1.519	1.518	1.519
5.2	1.535	1.535	1.535	1.535
6.1	1.522	1.522	1.520	1.521
6.2	1.500	1.500	1.500	1.500
7.1	1.511	1.508	1.506	1.508
7.2	1.517	1.518	1.518	1.518
C1	1.500	1.500	1.500	1.500
C2	1.516	1.516	1.517	1.516

Table G.10: Raw data used to calculate the mean of the filter and sediment weight of experiment 2 after 8 days

H

Physical-Chemical data

In this appendix, graphs from the physical-chemical parameters are depicted. These graphs are based on the measurements found in appendix I. The locations of the measurements can be found in figure 4.6 and figure 4.7.

Firstly, in figure H.1, figure H.2 and figure H.3, measurements of the different measurement days per site are depicted. The measurements days are October 2nd, 3rd and 8th 2025.

Furthermore, in figure H.4, figure H.5 and figure H.6, point maps of pH, redox potential and temperature are shown. Values for pH lie between 7.28 and 7.46. Potential redox values vary between -47.2 and 181.4. Temperature values lie between 27.07 and 32.72 where the outlier of 43.67 is taken as a measurement error. Similar to the salinity map shown in figure 5.12, generally no significant difference can be found between the reference areas and the Las Brujas area. What can be observed in figure H.6 is that the temperatures in Reference Area A are 2 to 3 degrees lower. This is, however, due to the fact that the measurements in Reference Area A were done early in the morning and the measurements in Las Brujas and Reference Area B were done in the afternoon. That way, the water in the latter areas had time to warm up by the sun.

Lastly, physical-chemical measurements were done in a river upstream of the Las Brujas area. The locations of these measurements are depicted in figure 4.6 and figure 4.7. The aim of these measurements was to compare these salinity values to the salinity values in the Las Brujas area to check the tidal influence in the area. Besides that, from the salinity values one could deduce the presence of various types of farms that could influence the mangrove growth conditions in Las Brujas. Observed can be that the salinity values in the upstream are significantly lower compared to the Las Brujas area as they lie between 0.05 and 0.09 PSU in the river area and between 0.2 and 0.3 in the area of Las Brujas. This low salinity rate in the river area suggests there is very little tidal influence in the river area. During a interview, a local inhabitant could confirm this (Lopéz, 2025). Furthermore, there seem to be no extreme values present in the salinity or pH values. This leads to the conclusion that there are no influential farms near the examined river. This was also confirmed by the local inhabitant. However, stated was that these kind of farms, such as shrimp and cattle farms, are located on private property. The actual influence of these farms on the river system and mangrove biotope is therefore hard to investigate (Lopéz, 2025).

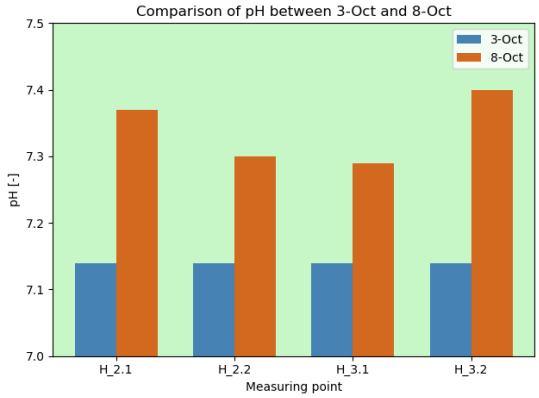

(a) Comparison of pH values in Helicopter area between October 3rd and 8th.

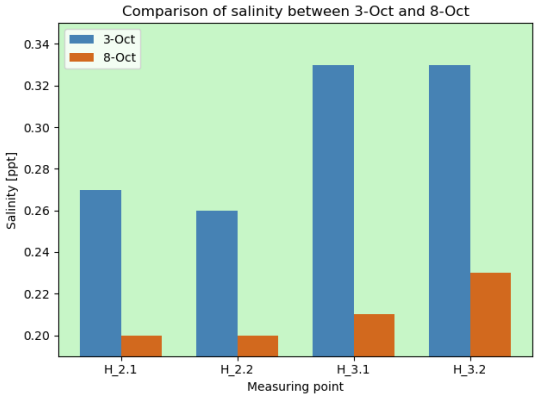

(b) Comparison of salinity values in Helicopter area between October 3rd and 8th.

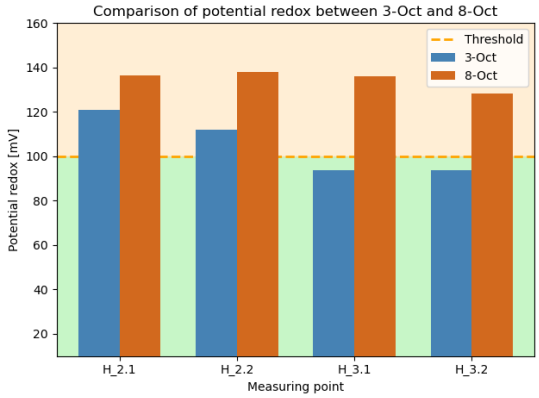

(c) Comparison of redox potential values in Helicopter area between October 3rd and 8th.

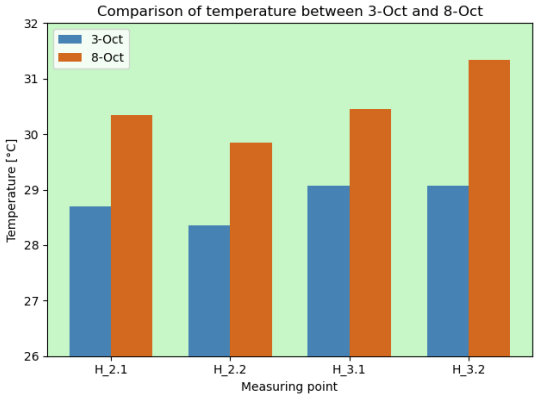

(d) Comparison of temperature values in Helicopter area between October 3rd and 8th.

Figure H.1: Comparison of physical-chemical values of the Helicopter area, measured on October 3rd and 8th. Measured values are pH levels (a), salinity (b), potential redox (c) and temperature (d). Blue bars represent measurements on October 3rd, brown bars represent measurements on October 8th. The graphs' backgrounds depict the healthy (green) and acceptable range (orange) for red mangroves to grow. (own image)

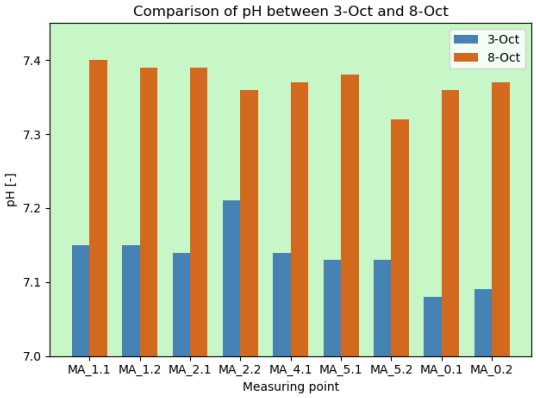

(a) Comparison of pH values in Marco Antonio area between October 3rd and 8th.

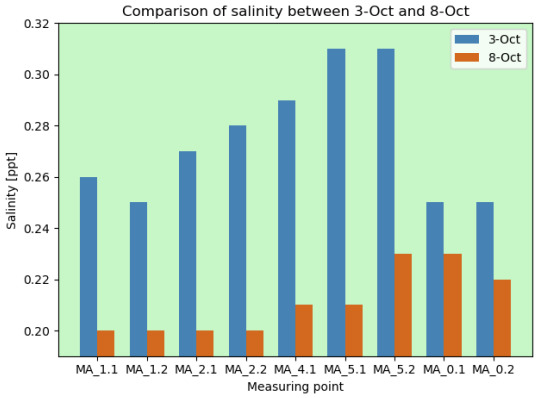

(b) Comparison of salinity values in Marco Antonio area between October 3rd and 8th.

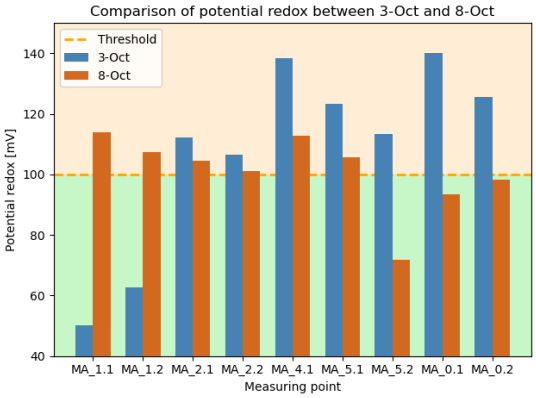

(c) Comparison of redox potential values in Marco Antonio area between October 3rd and 8th.

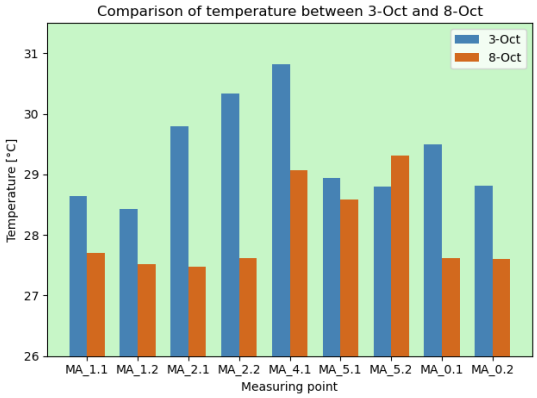

(d) Comparison of temperature values in Marco Antonio area between October 3rd and 8th.

Figure H.2: Comparison of physical-chemical values of the Marco Antonio area, measured on October 3rd and 8th. Measured values are pH levels (a), salinity (b), potential redox (c) and temperature (d). Blue bars represent measurements on October 3rd, brown bars represent measurements on October 8th. The graphs' backgrounds depict the healthy (green) and acceptable range (orange) for red mangroves to grow. (own image)

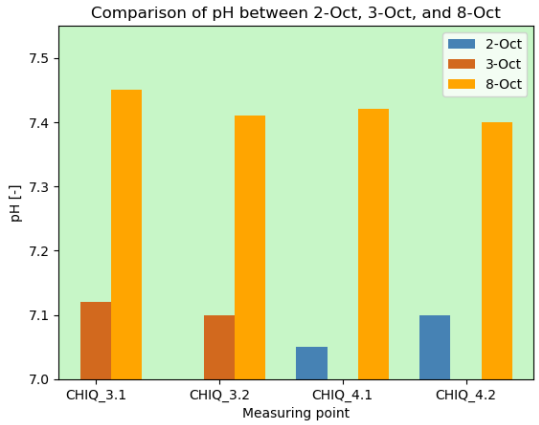

(a) Comparison of pH values in the Chiquimulilla river between October 2nd, 3rd and 8th.

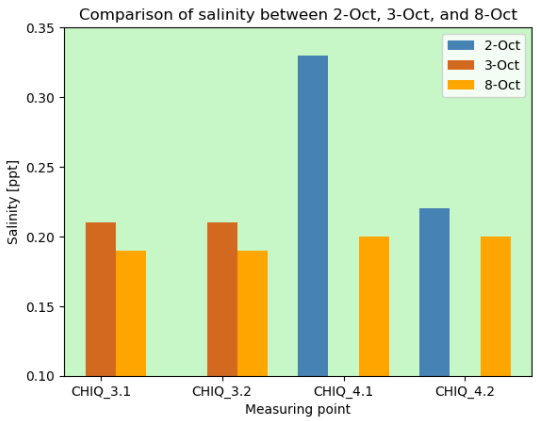

(b) Comparison of salinity values in the Chiquimulilla river between October 2nd, 3rd and 8th.

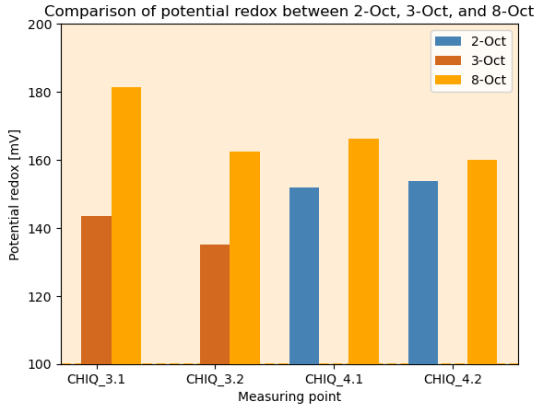

(c) Comparison of redox potential values in the Chiquimulilla river between October 2nd, 3rd and 8th.

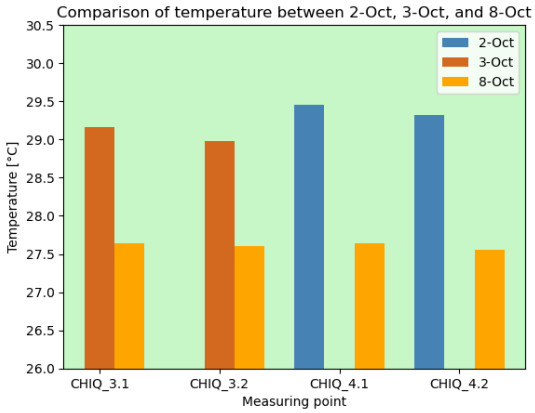

(d) Comparison of temperature values in the Chiquimulilla river between October 2nd, 3rd and 8th.

Figure H.3: Comparison of physical-chemical values of the Chiquimulilla river, measured on October 2nd, 3rd and 8th. Measured values are pH levels (a), salinity (b), potential redox (c) and temperature (d). Blue bars represent measurements on October 2nd, brown bars represent measurements on October 3rd and yellow bars represent measurements on October 8th. The graphs' backgrounds depict the healthy (green) and acceptable range (orange) for red mangroves to grow. (own image)

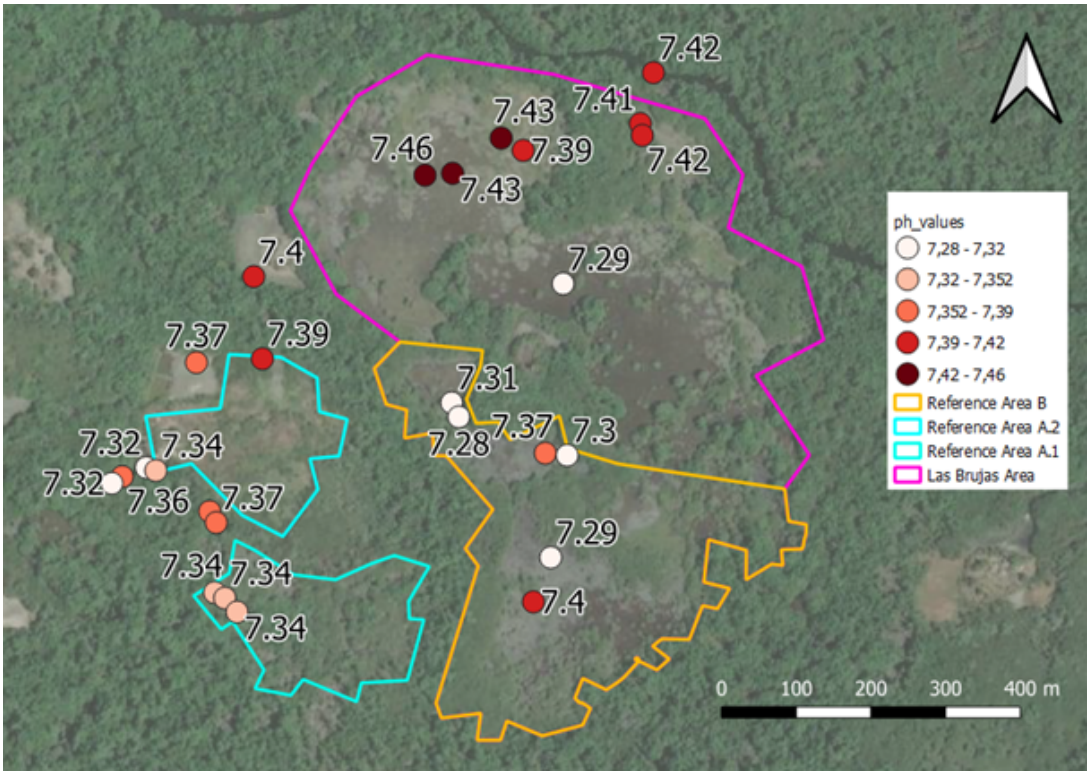

Figure H.4: Point map showing pH values in different areas around Las Brujas. All measurements are taken on October 8th, 2025. (own image)

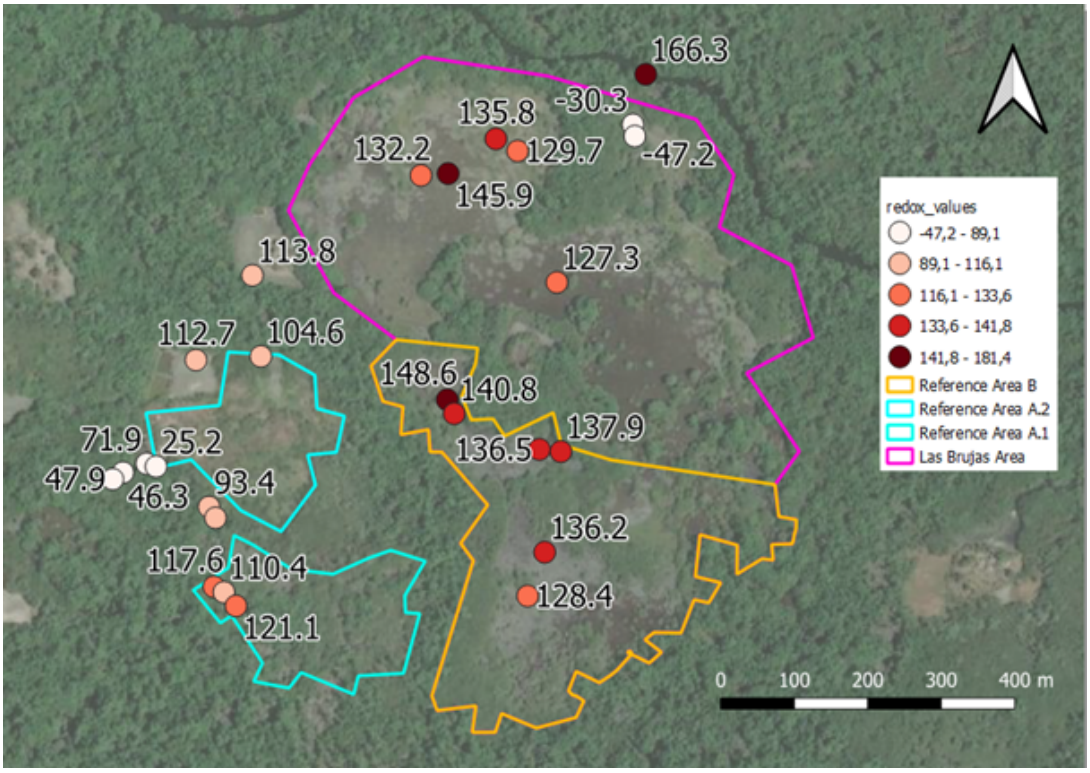

Figure H.5: Point map showing potential redox values in different areas around Las Brujas. All measurements are taken on October 8th, 2025. (own image)

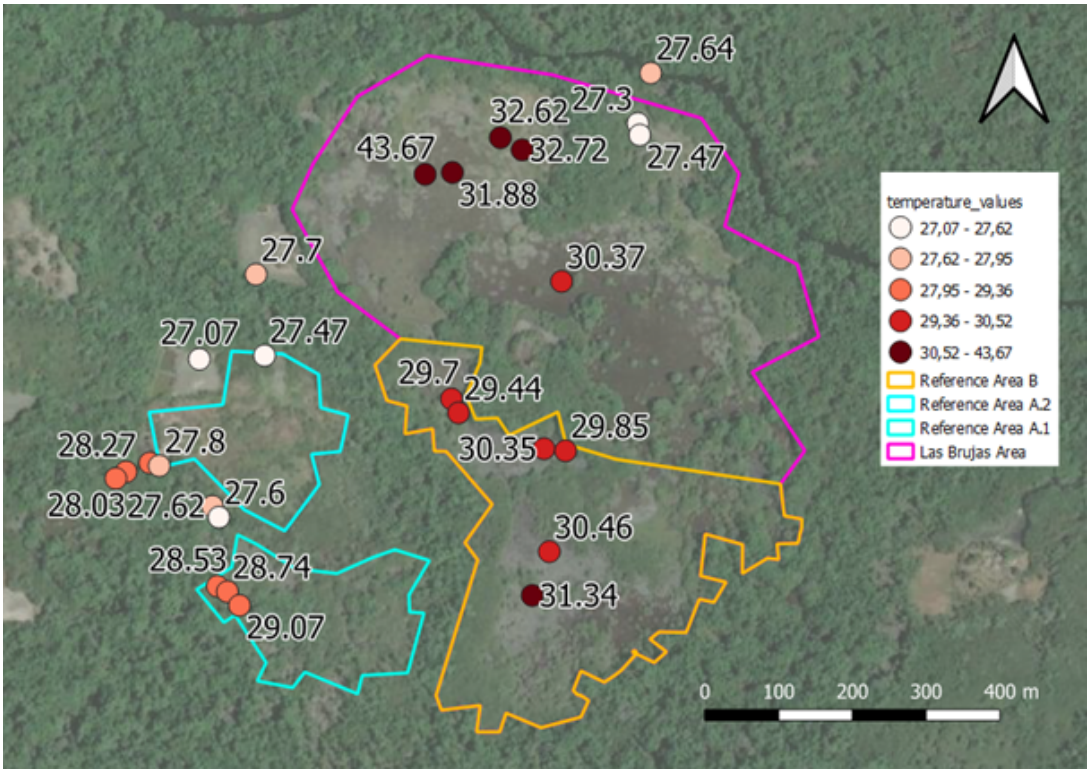

Figure H.6: Point map showing temperature values in different areas around Las Brujas. All measurements are taken on October 8th, 2025. (own image)

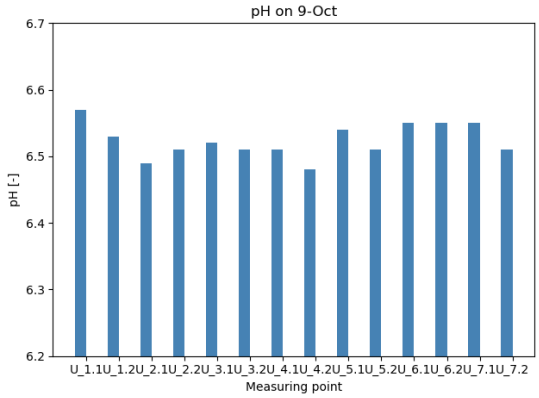

(a) Measurements of pH values in the upstream river area on October 9th.

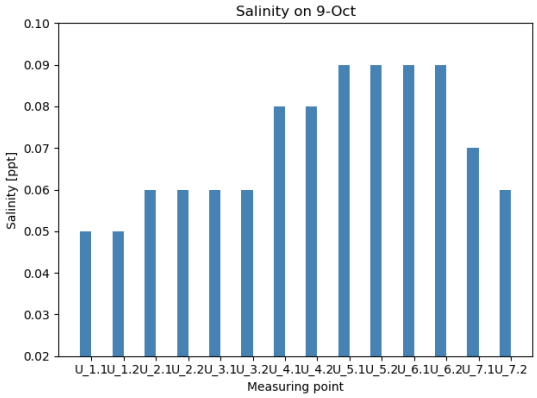

(b) Measurements of salinity values in the upstream river area on October 9th.

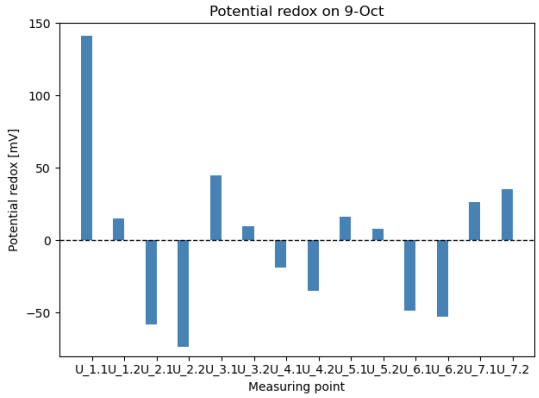

(c) Measurements of redox potential values in the upstream river area on October 9th.

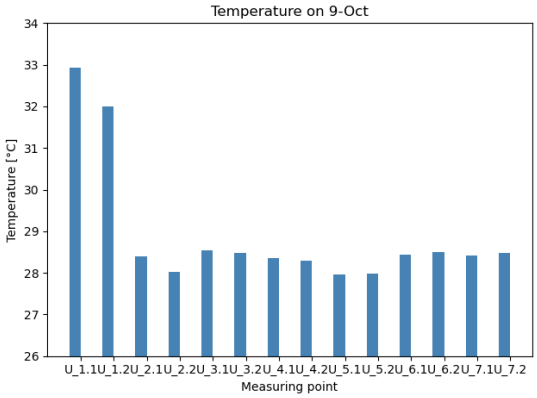

(d) Measurements of temperature values in the upstream river area on October 9th.

Figure H.7: Measured physical-chemical values of upstream area on October 9th. Measured values are pH (a), salinity (b), redox potential (c) and temperature (d) (own image)

I

Physical-Chemical Parameter measurements

In this appendix, the measured physical-chemical parameters can be found. In table I.1, table I.2 and table I.3, the values for 2, 3 and 8 October are denoted, respectively. The locations of the measurement points are depicted in figure 4.6 and figure 4.7.

site	point	depth [cm]	pH [-]	redox potential	salinity [PSU]	temperature [°C]
Chiquimullila	CHIQ 4.1	190	7.05	151.8	0.33	29.46
Chiquimullila	CHIQ 4.2	161	7.10	153.8	0.22	29.32
Chiquimullila	CHIQ 4.3	150	7.11	154.0	0.22	29.31
Brujas	BRU B1	60	7.22	177.4	0.23	32.07
Brujas	BRU B2	56	7.17	172.1	0.22	30.84
Brujas	BRU B3	60	7.19	168.3	0.22	31.44
Brujas	BRU C1	65	7.09	150.5	0.22	30.36
Brujas	BRU C2	68	7.12	118.1	0.17	29.95
Brujas	BRU C3	42	7.17	84.9	0.22	30.58
Brujas	BRU F1	57	7.23	150.0	0.23	31.55
Brujas	BRU F2	60	7.20	187.4	0.24	31.63
Brujas	BRU F3	52	7.17	190.3	0.23	31.17
Brujas	BRU G1	60	7.19	172.9	0.26	30.80
Brujas	BRU G2	55	7.13	179.7	0.25	30.95
Brujas	BRU G3	73	7.12	147.9	0.24	31.13

Table I.1: Measurements on October 2nd

site	point	depth [cm]	pH [-]	redox potential	salinity [PSU]	temperature [°C]
Brujas	H 4.1	55	7.19	125.4	0.36	28.20
Brujas	H 4.2	55	7.18	52.0	0.27	28.33
Brujas	H 4.3	55	7.19	53.9	0.26	28.23
Brujas	H 2.1	50	7.14	121.1	0.27	28.69
Brujas	H 2.2	50	7.14	111.9	0.26	28.36
Brujas	H 3.1	40	7.14	93.9	0.33	29.07
Brujas	H 3.2	45	7.17	90.2	0.32	29.11
Brujas	H 3.3	45	7.16	88.5	0.32	28.84
Brujas	H 3.4	45	7.13	84.1	0.32	28.57
Brujas	H 3.5	45	7.13	79.8	0.32	28.55
Brujas	MA 1.1	–	7.15	50.3	0.26	28.65
Brujas	MA 1.2	–	7.15	62.6	0.25	28.43
Brujas	MA 2.1	40	7.21	106.5	0.28	30.34
Brujas	MA 4.1	50	7.14	138.5	0.29	30.82
Brujas	MA 5.1	30	7.13	123.4	0.31	28.94
Brujas	MA 7.1	25	7.43	122.6	0.42	31.06
Brujas	MA 7.2	25	7.41	119.8	0.42	31.26
Brujas	MA 8.1	15	7.28	130.6	0.45	28.42
Brujas	MA 0.1	40	7.08	140.2	0.25	29.50
Brujas	CHIQ 3.1	195	7.12	143.5	0.21	29.16
Brujas	CHIQ 3.2	195	7.10	135.1	0.21	28.98

Table I.2: Measurements on October 3rd

site	point	depth [cm]	pH [-]	redox potential	salinity [PSU]	temperature [°C]
Brujas	BRU D1	65	7.41	-30.3	0.21	27.30
Brujas	BRU D2	70	7.42	-47.2	0.22	27.47
Brujas	BRU B1	75	7.46	132.2	0.20	32.67
Brujas	BRU B2	73	7.43	145.9	0.20	31.88
Brujas	BRU C1	60	7.43	135.8	0.20	32.62
Brujas	BRU C2	63	7.39	129.7	0.20	32.72
Brujas	BRU F1	73	7.34	138.1	0.20	30.74
Brujas	BRU F2	80	7.29	127.3	0.20	30.37
Chiquimullila	CHIQ 1.1	200	7.40	158.3	0.27	27.82
Chiquimullila	CHIQ 2.1	120	7.45	178.9	0.14	27.59
Chiquimullila	CHIQ 3.1	200	7.45	181.4	0.19	27.64
Chiquimullila	CHIQ 4.1	210	7.42	166.3	0.20	27.64
Marco Antonio	MA 0.1	58	7.40	113.8	0.20	27.70
Marco Antonio	MA 1.1	56	7.39	104.6	0.20	27.47
Marco Antonio	MA 2.1	54	7.37	112.7	0.21	29.07
Marco Antonio	MA 3.1	78	7.36	46.3	0.24	28.27
Marco Antonio	MA 4.1	70	7.32	71.9	0.23	29.31
Marco Antonio	MA 5.1	48	7.36	93.4	0.23	27.62
Marco Antonio	MA 6.1	70	7.34	117.6	0.30	28.53
Helicopter	H 1.1	70	7.31	148.6	0.20	29.70
Helicopter	H 2.1	60	7.37	136.5	0.20	30.35
Helicopter	H 3.1	60	7.29	136.2	0.21	30.46

Table I.3: Measurements on October 8th

Next to the measurement in the Las Brujas area, some physical-chemical measurements are done in a river area upstream of Las Brujas. The measurement locations are shown in figure 4.3. The data of the measurements are shown in table I.4.

point	depth [cm]	pH [-]	redox potential	salinity [PSU]	temperature [°C]
U 1.1	230	6.57	141.3	0.05	32.93
U 1.2	230	6.53	14.9	0.05	31.99
U 2.1	190	6.49	-57.9	0.06	28.39
U 2.2	190	6.51	-73.7	0.06	28.03
U 3.1	230	6.52	44.7	0.06	28.55
U 3.2	230	6.51	9.9	0.06	28.48
U 4.1	170	6.51	-19.1	0.08	28.36
U 4.2	170	6.48	-35.1	0.08	28.29
U 5.1	180	6.54	16.1	0.09	27.97
U 5.2	180	6.51	7.7	0.09	27.99
U 6.1	140	6.55	-48.4	0.09	28.44
U 6.2	140	6.55	-53.0	0.09	28.49
U 7.1	260	6.55	26.4	0.07	28.42
U 7.2	260	6.51	35.4	0.06	28.47

Table I.4: Measurements on October 9th in upstream river area

J

Reference projects

Many mangrove restoration projects have been executed over the years. These approaches vary in success. In this sub-chapter, the main takeaways of two projects comparable to this research project will be discussed.

Mikoko Pamoja, Kenya

Mikoko Pamoja is a community-led initiative focused on mangrove conservation and restoration in Gazi Bay, Kenya. It is the first project of its kind to fund conservation through the sale of carbon credits ("Mikoko pamoja," n.d.). A carbon market allows investors and corporations to trade both carbon credits and carbon offsets simultaneously. This mitigates the environmental crisis, while also creating new market opportunities (Credits, 2025). They conserved 117 hectares of land by involving the community in preventing deforestation, protecting the forest, and replanting 4,000 trees annually ("Mikoko pamoja," n.d.).

Mangrove action project (MAP)

The Mangrove Action Project is a small, education-focused non-profit organization. They facilitate educational and restoration projects all over the world using an approach called "Community-based ecological mangrove restoration". This method takes a holistic approach, emphasizing learning from nature and working with local communities. Their approach prioritizes research and analysis, focusing on local species, waterways, tides, and the surrounding communities. They maintain that mangrove loss inevitably disrupts natural systems, making it necessary to restore and reconnect waterways while addressing disturbances to the site's topography.

When looking at the project in Krabi, Thailand, several things can be remarked. Local community members and volunteers participated in the excavation of channels and reshaping the landscape to restore the natural system. To support mangrove repopulation, bees were introduced as pollinators. Byproducts such as pollen and honey were used by local communities as a source of income. Throughout and following the project education and knowlegde exchange with neighbouring towns and stakeholders remained a top priority (Project, 2019). This resulted in a restoration of 0.7ha of mangroves (Project, 2023).